DOE/PR/06010-T14
(DE83017239)

ENERGY CONSERVATION

EVALUATION OF O_2 AND CO MONITORING SYSTEMS FOR COMBUSTION CONTROLS

Final Report

By
C. Presser
H. G. Semerjian
M. Juberts

March 1983

Work Performed Under Contract No. AI01-76PR06010

National Bureau of Standards
U. S. Department of Commerce
Washington, D. C.

U. S. DEPARTMENT OF ENERGY

DISCLAIMER

This report has been reproduced directly from the best available copy.

Available from the National Technical Information Service, U. S. Department of Commerce, Springfield, Virginia 22161.

Price: Printed Copy A06
Microfiche A01

Codes are used for pricing all publications. The code is determined by the number of pages in the publication. Information pertaining to the pricing codes can be found in the current issues of the following publications, which are generally available in most libraries: *Energy Research Abstracts (ERA); Government Reports Announcements* and Index (*GRA* and I); *Scientific and Technical Abstract Reports (STAR);* and publication NTIS-PR-360 available from NTIS at the above address.

DOE/PR/06010-T14
(DE83017239)
Distribution Category UC-95f

Evaluation of O_2 and CO Monitoring Systems For Combustion Controls

Final Report

By

C. Presser
H. G. Semerjian
M. Juberts

Chemical Process Metrology Division
Center for Chemical Engineering
National Engineering Laboratory
National Bureau of Standards
Washington, D.C. 20234

Prepared for the
U.S. Department of Energy
Office of Industrial Programs
Washington, D.C. 20585
Under Contract No. EA-77-A01-6010

ABSTRACT

A study has been carried out to provide a comparative evaluation of in-situ O_2 and CO monitors used for combustion control. The experiments have been carried out in the NBS experimental furnace, which is equipped with a complete on-line gas sampling and analysis system used as a reference system. Chemical equilibrium calculations, carried out by the minicomputer based data acquisition system, also provide an indication of the extent of reaction, and a means to detect possible measurement errors. Specific areas of interest included evalution of the performance of the instruments over a wide range of operating conditions, effect of higher inlet temperatures on the stack gas composition, effect of furnace cavity pressure on the CO and O_2 measurements and the effect of variations in the stack gas temperature. The O_2 stack gas monitor has a ZrO_2 type sensor. The system performed reliably and provided the capability to operate at high process temperatures. The O_2 measurements, however, were found to be quite sensitive to air leakage when the furnace was kept below atmospheric pressure. On-line calibration of the instrument at the process temperature was also found to be necessary, especially for an aspirating type probe which is used to control the gas sampling rate. The in-situ CO monitoring system is based on infrared absorption measurements across the stack. The CO measurements were found to be quite sensitive to stack gas temperatures and this effect has been quantified in a heated test cell. The findings indicate that accurate measurements of CO concentration will require simultaneous measurement of gas temperatures and compensation of the CO reading. The stack gas composition was found to be dependent upon furnace cavity temperature and heat transfer processes which are influenced by physical geometry, fuel/air mixing and heat extraction rate. Experimental results are presented for both natural gas and No. 2 fuel oil fired systems. The results of this study indicate that stack gas monitoring is a valuable combustion control method when utilized with pre-established setpoints which are unique for a particular installation and load.

ACKNOWLEDGEMENT

This work was partially supported by the Department of Energy, Conservation and Renewable Energy, Office of Industrial Programs, under Contract No. EA-77-A01-6010. The technical program manager was Mr. Stanley F. Sobczynski. This support is gratefully acknowledged.

TABLE OF CONTENTS

LIST OF FIGURES

EXECUTIVE SUMMARY

Industrial efforts to improve the efficiency of boilers and furnaces have led to the development of a number of automatic control systems, which regulate the fuel and air flow rates and try to optimize the combustion and energy transfer processes. Most of the combustion control systems rely on measurement of the composition of flue gases, which is then used to adjust the fuel/air mixture in the combustion zone. In the past, gases have been sampled out of the exhaust stream, either in a continuous manner or in batches, and analyzed for a number of species. More recently, in-situ gas monitors have been developed to provide a continuous reading of species concentration in the flue gases with a faster response as compared to gas sampling systems. The general goal is to keep the fuel/air mixture as close to the stoichiometric mixture as possible, where the combustion and energy transfer processes are optimized, without generating excessive amounts of gaseous and particulate emissions.

The approach generally used for combustion control is to monitor the level of carbon monoxide (CO) and/or excess oxygen (O_2) in the flue gases, which are used as an indication of deviation from stoichiometric conditions. Optimum combustion performance is usually obtained with slightly fuel-lean flames, due to non-uniform fuel/air mixing. The CO monitors are based on the measurement of infrared absorption across the stack gases. The concentration of excess O_2 is determined by the electrochemical reaction occurring across a test-tube shaped ceramic probe, made up of yttria stabilized zirconium oxide

(ZrO_2). The current practice is to locate these monitoring systems in the boiler stack, far downstream of the combustion zone, where the gas temperatures are low and the chemical reactions are assumed to have been frozen or completed. At this point, the wall and gas temperatures are low enough so that any interference due to wall or gas radiation is not expected, and the lifetime of the instruments is substantially increased.

The objective of this study was to provide data on the performance of in-situ O_2 and CO monitors over a wide range of operating conditions, and to investigate the effect of heat transfer processes on the relationship between the combustion zone properties and stack gas measurements. Two stack gas monitoring systems, a ZrO_2 type O_2 sensor and an in-situ CO monitor based on infrared absorption, have been evaluated in the NBS experimental furnace. These instruments are typical of in-situ flue gas monitors that are used for combustion control in boilers and furnaces.

The experiments were designed to compare the measurements obtained with the in-situ CO and O_2 monitors to those obtained with the gas sampling system and to theoretical equilibrium calculations. Furnace conditions varied from a hot highly radiating environment, representative of industrial furnaces, to a cooler environment, representative of industrial boilers. Data were recorded over the equivalence ratio range of 0.75 to 1.05 for both natural gas and No. 2 fuel oil. Interest was centered around the desired region for

automatic controls; viz., $100 \leq CO \leq 300$ ppmv, $0 \leq O_2 \leq 2\%$ (excess) and $0.95 \leq \phi \leq 1.0$.

The ZrO_2 type O_2 monitor performed reliably over a long period of time, and provided quite repeatable measurements with an accuracy of 0.25% O_2 over the full range and a sensitivity of about 2% O_2 for a change of 0.1 in equivalence ratio. The instrument, however, did not have a provision for on-line calibration, and the O_2 measurements were found to be quite sensitive to the air aspiration rate, which controlled the gas sampling rate from the stack. The ZrO_2 sensor provides the capability for operating at high temperatures, nominally 1540°C (2800°F) and below, which is valuable especially for high temperature furnace applications. It also means that this sensor could be located closer to the combustion zone, and provide better time response.

Measurements with the in-situ CO monitoring system could only be carried out where the gas temperatures were more moderate, less than 370°C (700°F). In general, the readings obtained with the in-situ CO monitor were less than half of those obtained with the gas sampling system. This deviation was attributed primarily to the effect of gas temperature on the CO absorption coefficient. This effect was quantified in a set of experiments carried out in a heated cell. These findings indicate that any accurate measurement of CO concentration in the stack gases, using infrared absorption, will require a simultaneous measurement of gas temperature and compensation of the CO measurements. Additional effects due to CO_2 and water vapor absorption may also be important.

A definite dependence of stack gas composition measurement upon furnace temperature and heat transfer processes was displayed as the furnace heated up over a long period of time. These results indicate that the relationship between combustion fuel/air mixture and stack gas composition is not unique. It will vary as a function of furnace cavity temperature which is affected by physical geometry, burner geometry (and its effect on fuel/air mixing), and by the rate of heat extraction. The application of stack monitoring systems for combustion control, over the narrow range desired for optimal operation, will require static and/or dynamic allowances for these factors. The characteristics of a particular system should be carefully analyzed prior to implementation of a control system intended to optimize combustion at or near stoichiometric conditions. The results of this study indicate that stack gas monitoring is a valuable combustion control method, when utilized with pre-established setpoints. These setpoints can be expected to be unique for a particular installation and load.

These observations also point towards the need for combustion control systems, which do not necessarily rely on stack gas measurements, but rather on measurements made directly in the combustion zone.

I. INTRODUCTION

Industrial efforts to improve the efficiency of boilers and furnaces have led to the development of a number of automatic control systems, which regulate the fuel and air flow rates, and try to optimize combustion and energy transfer processes [1]. Most combustion control systems rely on measurement of the composition of flue gases, which is then used to adjust the fuel/air mixture in the combustion zone. In the past, gases have been sampled out of the exhaust stream, either in a continuous manner or in batches, and analyzed for a number of species. More recently, in-situ gas monitors have been developed to provide a continuous reading of species concentration in the flue gases with a faster response as compared to gas sampling systems. The general goal is to keep the fuel/air mixture as close to the stoichiometric mixture as possible, where the combustion and energy transfer processes are optimized, without generating excessive amounts of gaseous and particulate emissions.

The approach generally used for combustion control is to monitor the level of carbon monoxide (CO) and/or excess oxygen (O_2) in the flue gases, which are used as an indication of deviation from stoichiometric conditions. Excess air introduced into the combustion zone can result in lower flame temperatures as well as increased energy loss through the stack gases. A combustible mixture deficient of oxygen (or air) produces large amounts of combustible products (CO, hydrocarbons, particulates, etc.) and results in energy losses in the form of unburned fuel [2-4]. Optimum combustion performance is usually obtained with slightly fuel lean flames due to non-uniform fuel/air

mixing. For typical boiler configurations, automatic control is desirable over the CO concentration range of 100-300 ppmv, and excess oxygen range of 0-2% (about 0-10% excess air) [5-8].

The CO monitors are usually based on the measurement of infrared absorption across the stack gases [9]. The concentration of excess O_2 is often determined by the electrochemical reaction occurring across a test-tube shaped ceramic probe, made up of yttria stabilized zirconium oxide, ZrO_2 [10-12]. The current practice is to locate these monitoring systems in the boiler stack, far downstream of the combustion zone, where the gas temperatures are low and chemical reactions are assumed to have been frozen or completed. At this point the wall and gas temperatures are low enough, so that any interference due to wall or gas radiation is not expected, and the lifetime of the instruments is substantially increased.

The installation of these monitors in the stack may present additional problems. The stack conditions being monitored may not be entirely representative of conditions inside the combustion chamber. Air infiltration and/or stratification of flue gases can significantly influence the O_2 concentration, and to a lesser degree the CO level [13]. Disturbances in the furnace chamber may also result in control loop instabilities due to the increased response time of the monitoring system.

The relative advantages of using CO or O_2 monitoring systems, or both, for combustion control have been debated in the literature [14]. Depending on the particular combustor configuration, the type of fuel utilized in the system and the range of fuel/air mixtures over which control is desired, one of the two monitoring systems may be more

applicable. A number of studies carried out by industrial, government and academic institutions have identified automatic on-line control of combustion processes as a generic technology, which can provide energy savings and an improvement in process efficiency for a wide variety of industries [15-19]. The suggested approach has been to encourage increased and more efficient use of existing control technology, as well as development of new control techniques. CO monitoring systems have been cited often as a new technology, which is not fully utilized.

The application of CO monitors for combustion control, especially in high temperature processes, has been relatively limited, primarily due to a lack of detailed and reliable data on their performance and operating range. The purpose of this study was to provide such data by comparative evaluation of an O_2 monitor and a CO monitor in the NBS experimental furnace.

II. EVALUATION OF IN-SITU O_2 AND CO MONITORS

An evaluation of in-situ O_2 and CO monitors was carried out in the NBS experimental furnace. The objective of the experimental program was to provide data to establish the suitability of oxygen and carbon monoxide monitoring systems for combustion control over a wide range of operating conditions. The facility is equipped with a complete on-line gas analysis capability, which was used as a reference system. Specific areas of interest were evaluation of the performance of the instruments over a wide range of operating conditions; effect of higher inlet temperatures (for installations with heat recovery systems) on the stack gas composition; effect of furnace cavity (or stack) pressure level on the CO and O_2 measurements; and the effect of variations in the stack gas temperature.

Experimental Facility

The experimental furnace (Fig. 1) has a combustion chamber with the internal dimensions of 80 cm (W) x 110 cm (H) x 240 cm (L). A single burner fires horizontally through one end into the combustion chamber. The combustion products exhaust from the opposite end of the chamber, past a recuperator, and then up through the stack. The recuperator is designed to preheat incoming combustion air before reaching the burner. Several ports, located along the walls of the furnace, permit visual observation of the flame and the introduction of intrusive probes; viz., a water-cooled emission probe. A complete on-line gas analysis system is used for combustion gas sampling and

analysis. The system has the capability to analyze the effluents for the following species concentrations: CO, CO_2, O_2, NO/NO_x, SO_2 and total hydrocarbons (THC). The output of the gas analyzers, the temperature, pressure and flow rate of all the input and output streams, and other furnace parameters are continuously monitored by the DEC PDP 11/60* minicomputer-based data acquisition and control system (DAS). Removal of thermal energy from the furnace is achieved with a variable thermal load heat exchanger. A high temperature damper located in the stack is used to maintain positive furnace pressure during experiments. A more detailed description of the experimental facility is presented in Appendix A.

The in-situ O_2 monitor evaluated during this study utilizes an yttria stabilized zirconia tube probe to measure the excess O_2 content of stack gases. The monitor is located at the far end wall of the furnace in the plenum beneath the recuperator. The sensor probe uses an aspirating extraction technique to transport the sample gas from the probe inlet to the sensing cell which is kept at a constant temperature of 700°C (1300°F). The in-situ CO monitor selected for evaluation is an infrared device that uses a high resolution absorption

---

*Certain commercial equipment, instruments or materials are identified in this report in order to adequately specify the experimental procedure. In no case does such identification imply recommendation or endorsement by the National Bureau of Standards, nor does it imply that the material or equipment is necessarily the best available for the purpose.

Experimental Design

The experiments were designed so that the concentrations recorded by the in-situ O_2 and CO monitors could be compared with those measured with the gas sampling system. The fuel/air equivalence ratio derived from the latter [20] was then compared to the measured input input fuel/air ratio, to check for internal consistency. In addition, on-line chemical equilibrium calculations [21] were carried out based on input fuel and air flow rates, and for selected temperatures; e.g., adiabatic flame temperature, measured furnace cavity temperature or stack gas temperature. A typical set of calculations for methane/air combustion, based on adiabatic flame temperatures, are shown in Fig. 2. The predicted gas composition can then be compared with measured species concentrations to give an indication of the extent of reaction, effect of local temperature, possible measurement errors, and dilution effects.

The measurements were carried out at various furnace operating conditions; i.e., high and low heat throughput rates, after different periods of furnace preheating, with different rates of furnace heat extraction, and with different burner inlet air temperatures. Experiments were conducted with both natural gas and No. 2 fuel oil. The fuel/air equivalence ratio (ratio of actual fuel to air ratio to the stoichiometric fuel to air ratio) was varied from about 0.75 to 1.05, the region around =1.0 being the main area of interest. spectroscopy technique. The CO concentration can be monitored over the range of 0-1000 ppmv, in flue gases which are below 370°C (700°F). A more detailed description of each monitor is given in Appendix B.

Measurements Below the Recuperator

For the first set of experiments, both the O_2 and CO in-situ monitoring systems were located in the region beyond the curtain wall but below the recuperator (see Fig. 1). The gas temperatures encountered in this zone (500-750°C) were more typical of conditions to be found in an industrial furnace stack, where no recuperator existed. The in-situ O_2 probe was located on the far end wall, 23 cm (9 in) above the sighting port which is in line with the burner (see Fig. 3). The in-situ CO monitoring system was located at the same height as the O_2 probe. The source and the analyzer units were located on the side walls of the stack cavity (behind the curtain wall) such that the infrared beam crossed the stack 31 cm (12 in) in front of the end wall. The stack gas sampling probe was inserted into the stack through a port 23 cm (9 in) to the side of the O_2 probe, and 9 cm (3.5 in) above, enabling gases to be sampled from the area immediately above the region where the infrared beam traverses the stack cavity.

The results obtained in this region, below the recuperator, are shown in Figs. 4-6 for natural gas and Figs. 7-9 for No. 2 fuel oil. The furnace pressure was kept positive, thereby preventing air infiltration into the furnace. The furnace was generally preheated for 3-4 hours (to about 900°C) before data acquisition was initiated. Typical CO_2, O_2 and CO measurements as a function of fuel/air equivalence ratio are shown in Figs. 4-9 ($\phi<1$ is a fuel lean mixture, $\phi>1$ a fuel rich mixture, and $\phi=1$ is a stoichiometric mixture). Included are results obtained with the gas sampling/analysis system,

with the ZrO_2 in-situ O_2 monitor, and from equilibrium calculations based on stack gas temperature measurements. The CO_2, O_2 and CO measurements obtained from the gas analysis system are "dry" measurements, since all the water is removed from the gas sample before analysis (see Appendix B). These readings are then corrected by using the measured species concentrations of the flue gas to calculate the corresponding amount of water formed during combustion [20]. The measurements are then reported as the "wet" values. These are, of course, the appropriate values for comparison with the in-situ measurements and the equilibrium calculations. The general trends show that as the fuel/air mixture becomes richer (i.e., as ϕ increases) and approaches a stoichiometric mixture, the maximum theoretical value of CO_2 concentration (wet) is attained (9.5% for natural gas and 13.3% for No. 2 fuel oil) at approximately ϕ =1, and then starts decreasing beyond that point due to lack of available oxygen. This is clearly indicated in Figs. 5 and 8, where the excess O_2 falls steadily with increasing ϕ, until the stoichiometric mixture is reached, beyond which point no more oxygen is detected. The CO concentration remains below 20 ppmv for fuel lean mixtures, and rapidly rises beyond ϕ=1 (see Figs. 6 and 9). The equilibrium calculations are included in each case, and the general trends agree with the measurements. Indeed, it is surprising to see such good agreement between the CO concentrations and the computed equilibrium values. It indicates that the CO oxidation proceeds fast enough to reduce the CO concentration from the high levels expected to exist in the combustion zone (see the CO equilibrium levels based on flame temperature in Fig. 10) to the much lower levels

that correspond to an equilibrium at the lower stack temperature.

This behavior should be unique to systems where the overall furnace cavity temperature remains high, and the amount of total heat extraction is relatively modest; i.e., low enough not to quench the CO oxidation. Indeed in most industrial applications, the CO concentrations are found to be much higher, as reported by Gilbert [5]. Figure 4 of Ref. 5 is reproduced here as Fig. 11, which indicates that automatic control of boilers, kilns and furnaces for maximum combustion efficiency could be achieved over the range 120-250 ppmv CO and 0-2.2% excess O_2.

To allow for a direct comparison, the experimental data obtained in the furnace over the range $0.96 \leq \phi \leq 1.04$ is expanded and shown in Fig. 12 for natural gas, and Fig. 13 for No. 2 fuel oil. A closer examination of Figs. 11-13 shows that the measured CO and excess O_2 curves intersect outside the limits proposed by Gilbert (i.e., less than 100 ppmv CO at 0.1-0.2% O_2) for natural gas and just inside the limits for No. 2 fuel oil, with the oil flame requiring more excess O_2, as expected. These results indicate that, under certain circumstances, the expected relationship between the conditions existing in the combustion zone and those monitored in the stack could be significantly different. They also suggest that the range of the control parameters (i.e., CO and O_2 concentration) to be utilized may strongly depend on the particular combustion system configuration and heat extraction profile.

The O_2 measurements obtained with the ZrO_2 probe are also shown in Figs. 5 and 8. For the fuel lean flames, these readings are observed to deviate from the gas sampling measurements by more than

0.5% O_2. As the flame becomes richer this difference is reduced; however, the percent difference remains about the same. Part of this discrepancy was attributed to a lack of a calibration procedure, except at ambient air conditions. An attempt was made to pass calibration gas over the ZrO_2 cell at normal furnace operating conditions in order to check the instrument calibration and to verify that the ZrO_2 cell was still functioning properly. The aspirator air hose was replaced by tubing that was connected to calibration gas bottles. The open end of the aspirator was blocked so that the calibration gases would flow back past the sensor cell and out through the sampling pipe into the furnace cavity. The monitored O_2 level was checked with 2.09% and 3.94% O_2/N_2 calibration gas and the agreement was good, thus indicating that the ZrO_2 cell was working properly.

It was also realized that the readings could be affected by varying the aspiration flow rate. Fig. 8 presents two sets of data taken at different aspirator air flow rates for varying fuel/air ratio. It was found that the in-situ O_2 readings could be changed significantly (compare open and solid symbols, Fig. 8) and be made to correspond with the on-line analyzer measurements for an aspirator downstream pressure of 2.5 KPa (10 in H_2O gauge). This pressure was used throughout the remaining reported tests. The discrepancy which developed during later tests between the monitored O_2 level and the gas sampling O_2 analyzer shows that the aspirator air flow should be readjusted for each furnace run, according to the furnace pressure.

These tests were all performed with a positive furnace pressure of 15-25 Pa (0.06 - 0.1 in H_2O) in order to prevent any dilution

effects, through leakage of outside air into the furnace, which could effect the ZrO_2 probe readings or influence the combustion processes occuring upstream of the probe. The influence of varying the fuel/air ratio, over the range $0.5 \leq \phi \leq 1.1$, upon the furnace pressure was found to be relatively small, and hence the effect on oxygen measurements to be negligible. Any substantial variation in the furnace pressure, however, could effect the flow rate of sampled gases over the ZrO_2 sensor. Figure 14 presents the variation of the excess O_2 concentration with equivalence ratio for both the in-situ O_2 monitor and the on-line O_2 analyzer. The experiment, performed with No. 2 fuel oil, showed a definite increase in the O_2 readings with a negative furnace pressure, indicating air infiltration and dilution effects.

Measurements with the in-situ CO monitoring system were also attempted at this location below the recuperator, where the gas temperatures are at or above 500°C (930°F). This was considered to be representative of typical industrial furnace-type applications. In the experimental furnace, the high temperature gases from the combustion zone flow past two large water tube heat exchangers, located upstream of the curtain wall (see Fig. 1), where about 30-50% of the thermal energy is removed.

The CO monitoring system was set-up for a nominal optical path of 91 cm (3 ft) across the stack cavity. This corresponded to the inner wall dimensions, since the cooling air for the sapphire windows also purged the circular passages between the external (source or analyzer) units and the furnace inner wall. This air flow, however was assumed to be small enough not to penetrate the central part of the stack, and

simply flow up along the walls with a minimum amount of influence on the CO readings. This indeed may be the case for industrial applications, where the in-situ CO monitoring system is usually placed on a boiler stack with a diameter several times that of the experimental furnace, with correspondingly larger flow rates.

Unfortunately, because of the smaller size of the furnace, the cooling air was found to penetrate into the stack gases, effecting not only the CO readings, but also the measurements obtained with the ZrO_2 probe and the gas sampling probe. Both of these probes were located near the center of the stack, indicating substantial air penetration. Attempts were made to minimize the cooling air flow; however, the readings obtained from the in-situ CO monitor were still far lower than those obtained from the gas analysis system (see Fig. 9). In addition, it was also observed that radiation emitted from the hot furnace walls, especially after several hours of heating, affected the detector signal quite substantially. This radiant energy, however, is emitted as a continuum and effects only the d.c. level. The frequency discrimination capability of the monitor should therefore compensate for this effect.

Based on these observations, it was concluded that our inability to obtain reliable data at this location was primarily due to the higher stack gas temperatures, which resulted in a reduced absorption coefficient, and hence reduced the indicated CO levels. It was therefore decided to relocate the in-situ CO monitoring system in the stack above the recuperator, where the gas temperatures are substantially lower.

Measurements Above the Recuperator

The in-situ CO monitor was fixed to the tapering portion of the stack above the recuperator as shown in Fig. 15. This provided a 91 cm (3 ft) separation between the source and analyzer units of the monitor. The gas sampling probe drew effluent at a location 15 cm (6 in) above the infrared beam so that one could detect dilution effects by the CO monitor cooling blowers. The excess O_2 reading could then be compared with the in-situ ZrO_2 monitor located below the recuperator. A discrepancy in the two excess O_2 readings would indicate a change in the effective path length through dilution. The absence of an increase in the O_2 level would indicate that the air flow introduced by the CO monitoring system does not perturb the flue gases and that the stack readings could be assumed indicative of upstream combustion processes.

The initial tests produced a large increase in the excess O_2 as illustrated in Figs. 16 and 17 (natural gas) and Figs. 18 and 19 (No. 2 fuel oil) where approximately 5% excess O_2 was recorded at stoichiometric conditions. As expected this reduced significantly the CO_2 concentration when compared to the equilibrium computations.

In an attempt to reduce the dilution effect of the cooling air and match the O_2 reading in the stack with the value monitored below the recuperator, the cooling air blower outlet was restricted with 2.54×10^{-3} cm (0.001 in) thick brass shim stock. After restricting the blower output with several pieces of shim stock, it was found that when the center of the restriction contained a 0.3 cm (1/8 in) diameter opening the monitor output signal voltage would drop until the instrument could no longer function. The monitor panel indicated an

increase in the beam opacity beyond 80%. Insufficient air cooling allowed flue gases and soot particles to enter the instrument connecting flanges. Consequently, the indicated CO level increased until the monitor output went off-scale. The 0.3 cm (1/8 in) restriction also induced excessive blower heating (operating at 540 watts) which caused an increase in the air temperature by 12-14°C (20-25°F).

This problem was alleviated partially by replacing the blowers with air-conditioned air from the room ventilation system. This provided cooler air at lower flow rates and pressure than was achieved with the in-situ CO monitor blowers. The cooler air was also used to provide additional cooling for the instrument electronics. The best operating conditions were obtained with the air-conditioned air and a 0.6 cm (1/4 in) restriction in the line, which caused a 0.5% increase in the stack excess O_2 and a reduction in the detector electronic signal from 2V to 1-1.5V. It was impossible to produce a full 2V signal (recommended operating level) without increasing significantly the stack excess O_2. The beam path length was not known accurately since insufficient cooling air permitted effluents to enter the instrument connecting flanges. Soot had been discovered on the inside face of the 0.6 cm (1/4 in) restriction after using the No. 2 fuel oil, which indicated reduced beam transmission near the sapphire windows. The inability to obtain a strong detector signal without excess O_2 dilution may indicate that the cooling air does not pass through the connecting flanges uniformly, and permits effluents to move into the flanges at the same time. The air may pass into the flanges

tangentially and develop a swirling motion with a central recirculating zone which draws flue gases toward the sapphire windows.

Another problem arose due to the heat rising from the recuperator which increased the detector electronic's temperature above 49°C (120°F). This problem was resolved by cooling the detector cabinet with air-conditioned air and by insulating the detector cabinet from the recuperator.

The measurements of CO_2, CO and O_2 concentration for the range $0.8 \leq \phi \leq 1.04$ are presented in Figs. 20-22 for natural gas and Figs. 23-25 for No. 2 fuel oil. These show the effect of the 0.5% excess O_2 in the stack flue gases. The furnace was relatively warm; e.g., for the No. 2 fuel oil case the furnace gas temperature (T_F) was approximately 888°C (1630°F) and the stack gas temperature (T_{STK}) was about 290°C (550°F) at =1.

Figures 20-22 illustrate the effect of permitting the pilot light to burn continuously in order to prevent flame outs. The extra natural gas shifts the measured readings from both the gas sampling and in-situ instruments to the lean side because the additional fuel is unaccounted for in ϕ. The effective change in ϕ is 4%.

Data obtained without the pilot flame, Fig. 23, indicates that the CO_2 peak is shifted to slightly larger than ϕ=1 because of the lower furnace temperature. The maximum value attained is lower than the theoretical maximum due to the 0.5% excess O_2. The CO level will consequently rise when the flame is slightly richer than expected and the excess O_2 reaches its minimum past the stoichiometric point. Comparison with the in-situ CO monitor in Figs. 22 and 25 shows that

the CO level remains at 10-40 ppmv for lean flames. Past stoichiometric conditions both CO readings rise simultaneously, but the in-situ monitor readings generally remain at less than half the gas sampling value (originally, with the cooling blowers, this ratio was 1:3-4). For automatic control purposes the in-situ instrument could be used as an indicator of the presence of CO, but not necessarily to provide an accurate measurement of the CO concentration. Good agreement between in-situ O_2 monitor (Figs. 21 and 24) and the gas sampling data is primarily due to the adjusted setting of the air aspiration rate. Note that the minimum reading of excess O_2 is 1% on the instrument. This monitor would be suited for automatic control of boilers (Ref. 5, Fig. 4) where the desired control range is 1-2% excess O_2 (at approximately 100-300 ppmv CO); however, for gas and oil fired systems, the indications in the lower range need to be improved since excess O_2 levels range from 0-0.6%.

For furnace gas temperatures below 540°C (1000°F), along with heat removal by the two combustion chamber heat exchangers and the recuperator, conditions in the stack may be considered similar to that of a boiler except for the effect of the high temperature flame and furnace wall radiation on completion of combustion processes. In order to simulate boiler conditions where wall incident energy is removed by heat exchangers, an attempt was made to keep the furnace gas temperature below 540°C by minimizing the thermal energy content of the flame. The flame was stabilized by keeping the pilot on continuously. The procedure did not prove to be successful since, for the oil flame, the furnace gas temperature (T_F) rose above 540°C almost immediately,

and for the natural gas flame, the fuel/air ratio was altered 4% due to the extra pilot gas.

Another approach was attempted in which data were recorded during the furnace transient start-up. Although long tests with rich flames could not be attempted, some data could be acquired for lean flames under quasi-steady conditions.

Several tests were performed for different equivalence ratios. The results presented in Figs. 26-29 are for ϕ=0.5 with gas sampling in the stack. The length of each test was approximately 30 minutes which depended upon our ability to keep the stack gas temperature between 150-190°C (300-375°F). The furnace gas temperature rose to 685°C (1265°F) during this trial. Upon flame ignition the cold furnace walls produced an initial surge of CO (Figs. 28 and 29) for the very lean flame due to the poor fuel/air mixing and freezing of chemical reactions. The CO level peaks after several minutes and then drops exponentially as the stack gas temperatures grow. During the initial startup (the first 100 sec) the CO_2 concentration (Fig. 26) increases and the O_2 concentration (Fig. 27) decreases rapidly. The rate of change in CO_2 and O_2 is then reduced as the rate of change in CO decreases. The CO concentrations recorded from the in-situ device are also shown in Figs. 28 and 29. CO readings above 1000 ppmv (beyond the panel meter scale) were also measured by connecting the analog output signal (linear) to a strip chart recorder. It is again observed that the in-situ CO monitor provides readings which are about half the value obtained with the gas analysis system throughout its operating range.

The ZrO_2 sensor reading stayed within 0.5% of the gas sample measurements. When the air-conditioned air flow across the sapphire

windows of the in-situ CO monitor was slightly increased there were no significant changes. However, when the fuel/air ratio was increased to ϕ=0.56, the initial surge of CO was reduced and vanished for the richer flames. The increase in combustion air inlet temperature was insignificant.

Heat Transfer Effects on Stack Gas Composition

Figures 30-32 present data taken during the same experiment shown in Figs. 23-25; however, the furnace gas temperature had risen from a temperature of T_F = 888°C to T_F = 920°C at ϕ=1. A shift in the experimental curves toward the lean side was realized due to increased furnace gas temperature and higher combustion air inlet temperature.

Figs. 33-41 illustrate this heat transfer effect for a 7 hour test using No. 2 fuel oil. Three sets of data were obtained over a 2 hour interval each, with one hour of furnace preheating which ensured flame stability. Presented are the CO_2, O_2 and CO concentrations for $0.78 \leq \phi \leq 1.04$. The furnace gas temperature (T_F) for the 3 tests (ie., cold, warm and hot, respectively) were 870, 910 and 945°C at $\phi \simeq 1$, along with combustion air inlet temperatures (T_A) of 177, 249 and 270°C. Gas samples were extracted from the plenum beneath the recuperator, where the gas temperatures were 588, 677 and 717°C, respectively, at $\phi \simeq 1$. The in-situ CO monitor was inoperable for this experiment.

For the "cold" test (Figs. 33-35) the CO_2 concentration is lower than the equilibrium values (based on the stack gas temperatures) on the lean side of stoichiometric mixture indicating reduced combustion

efficiency which may be, in part, due to poor fuel evaporation and nonuniform fuel/air mixture. As the flame becomes richer the CO_2 concentration reaches the same maximum value as predicted theoretically, but on the rich side of the stoichiometric fuel/air value. The CO level similarly does not grow until the flame is fuel rich, and the amount of excess O_2 remains greater than the equilibrium value until it is depleted on the fuel rich side of the fuel/air stoichiometric point. The discrepancy in the readings by the ZrO_2 sensor is again due to the incorrect adjustment of the aspiration rate.

For the "warm" test (Figs. 36-38) the furnace temperatures are somewhat higher. The CO_2 concentration appears to reach its maximum value at the fuel/air equivalence ratio predicted by the equilibrium calculations, with the two curves almost overlapping one another. The CO and excess O_2 concentrations are also in better agreement with the equilibrium calculations.

For the "hot" test (Figs. 39-41), gas temperatures are generally higher than the above cases. The maximum CO_2 level is attained for fuel lean mixtures, contrary to the earlier observation with the cooler flame, which may be an indication of improved combustion processes. Less excess O_2 is available as compared to the theoretical values. Correspondingly, the CO level is observed to start increasing at a leaner fuel/air mixture.

Goldman and Timnat [22] tend to support these findings for No. 2 fuel oil (refer to Fig. 7 of Ref. 22). The variation of CO_2, CO and O_2 concentration is presented for two burner tunnels. Effluent was sampled 94 cm (37 in) downstream of the burner. One tunnel has a

relatively large volume whose ability to develop hot combustion gas recirculation in the sudden expansion region is much less than a second smaller tunnel which utilizes its internal volume more effectively. The latter tunnel develops a strong recirculation zone which enhances fuel droplet evaporation. Their results show that higher tunnel gas temperatures associated with the smaller tunnel enhance combustion efficiency and appear to shift the concentration curves to leaner flames. A similar phenomenon is occurring for the NBS furnace as it approaches steady state conditions.

In-situ CO Monitor: Investigation of the Effect of Stack Gas Temperatures

It was pointed out earlier that the relatively low CO concentrations measured in the stack gases, with the in-situ CO monitor, were primarily attributed to the higher temperatures encountered in the stack. In order to clearly identify and quantify this effect, an absorption cell was fabricated, where the gas temperature, pressure and composition could be carefully controlled, and CO measurements could be made using the CO monitoring system. A sketch of the experimental set-up, and a picture of the test cell are shown in Figs. 42 and 43, respectively.

The cell was 91.5 cm (3 ft) long and was encased by high vacuum flanges. Two sapphire windows, located on the end flanges, allowed optical access into the cell. The sapphire windows were identical to the ones used in the CO monitoring system, so that the spectral response of the system would not be altered. The cell was made of 12 cm (4 3/4 in) I.D. steel tube. The end flanges were made of stainless

steel. The cell was heated with a 0.63 mm (0.025 in) Nichrome wire which was wrapped around the steel tube. The temperature was controlled with three powerstat variable transformers and measured with three T-type thermocouples inserted into the cell. The temperatures were monitored with a digital LED meter and a multipen strip chart recorder. The cell pressure was kept constant throughout the tests at near atmospheric pressure. The source and analyzer units of the CO monitoring system were then mounted on the two sides of the cell.

Before the tests, the test cell was flushed with dry N_2 for several hours in order to remove any residual gases. Then a calibration gas mixture of 779 ppmv CO/N_2 was introduced into the cell from one end, and the gases exiting from the other end were fed into the gas sampling/analysis system, where the CO concentration was continuously monitored with the non-dispersive infrared (NDIR) CO analyzer. The concentration measurements provided by both the in-situ stack monitoring system and the NDIR analyzer were recorded, and these values agreed relatively well (the in-situ monitor gave a reading of 730 ppmv instead of 779 ppmv). The calibration provided by the manufacturer for the in-situ monitor was not altered, which could have been done to obtain an exact agreement. But this was not considered to be critical for this set of experiments.

The cell was then gradually heated, and the results obtained with both the in-situ monitor and the NDIR analyzer were shown in Fig. 44. The experiments were limited to temperatures below 275°C (530°F), because of the sealant used to fix the sapphire windows to the stainless steel flanges. It can be seen that, while the reading from the NDIR analyzer stayed constant, the measurements obtained with the

in-situ monitor decreased by more than twofold as temperature increased from 20°C to 260°C. This cycle was repeated as the cell was allowed to cool down to room temperature, and the values obtained duplicated very closely those obtained during the heating cycle. It should be noted that the NDIR analyzer measurements are carried out at a constant temperature within the instrument itself, and therefore are not expected to be effected by ambient temperature variations.

The results obtained during these experiments document the sensitivity of the CO concentration measurements, obtained with the in-situ monitor, on the stack gas temperature. This dependence on temperature is due to the variation of the absorption coefficient $K = NQ$, which then affects the infrared light transmission through Beer's Law:

$$T = I/I_0 = \exp(-KL)$$

where T is the transmittance, I and I_0 are transmitted and incident intensities, respectively, and L the optical path. The absorption coefficient could change either due to changes in the molecular number density, N (cm^{-3}), or the absorption cross section, Q (cm^2). The observed reduction in measured absorption, with increasing temperature, could be attributed, to a large extent, to a decrease in the number density, since the pressure was kept constant. This does not, however, account completely for the observed effect. When the data (see Fig. 14) are corrected for density effects, using the ideal gas law, the measured curve still shows a significant drop (18%) in the CO concentration at 260°C. The remaining change has to be attributed to changes in Q, with temperature, over the spectral bandwidth of the absorption measurements. A typical variation of the absorption

coefficient and spectral features are shown in Fig. 45, which has been reproduced from Ref. 23. It can be seen that the dependence on temperature could be quite significant, and it will depend on the bandwidth used for the measurements. This bandwidth was not available, and therefore an accurate estimate of this effect could not be made.

Results obtained with this simple experiment suggest that accurate measurements of CO concentration in stack gases, using line-of-sight infrared absorption techniques, will require an appropriate correction for changes in the stack gas temperature. Even if the temperature does not change over a large range, the instrument has to be calibrated for the appropriate mean gas temperature. Hence, an on-line temperature correction, based on actual stack gas temperature measurements, would be most appropriate to realize the full potential of in-situ CO monitoring systems.

III. CONCLUSIONS

The objective of this study was to provide data on the performance of the two stack gas monitoring systems over a wide range of operating conditions, and to investigate the effect of heat transfer processes on the relationship between the combustion zone properties and stack gas measurements. Two in-situ monitoring systems, a ZrO_2 type O_2 sensor and a CO monitor based on infrared absorption, have been evaluated in the NBS experimental furnace. These instruments are typical of in-situ flue gas monitors that are used for combustion control in industrial boilers and furnaces.

The experiments were designed to compare the measurements obtained with the in-situ CO and O_2 monitors to those obtained with the gas sampling system and to theoretical equilibrium calculations. Furnace conditions varied from a hot highly radiating environment representative of industrial furnaces to a cooler environment representative of industrial boilers. Data were recorded over the equivalence ratio range of 0.75 to 1.05, for both natural gas and No. 2 fuel oil. Interest was centered around the desired region for automatic controls; viz., $100 \leq CO \leq 300$ ppmv, $0 \leq O_2 \leq 2\%$ (excess) and $0.95 \leq \phi \leq 1.0$.

The ZrO_2 type O_2 monitor performed reliably over a long period of time, and provided quite repeatable measurements with an accuracy of 0.25% O_2 over the full range and a sensitivity of about 2% O_2 for a change of 0.1 in equivalence ratio. The instrument, however, did not have a provision for on-line calibration, and the O_2 measurements

were found to be quite sensitive to the air aspiration rate, which controlled the gas sampling rate from the stack. The ZrO_2 sensor provides the capability for operating at high temperatures, nominally 1540°C (2800°F) and below, which is valuable especially for high temperature furnace applications. It also means that this sensor could be located closer to the combustion zone, and provide better time response.

Measurements with the in-situ CO monitoring system could only be carried out where the gas temperatures were more moderate, less than 370°C (700°F). In general, the readings obtained with the in-situ CO monitor were less than half of those obtained with the gas sampling system. This deviation was attributed primarily to the effect of gas temperature on the CO number density, but also partly to the effect of gas temperature on the the CO absorption coefficient. This effect was quantified in a set of experiments carried out in a heated cell. These findings indicate that any accurate measurement of CO concentration in the stack gases, using infrared absorption, will require a simultaneous measurement of gas temperature and compensation of the CO measurements. Additional effects due to CO_2 and water vapor absorption may also be important.

A definite dependence of stack gas composition measurement upon furnace temperature and heat transfer processes was displayed as the furnace heated up over a long period of time. These results indicate that the relationship between combustion fuel/air mixture and stack gas composition is not unique. It will vary as a function of furnace cavity temperature which is affected by physical geometry, burner geometry (and its effect on fuel/air mixing), and by the rate of heat

extraction. The application of stack monitoring systems for combustion control, over the narrow range desired for optimal operation, will require static and/or dynamic allowances for these factors. The characteristics of a particular system should be carefully analyzed prior to implementation of a control system intended to optimize combustion at or near stoichiometric conditions. The results of this study indicate that stack gas monitoring is a valuable combustion control method, when utilized with pre-established setpoints. These setpoints can be expected to be unique for a particular installation and load.

These observations also point towards the need for combustion control systems which do not necessarily rely on stack gas measurements, but rather on measurements made directly in the combustion zone.

REFERENCES

1. Robertson, J.L. and Clarke, P.R., "Microprocessors and Instrumentation in Furnace Control," Industrial Heating, Vol. 48, No. 5, pp. 9-12, May 1981.

2. Richardson, D.M., "Combustion Efficiency through Use of Flue Gas Analyzers," Industrial Heating, Vol. 45, No. 5, pp. 20-21, May 1978.

3. Anson, D., Clarke, W.H.N., Cunningham, A.T.S. and Todd, P., "Carbon Monoxide as a Combustion Control Parameter," Combustion, Vol. 43, No. 9, pp. 17-20, March 1972.

4. Pruce, L.M., "Maximum Boiler Efficiency and Save Fuel with CO Monitoring," Power, Vol. 124, No. 1, pp. 70-72, January 1980.

5. Gilbert, L.F., Sr., "CO Control Heightens Furnace Efficiency," Chemical Engineering, Vol. 87, No. 15, pp. 69-73, July 1980.

6. Spanbauer, J.P., "Energy Savings Through Advanced Boiler Control," paper presented at the 1980 Annual Meeting of the Technical Association of the Pulp and Paper Industry, 1980.

7. Jutila, J.M., "Guide to Selecting Stack Gas Monitors," Industrial Technology, Vol. 27, No. 11, pp. 43-54, November 1980.

8. Gilbert, L.F., "Precise Combustion-Control Saves Fuel and Power," Chemical Engineering, Vol. 83, No. 13, pp. 145-150, June 1976.

9. McArthur, L., Lord, H.C. and Gilbert, L.F., "Efficient Combustion Through Boiler Air-Fuel Ratio Control," Final Control Elements, Vol. 3, 3rd Control Valve Symposium and Process Control Technology, Instrument Society of America, Pittsburg, pp. 101-106, 1977.

10. Hoffman, A.R., "Nature of Platinum-Zirconia Oxygen Sensor," Industrial Heating, Vol, 47, No. 7, pp. 32-33, July 1980.

11. "Considerations for Energy Savings in Design and Use of Continuous Heat Treating Furnaces - Part I - Role of Controls," Industrial Heating, Vol. 48, No. 6, pp. 33-37, June 1981.

12. Shafer, R.V., "Oxygen Measurement and Control for More Efficient Operation of Soaking Pits," Industrial Heating, Vol. 48, No. 8, pp. 14-19, August 1981.

13. Opel, A.E. and Gilbert, L.F., "Closed Loop Source Monitoring Saves Energy and Money," ASME Paper No. 78-WA/APC-6, December 1978.

14. Molloy, R.C., "Microprocessor Based Combustion Monitoring and Control Systems Utilizing In-Situ Opacity, Oxygen, and CO Measurements," presented at the 4th World Energy Engineering Conference in Atlanta, Georgia, Oct. 12-15, 1981 and also presented at the 3rd Annual Industrial Energy Conservation Technology Conference and Exhibition, Houston, Texas, April 26-29, 1981.

15. Hall, E.H., et al, "Evaluation of the Theoretical Potential for Energy Conservation in Seven Basic Industries," Battelle Columbus Laboratory, Report to FEA, January 1975.

16. Hamm, J.R., et al, "Energy Conversion Alternatives Study (ECAS) - Vol. III: Combustors, Furnaces and Low Btu Gasifiers," Westinghouse Electric Corp. Research Laboratories, NASA CR-134941, February 1976.

17. Resource Planning Associates, "Implementation of Energy Conservation Technology in the Pulp and Paper Industry," Report for Office of Industrial Programs, Dept. of Energy, September 1980.

18. Fam, S.S., "Impact on Energy Conservation of Automatic Control Systems Utilization in the U.S. Pulp and Paper Industry," Thermo Electron Rpt. No. TE4265-20-80, 1980.

19. "Basic Research in Engineering - Workshop on Fluid Dynamics and Thermal Processes," Engineering Societies Commission on Energy, Inc., February 1980.

20. "Procedure for the Continuous Sampling and Measurement of Gaseous Emissions from Aircraft Turbine Engines," Society of Automotive Engineers, Inc., ARP 1256, October 1971.

21. Brinkley, S.R., "Computational Methods in Combustion Calculations," Combustion Processes, Sect. C., High Speed Aerodynamics and Jet Propulsion, Vol. 2, edited by B. Lewis, R.N. Pease and H.S. Taylor, Princeton University Press, Princeton, N.J., 1956.

22. Goldman, Y. and Timnat, Y.M., "Study of Liquid Fuel Combustion in Tunnel Burners," Israel Journal of Technology, Vol. 14, Nos. 4-5, pp. 179-186, 1976.

23. "Handbook of Infrared Radiation from Combustion Gases," eds. R. Goulard, and J.A.L. Thompson, NASA SP-3080, 1973.

24. Young, S.B., "High Temperature Waste Heat Recovery Systems for Forge and Other Furnaces," Industrial Heating, Vol. 47, No. 7, pp. 16-18, July 1980.

APPENDICES

APPENDIX A

DESCRIPTION OF THE EXPERIMENTAL FURNACE FACILITY

The experimental facilities installed at the National Bureau of Standards include a pilot-scale industrial furnace (see Fig. 46), a complete gas sampling/analysis system and an automatic data acquisition and processing system.

The Experimental Furnace

The experimental furnace has a combustion chamber, with the internal dimensions of 80 cm (W) x 110 cm (H) x 240 cm (L). A single burner fires horizontally through one end into the combustion chamber. The combustion products exhaust from the opposite end of the chamber, past a recuperator, and then up through the stack. The furnace walls are made up of lightweight castable refractory and insulation materials, anchored to a steel outer wall. The exit of the furnace is formed by a curtain wall, which is perforated to allow for passage of the gases. The plenum between the curtain wall and the insulated side and end walls serves as a passage for exhaust gases to the recuperator (Fig. 1).

The experimental furnace has a rated capacity of 300 kw (1×10^6 BTU/hr). At steady state, the outer wall temperature is designed to stay below 70°C (160°F) when the chamber temperature reaches 1350°C (2460°F). The furnace is sealed with high temperature RTV silicone caulking compound in order to reduce furnace leakage. Several ports

are located along both furnace side walls and the downstream end wall (Fig. 47). These ports permit visual observation of the flame, the introduction of intrusive probes and provides an optical path across the furnace. Fig. 1 indicates the location of each access port.

A Transjet burner, designed by Hague International [24], is fitted into a 32.5 cm (12.8 in) diameter corbel which is cast from high temperature alumina and sits normal to the front end face of the furnace. The burner is capable of withstanding a combustion air inlet temperature of 900°C (1650°F). The burner (Fig. 48) is designed to recirculate and entrain combustion products with incoming fresh combustion air, thereby enhancing flame stability. The burner air passageways are thermally insulated in order to accomodate the high inlet air temperatures.

Either natural gas or No. 2 fuel oil can be supplied to the burner. An exchange of nozzles and fuel feed lines is required to convert the burner from one fuel to another. The central core of the burner serves to house the fuel and atomizing air lines, the electric spark ignited pilot flame and the Fireye ultraviolet flame sensor.

The atomizing compressed air is regulated to a pressure of 100 KPa (15 psig) and a volumetric flow rate of approximately 450 l/min (16 ft^3/min). This air is mixed with the liquid fuel, externally, immediately downstream of the nozzle head. The No. 2 fuel oil is supplied at approximately 55 KPa (8 psig) and can reach a maximum volumetric flow rate of 0.48 l/min (7.6 gph). There are 8 fuel outlets in the nozzle head which allow the atomizing air to flow tangentially around the adjacent fuel openings. For natural gas, fuel is expelled radially outward through 8 openings which are located around the head

of the gas supply line. Natural gas is supplied at 14 KPa (2 psig) with a maximum volumetric flow rate of 510 l/min (18 ft^3/min).

Cooling air is bled from the combustion air blower and passed around the fuel injector in order to reduce thermal decomposition of the fuel. The cooling air flow is 255 l/min (9 ft^3/min) at a pressure of 2.5-3.5 KPa (10-14 in H_2O), which accounts for about 1% of the air blower capacity. A refractory stabilizer plate, which surrounds the cooling air passageway inside the burner, provides a separation between the preheated combustion air and the fuel supply line.

Combustion stability is enhanced by holes located on the downstream face of the stabilizer plate which generate hot combustion gas recirculation. An electrically ignited pilot is used to fire the main flame. The Fireye sensor is used to check for flame ignition and continued combustion. During flame shutdown, compressed purge air is provided at 21 KPa (3 psig) in order to remove any residual fuel in the fuel line.

The recuperator is designed to preheat incoming combustion air before reaching the burner. A ceramic heat exchanger, containing 30 silicon carbide tubes, is the main component of the recuperator which is capable of withstanding long term exposure to gas temperatures of 1550°C (2820°F), (see Fig. 49). The heat transfer elements of the recuperator are of a tubular configuration with an enhanced heat transfer surface on both the exterior and interior of the tube. The external surface area is increased by means of a spiral wound fin and the internal bore is enhanced by longitudinal fins. The tubular

elements are nested together and arranged to provide the optimum transfer of heat between the outgoing flue gases and the incoming combustion air. The tubes are provided with seals to minimize incoming combustion air losses due to leakage.

The ceramic elements are arranged to provide one cross-flow pass on the exhaust gas side and one pass through the tubes on the combustion air side. Metal tubes are used to bring the combustion air to the ceramic elements inside the recuperator which are held in place by adapters and compression springs. At the exit, heated combustion air is passed from the ceramic elements through short metallic tubes to an insulated header. Inlet temperatures of 274°C (525°F) have been achieved for furnace gas temperatures of approximately 882°C (1620°F). This corresponds to flue gas temperatures of 735°C (1355°F) entering the recuperator and 404°C (760°F) leaving the recuperator. The furnace gas temperature is measured by a Pt-Pt/10% Rh (S-type) thermocouple stationed in front of the furnace load probes. Chromel-alumel (K-type) thermocouples are located at several sites along the recuperator's 28 cm diameter exit duct. This passageway is insulated so that heat losses from the combustion air are minimized.

A pneumatically controlled stainless steel high temperature damper located inside the stack is used to maintain positive furnace pressure during experiments. Typical furnace overpressures of 0-50 Pa (0-0.2 in H_2O) are required to prevent air infiltration into the combustion chamber.

A 4kw (5hp) turbo-blower supplies combustion air from the surroundings to the burner. The blower has a rated maximum capacity of 23,100 l/min (49,100 ft^3/hr) at 6.9 KPa (16oz/in^2) gauge pressure.

copper-constantan (T-type) thermocouple and the line pressure is measured by a pressure transducer in order to correct the oil flow for viscosity effects.

Commercially supplied natural gas (96.9% CH_4, 2% C_2H_6, 1.1% others) is pressure regulated down to 14 KPa (2 psig). Some of this gas is tapped off to the pilot burner before the gas reaches a manual reset and motorized shut-off valve train which is used for gas flow control. As a safety feature, low and high gas pressure switches set pressure limits for the shut-off valve. The volumetric flow rate is read from a rotameter (max: 510 l/min CH_4 at 21°C, 100 KPa) while a laminar flow device (max: 565 l/min at ΔP = 2 KPa, for flow conditions at 21°C and 100 KPa) and a pressure transducer provide the output signal to the DAS. Flow control is accomplished in the same way described for the No. 2 fuel oil supply; i.e., with a prove switch, motorized valve and cam, and a solenoid valve. The line gas temperature is measured with a T-type thermocouple.

Heat extraction from the furnace is achieved with a variable thermal load heat exchanger consisting of two water-cooled 25.4 cm (10 in) diameter stainless steel tubes, passing vertically downward through the furnace roof at a station 170 cm downstream of the burner. Water is supplied to the system at a pressure of 210 KPa (30 psig) before passing through a filter. The volumetric flow rate is controlled downstream of the filter with a pneumatic actuator and valve. The flow rate is measured by a stainless steel orifice plate with a 1.3 cm (0.527 in) bore. The output is read by a flow gauge having a maximum flow of 38 l/min (10 gpm).

The water supply is split into 2 segments, one supply line for each heat exchanger probe. Each leg contains a ball valve, a turbine flowmeter which provides a flow reading for the DAS, and copper-constantan (T-type) thermocouples which are placed on both the upstream and downstream sides of the thermal load cells.

Gas Sampling and Analysis System

A complete on-line gas analysis system is used for combustion gas sampling and analysis (Fig. 51). A water-cooled sampling probe was fabricated as shown in Fig. 52. The probe has a 1.27 cm (0.5 in) diameter hemispherical stainless steel head and shaft, with a water-cooled jacket covering the gas collection channel. The 0.11 cm (0.043 in) inlet diameter is designed to choke the flow at temperatures above 260°C (500°F) for gas suction at 0.2 l/min (0.5 ft^3/hr). The 84 cm (33 in) long probe which is situated at the far end furnace wall below the recuperator (Fig. 53), is designed to reach the curtain wall.

The gas sample is delivered to a heated metal bellows vacuum pump through a 460 cm (15 ft) section of heated line. The vacuum pump operates at 14 l/min (0.5 ft^3/min) for a bellows speed of 1725 rpm. A second uncooled probe was also used to sample effluents below the recuperator and inside the stack. The gas sample is then delivered through a 1070 cm (35 ft) section of heated line to the analyzer manifold. The heated lines and the vacuum pump are maintained above 150°C (300°F) in order to prevent condensation of hydrocarbons and water vapor. The line and pump temperatures are continuously monitored

and controlled by temperature controllers (max: 300°C). The pump manifold temperature is measured with a bi-metallic thermometer (max: 300°C) and the pump pressure is read from a 76 cm Hg (30 in Hg) vacuum gauge. A nitrogen purge system is used to clear the probe, heated lines and the analyzer manifold of large particulates whenever the gas sample flow is significantly reduced. Two electro-mechanical valve actuators are used to control the flow of gases through the manifold (see Fig. 54).

The gas sample is delivered to the gas analyzers which are connected in parallel. The sample first enters a flame ionization detector (F.I.D.) type total hydrocarbon analyzer which provides a wet reading. The manifold then leads into a stainless steel gas dryer (Permapure) used to remove any water vapor present in the sample by permeation distillation through a plastic tube bundle, and to prevent the interference of water vapor inside the non-dispersive infrared CO and CO_2 analyzers. Compressed air is introduced into the dryer and used to carry the water vapor out of the system via an 8 l/min rotameter. The resulting dry gas is then introduced into the CO, CO_2, O_2, NO/NO_x and SO_2 analyzers. The flow rates through each analyzer are carefully monitored by rotameters placed upstream of each instrument. Unused sample gas is finally bypassed into the sample dump manifold.

The Beckman Model 402 hydrocarbon analyzer utilizes the flame ionization method of detection (F.I.D.) for determining total hydrocarbon concentration. The sensor is a burner in which a regulated flow of sample gas is passed through a H_2/O_2 flame sustained by regulated flows of compressed air and 40% H_2/N_2 fuel. The fuel and air pressures are adjusted to 172 KPa (25 psig) and 103 KPa (15 psig),

respectively. Seven ranges of concentration are provided with the instrument; viz., 10, 25, 100, 250, 1000, 2500, 10000 ppmv. Both speed and magnitude of the analyzer response are affected by the type of hydrocarbon being sampled. The system is therefore calibrated with hydrocarbons that are representative of those to be sampled. Propane is used as the reference span gas and compressed air is used to zero the instrument. The sample gas is supplied to the burner at a regulated pressure of 21 KPa (3 psig) and a flow rate of 1.9 l/min (4 ft^3/hr) as measured by the F.I.D. sample bypass rotameter.

A Thermo Electron (TECO) Model 10AR chemiluminescent NO/NO_x gas analyzer is used to determine the concentration of nitrogen oxides (NO, NO_2) in the sample. The monitor provides 8 linear, full-scale ranges including 0-2.5, 0-10, 0-25, 0-100, 0-250, 0-1000, 0-2500 and 0-10,000 ppmv. Calibration gases include compressed air for zero gas and NO/N_2 mixture for calibrating the instrument. The sample and calibration gas flow rate is 1.2 l/min (2.5 ft^3/hr).

The Beckman Model 755 oxygen analyzer measures the paramagnetic susceptibility of oxygen. This susceptibility is much higher for oxygen than other common gases. The instrument measures the total magnetic susceptibility of the sample. This total is almost entirely due to the oxygen present, so the measurement gives an accurate indication of oxygen content. The unit is supplied with 4 switch-selectable ranges, 0-1, 0-2.5, 0-5 and 0-10% oxygen. The calibration is accomplished with O_2/N_2 span gas mixture and nitrogen is used to zero the instrument. Calibration and sample gases flow through the analyzer at 0.3 l/hr and are monitored using a rotameter (max: 0.9 l/min at 21°C and 100 KPa).

A Thermo Electron (TECO) Model 40 SO_2 pulsed fluorescence analyzer is available to carry out measurements of SO_2, when necessary. The instrument provides 5 ranges; 0-50, 0-100, 0-500, 0-1000 and 0-5000 ppmv SO_2. Zero adjustment of the analyzer is accomplished with nitrogen, and SO_2/N_2 span gas mixture is used to calibrate the instrument. Recommended sample and calibration gas flow rates are 0.9-3.8 l/min (2-8 ft^3/hr).

Two Beckman Model 865 non-dispersive infrared (NDIR) analyzers are used to measure CO and CO_2 concentrations in the sample gas. The CO analyzer has one sampling cell and provides 3 scales, 0-1000, 0-2000, and 0-5000 ppmv CO. The instrument is zero adjusted with nitrogen and calibrated with CO/N_2 span gas mixture. The CO_2 analyzer is also a single cell unit having 3 ranges which include 0-5, 0-10 and 0-20% CO_2. It uses nitrogen for zero gas and CO_2/N_2 mixture for span gas. Each range on both instruments has a nonlinear response and are used with appropriate calibration curves. Required sample and calibration gas flow rates are 0.5-0.9 l/min (1-2 ft^3/hr) which is measured using a rotameter.

Response characteristics and linearity of the individual analyzers are investigated using a Thermo Electron Model 900 heated sampler. This dilution apparatus provides a means for filtering and diluting a gas of known concentration at a specific rate and then introducing the diluted gas to the analyzers. The instrument accurately blends dry air with the sample in order to reduce the dew point and prevent condensation at room temperature. The sample flow rate is approximately 3.3 l/min (7 ft^3/hr) at 69 KPa (10 psig). This is an especially useful diagnostic tool because it enables the determination

of instrument response characteristics over a wide concentration range.

All analyzers are checked and calibrated prior to start of and during a test sequence. The calibration gases are brought to a patch panel located near the analyzers. The various gases are connected to the analyzers with quick disconnects and eliminate the need for intricate valving. Excess dry sample gases are bypassed from the system through a rotameter (max: 8 l/min).

Data Acquisition System (DAS)

The Digital Equipment Corp. (DEC) PDP 11/60 minicomputer based data acquisition and control system (Fig. 55) is used to monitor and record the many instrument variables involved in operating the furnace during experiments which often run several hours. Since the computer facility is located 610 m (2000 ft) away from the furnace, a Remote Industrial Control (ICR) I/O subsystem is used to interface the process instrumentation and control signals to the minicomputer. The ICR contains an analog to digital converter board and has multiplexing for 40 differential input channels. System gains of 1000, 200, 100, 50, 20, 10, 2 and 1 are available to the user. The A/D converter has a scan rate of 200 samples per second when scanning all the channels. The following furnace input and output parameters are converted and entered into the computer mass storage: coolant water flow, air flow, natural gas and oil flows, and stack emissions by the gas sampling system (CO, CO_2, O_2, SO_2, NO/NO_x and total hydrocarbons).

A Fluke Model 2240B data logger is used to process and record the various furnace temperatures. It presently uses 40 channels for analog input data. With the A/D converter the data acquisition rate is

approximately 13-15 channels/sec when remotely connected to the minicomputer. A high performance A/D converter is used for the temperature measurements to obtain 1 μv resolution on the 40 mv range for low level S-type thermocouples.

The Fluke data logger is compatible with T, K, R and S type thermocouples. Automatic reference junction compensation corrects over the temperature range 0°-50°C (0-120°F). Typical system accuracy for fast scan temperature measurements is: ±0.6°C for K-type, ±0.5°C for T-type, ±1.4°C for R-type and ±1.4°C for S-type thermocouples.

During an experiment the acquired data is temporarily stored on the DAS disk system. After completion of the test the raw data is processed and transferred to a Kennedy 75 ips, 9 track, 800 or 1600 bpi magnetic tape transport system. A Versatec high speed printer/plotter is used for hard copy listings of program files and for plotting experimental results.

APPENDIX B

DESCRIPTION OF THE IN-SITU O_2 AND CO MONITORS

In-Situ Oxygen Analyzer

An in-situ O_2 monitor, with an yttria stabilized zirconia tube probe, is located at the far end wall of the furnace and is used to monitor excess oxygen content of the stack gases (see Fig. 56). The probe consists of zirconium oxide (ZrO_2) high temperature solid electrolyte ceramic material shaped like a test tube. Two porous platinum electrodes coat the inside and outside surfaces of the zirconia substrate and conduct electricity by means of oxygen ion transport across the cell. The platinum acts as a catalyst to help promote the electrochemical reaction. A cross section of the monitor is shown in Fig. 57.

The monitor continuously measures excess O_2 in the stack and, if desired, trims the concentration to a preset level that ensures maximum combustion efficiency and fuel savings. The oxygen concentration of stack gases is sensitive to naturally varying conditions in the fuel and air flows such as fuel and air temperature, pressure, specific gravity, calorific value, barometric pressure and humidity. In order to ensure that no unburnt fuel is carried through the stack, most combustors operate with excess air. This air leaves the stack, however, at high temperatures, thereby wasting useful energy. Improved efficiency can be achieved by reducing the level of excess O_2 and by maintaining this level within strict limits. A Readout/Control cabinet

provided with the ZrO_2 cell enables one to compare the stack O_2 content to the desired preset level and maintain this level by trimming the fuel/air ratio.

Oil-free air is generally used as a reference gas since the oxygen content of air is normally constant at sea level (20.9% O_2). When this air comes in contact with the inner probe surface, the oxygen is converted to $O^=$ while removing electrons from the ZrO_2;

$$O_2 \rightarrow 2\ O$$

$$2\ O + 4\ e^- \rightarrow 2\ O^=.$$

The ions travel through the probe to the outer surface where oxygen from the flue gases is at a lower concentration. A similar but opposite reaction occurs on this surface where $O^=$ changes back to oxygen and free electrons;

$$2\ O^= \rightarrow 2\ O + 4\ e^-$$

$$2\ O \rightarrow O_2.$$

As the oxygen concentration on both surfaces varies, so do their reaction rates. The differential transport of ions and electrons give rise to an electrical potential between the two surfaces. As the ions deposit their electric charge on the inner and outer surfaces a voltage builds up between the two electrodes and inhibits the flow of ions through the cell wall. An equilibrium is reached when the voltage across the electrodes exactly balances the driving force caused by the difference in oxygen concentration across both faces of the probe. The resulting voltage is given by the Nernst equation;

$E = kT \ln (P_2/P_1)$

where $k = 2.15 \times 10^{-5}$ (V/°K)

T = temperature (°K)

P_2 = oxygen partial pressure on the reference side of the cell

(20.9% for air)

P_1 = oxygen partial pressure on the sample side of the cell.

In addition to the O_2 concentration on both surfaces of the probe, the voltage is also dependent upon the absolute temperature of the sensor. In order to ensure good ion conduction across the cell, the sensor temperature must be in the range 650-1000°C (1200-1900°F). At lower temperatures, operation can be sluggish and at higher temperatures, operating life can be significantly reduced due to reduced chemical stability of the electrodes. The probe is designed to withstand temperatures of 1500°C (2800°F) for extended periods.

The operating temperature of the probe is 704°C (1300°F). This temperature is maintained by a ceramic oven which surrounds the cell. The heater also serves to keep the flue gas hot and to burn away any combustible material around the cell. Uncontrolled sooting can be detrimental to proper sensor operation. The cell temperature is sensed by a K-type thermocouple. When the temperature falls 3°C (5°F) below the specified oven temperature, the heater is turned on and power is supplied to the cell heater element. A light on the Readout/Control panel is used to indicate when the heater is operating.

The sensor probe uses an aspirating extraction technique, based on the Venturi principle, to transport the sample gas from the probe inlet to the sensing cell. Air at 25.4 cm (10 in) H_2O gauge pressure flows past a tube leading from the cell cavity. This draws air up through

the tube to the aspirating air outlet which in turn causes flue gas to flow down the sampling tube to the sensor. The silicon carbide sampling tube is a straight passageway lined with mullite capable of withstanding the high flue temperatures.

The Readout/Control cabinet has 4 major functions. It gives a readout from the sensor in % volume excess O_2 on a wet gas basis, controls the sensor cell temperature as indicated by the panel light, generates a process control signal by comparing cell output to the setpoint and permits selection of setpoints and modes of operation. Printed circuit boards in the cabinet are used to provide power for all the electronics, to amplify the probe signal, to control the probe heater and to determine fuel/air ratio trim control. A meter zero knob on the cabinet panel compensates for the small off-set voltage from the cell when it is exposed to air on both surfaces. When the unit is switched to calibrate mode, the control function is disabled and the meter can then be corrected with the zero knob in order to match the O_2 concentration with the calibration gas (generally atmospheric air = 20.9% O_2).

In-Situ Carbon Monoxide Analyzer

The in-situ CO monitor (Fig. 58) is an infrared device that uses a high resolution absorption spectroscopy technique to measure CO in the range of 0-1000 ppmv. An infrared beam of light is transmitted from a light source compartment across a stack or duct to a detector compartment on the opposite side. The minimum required beam path length is 91 cm (3 ft). An infrared globar light source emitting a wide beam of polychromatic light is mechanically chopped at a frequency

of 63 Hz and collimated before being transmitted through a sapphire window interface and across the furnace stack to a duplicate sapphire window and collecting mirror on the detector side. Blowers with a flow capacity of 1450 l/min (51 ft^3/min) protect the sapphire windows from combustion products, soot and high stack temperatures. The detector cell collecting mirror directs the attenuated beam into a wavelength discrimination module which employs a gas cell correlation technique.

The light beam is passed through a rotating wheel containing three sealed gas cells (Fig. 59). One chamber contains 100% CO, the second has 100% N_2, and the third is filled with approximately 10% CO. A narrow band filter (transmitting at approximately λ = 4.7 μm) located in front of the beam detector allows only the CO sensitive portion of the infrared spectrum that is not absorbed by the stack emissions to pass. The intensity at this wavelength from each discriminator gas cell is transmitted to an electronically cooled lead-selenide detector.

Each signal is amplified and transmitted via a signal cable to the control room module. After the signals are again amplified and fed into an analog/digital converter, the resulting digital signal is passed into an Intel 8085 microprocessor. The microprocessor is programmed to measure the difference between the signal level from the nitrogen cell and the signal from the CO chambers. The flue gas CO concentration is then computed from the ratio.

The instrument calibration is checked by comparing the indicated CO level to a preset check value of 780 ppmv CO which is based on a 91 cm (3 ft) path length. The zero adjustment must be set initially for no measurable CO concentration. The calibration can be checked at any

time by adding 780 ppmv to the present CO level as long as the sum is below 1000 ppmv and the zero setpoint has not been changed.

Using an oscilloscope the peak to peak signal voltage from each cell can be monitored as illustrated in Fig. 60. The voltage level should be 2.0±0.5 V, through the 100% N_2 chamber (cell#1). The voltage can be adjusted with the detector amplifier located above the cell discriminator wheel. When the signal level drops below 1.0 V the opacity in the stack is 80% or greater and insufficient light is transmitted across the stack. The CO level will then read off scale. Warning lights will also indicate when data from the detector or to the microprocessor are invalid.

APPENDIX C

FIGURES

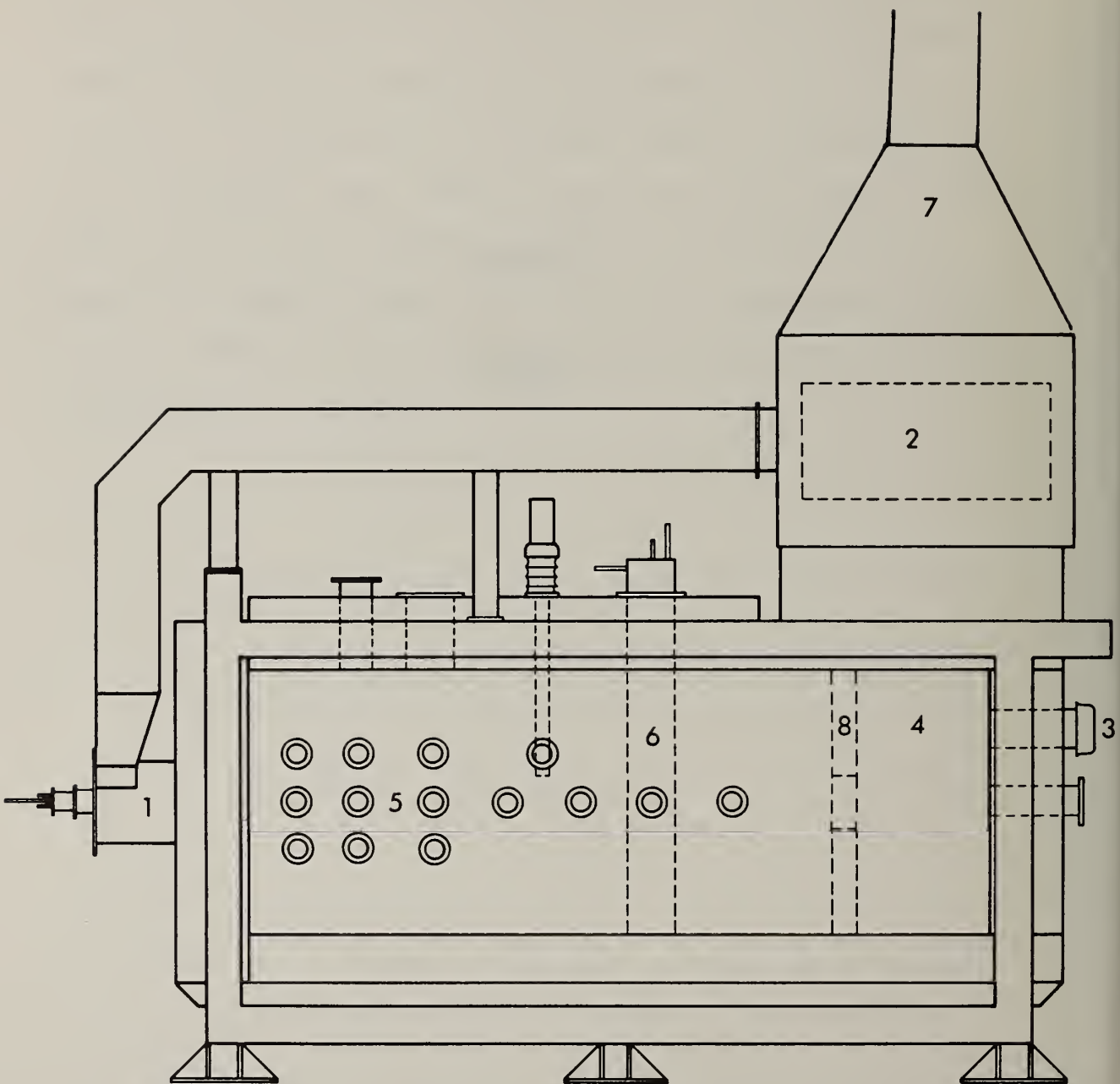

Fig. 1 - NBS Experimental Furnace : 1) Burner; 2) Recuperator; 3) Location of in-situ O_2 monitor; 4) Location of in-situ CO monitor below recuperator; 5) Combustion chamber portholes; 6) Heat exchanger probes; 7) Location of in-situ CO monitor in the stack; 8) Curtain wall.

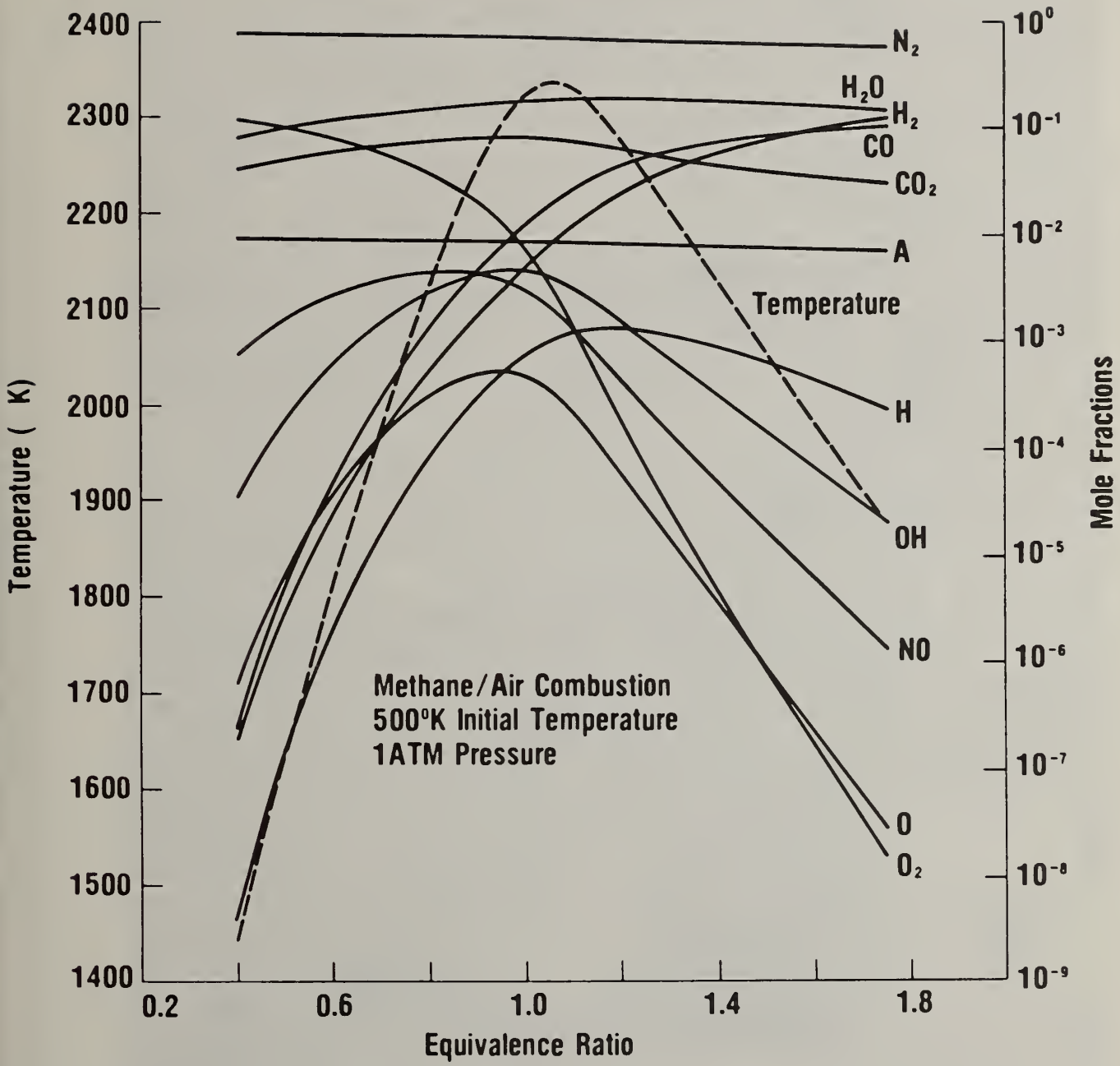

Fig. 2 - Typical results of equilibrium calculations for adiabatic flames.

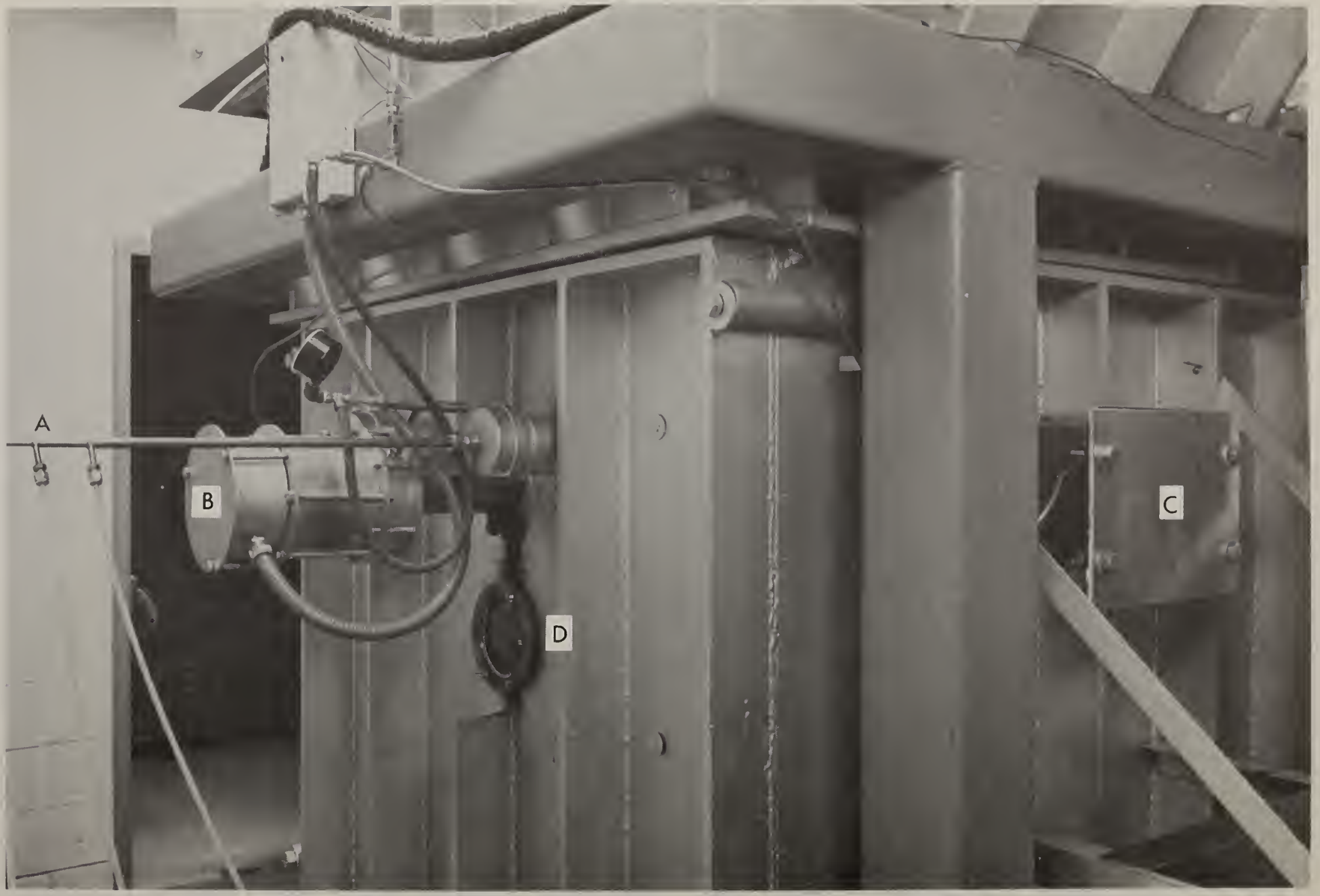

Fig. 3 - Location of gas sampling probe (A), in-situ O_2 monitor (B), flange where CO monitor was installed below the recuperator (C), and porthole of the furnace end wall (D).

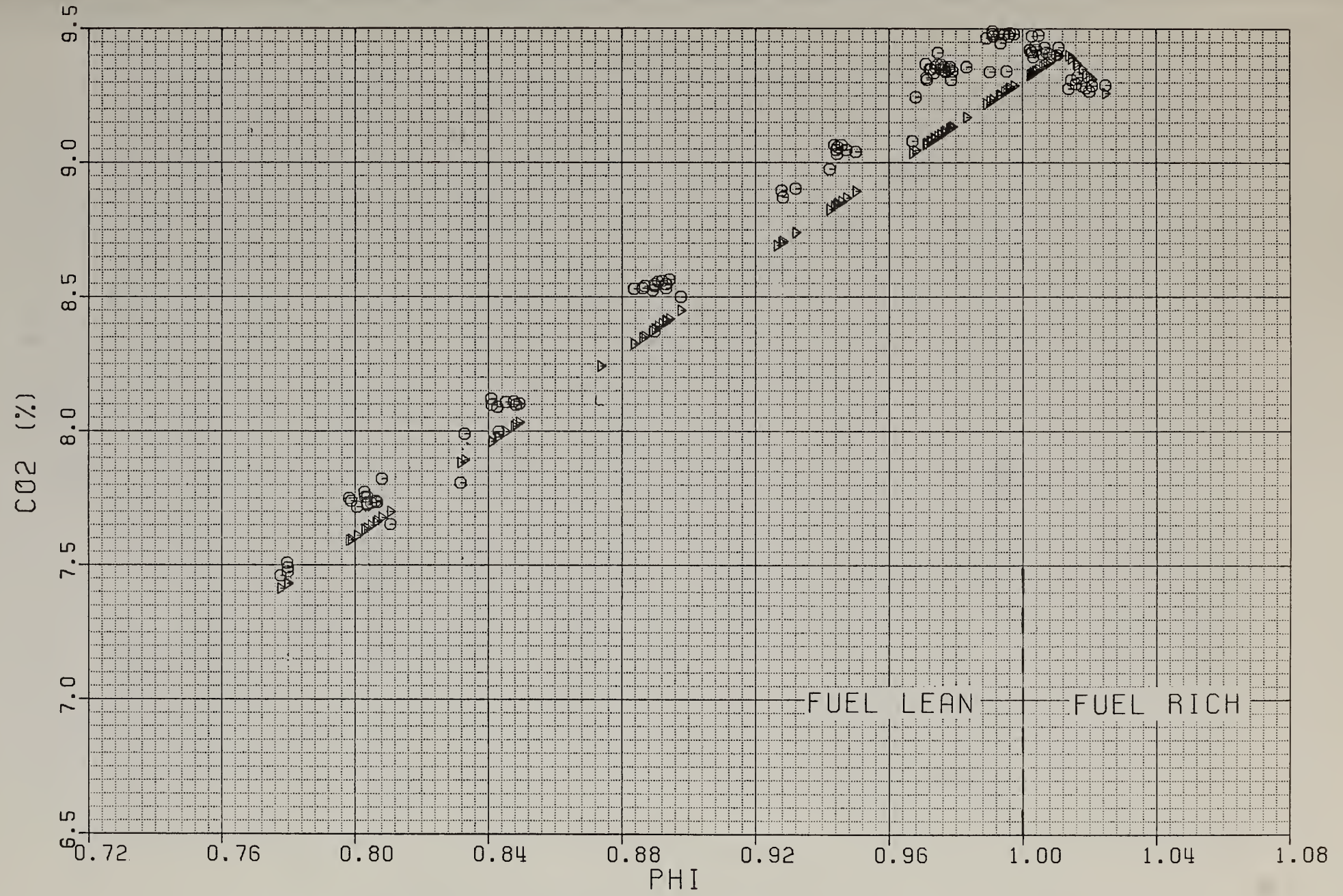

Fig. 4 - Variation of CO_2 concentration with equivalence ratio; Fuel = Natural Gas; Sampling below recuperator; (o - Gas Sampling; Δ - Equilibrium Calculation Based on Stack Temperature).

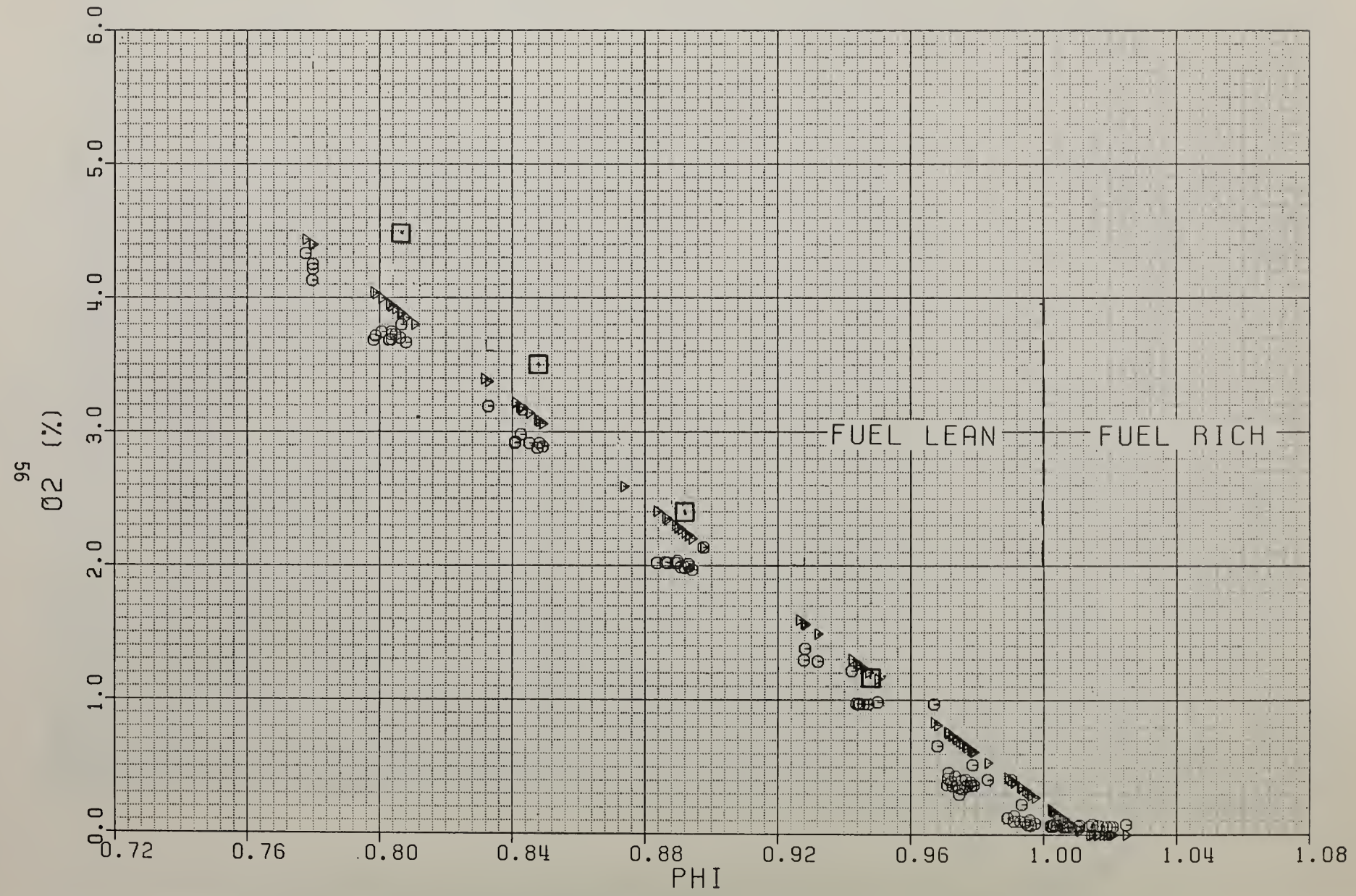

Fig. 5 - Variation of O_2 concentration with equivalence ratio; Fuel = Natural Gas; Sampling below recuperator; (o - Gas Sampling; Δ - Equilibrium Calculation Based on Stack Temperature; □ - In-Situ Monitor).

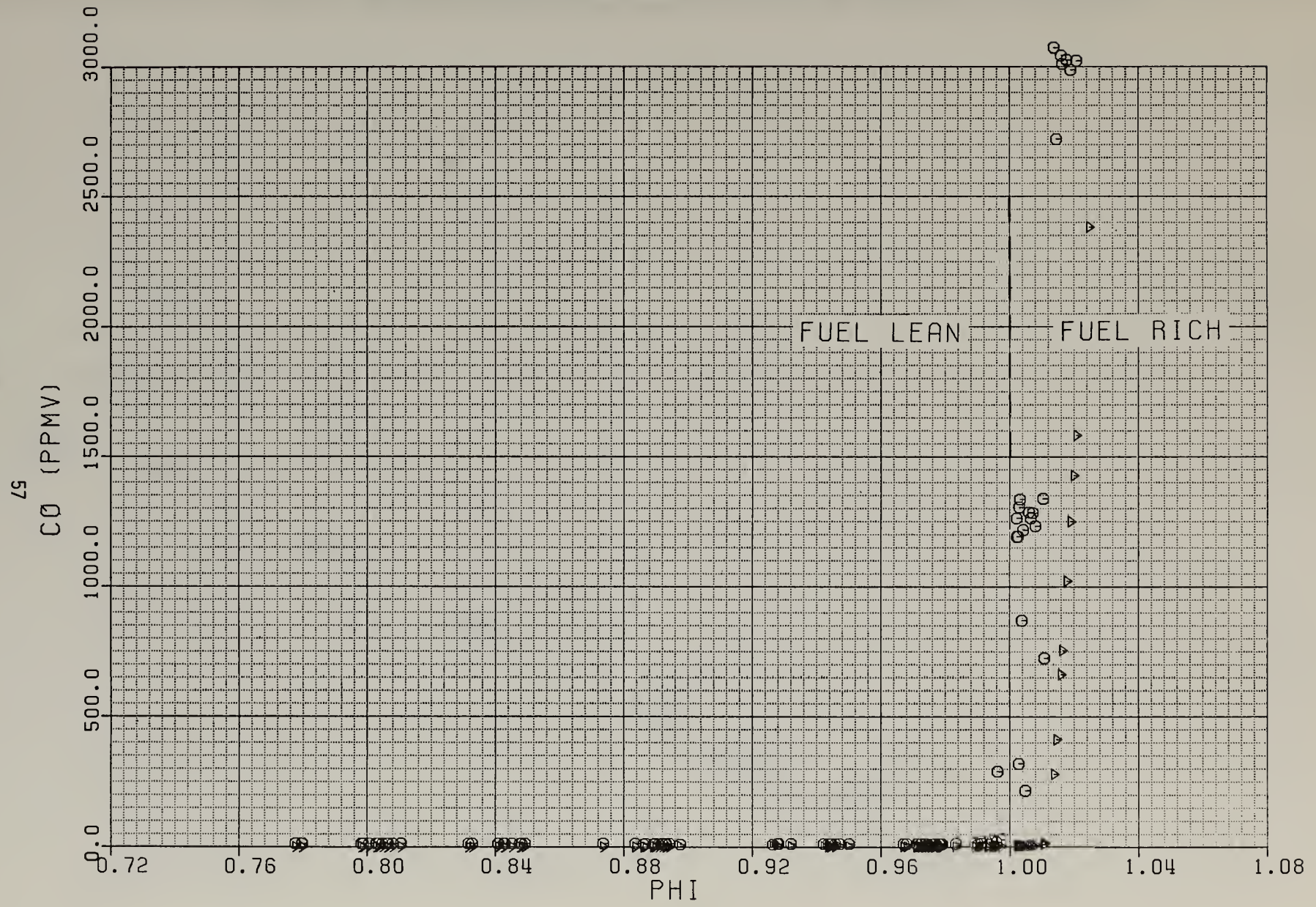

Fig. 6 - Variation of CO concentration with equivalence ratio; Fuel = Natural Gas; Sampling below recuperator; (o - Gas Sampling; Δ - Equilibrium Calculation Based on Stack Temperature).

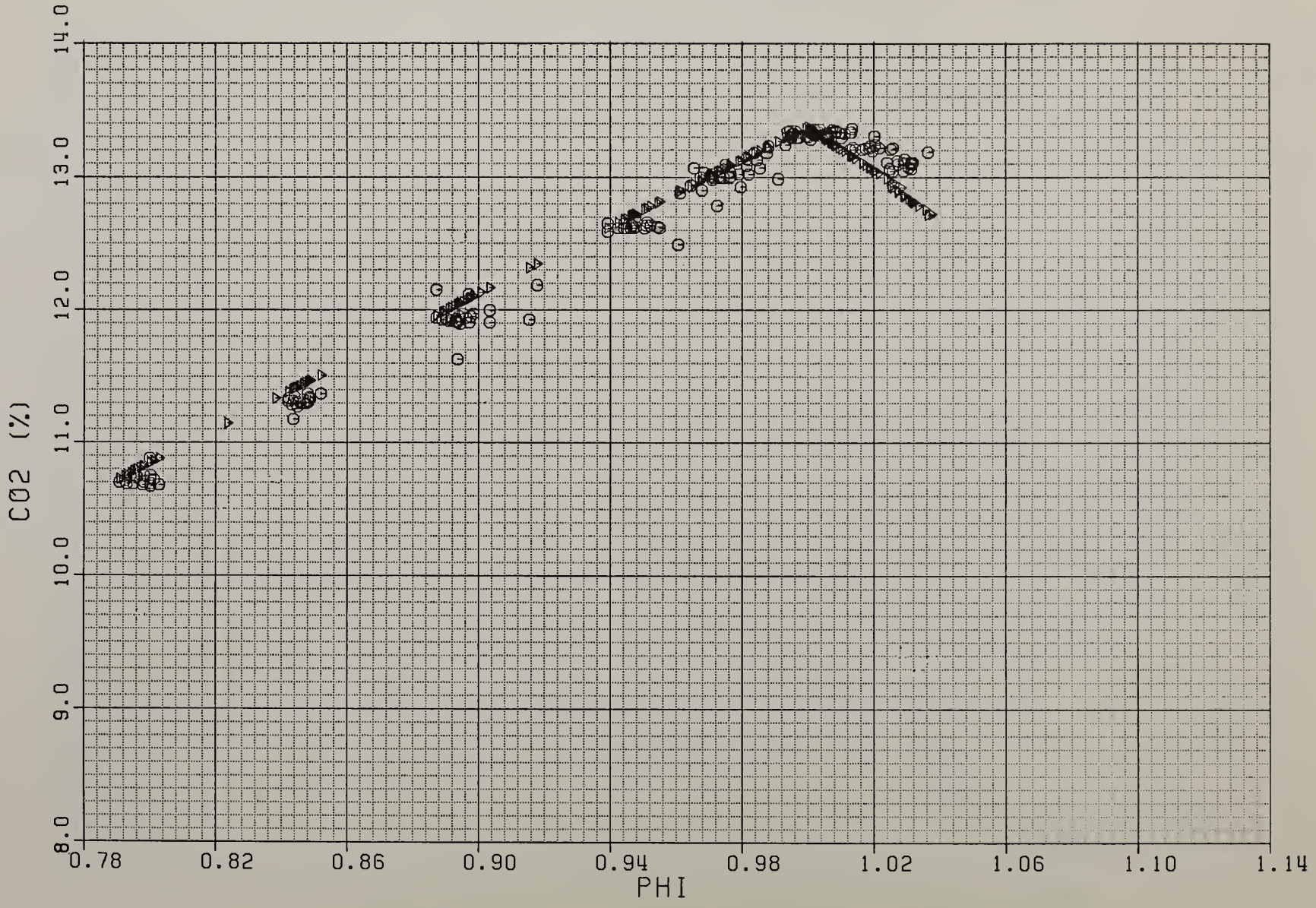

Fig. 7 - Variation of CO_2 concentration with equivalence ratio; Fuel = No. 2 Fuel Oil; Sampling below recuperator; (o - Gas Sampling; Δ - Equilibrium Calculation Based on Stack Temperature).

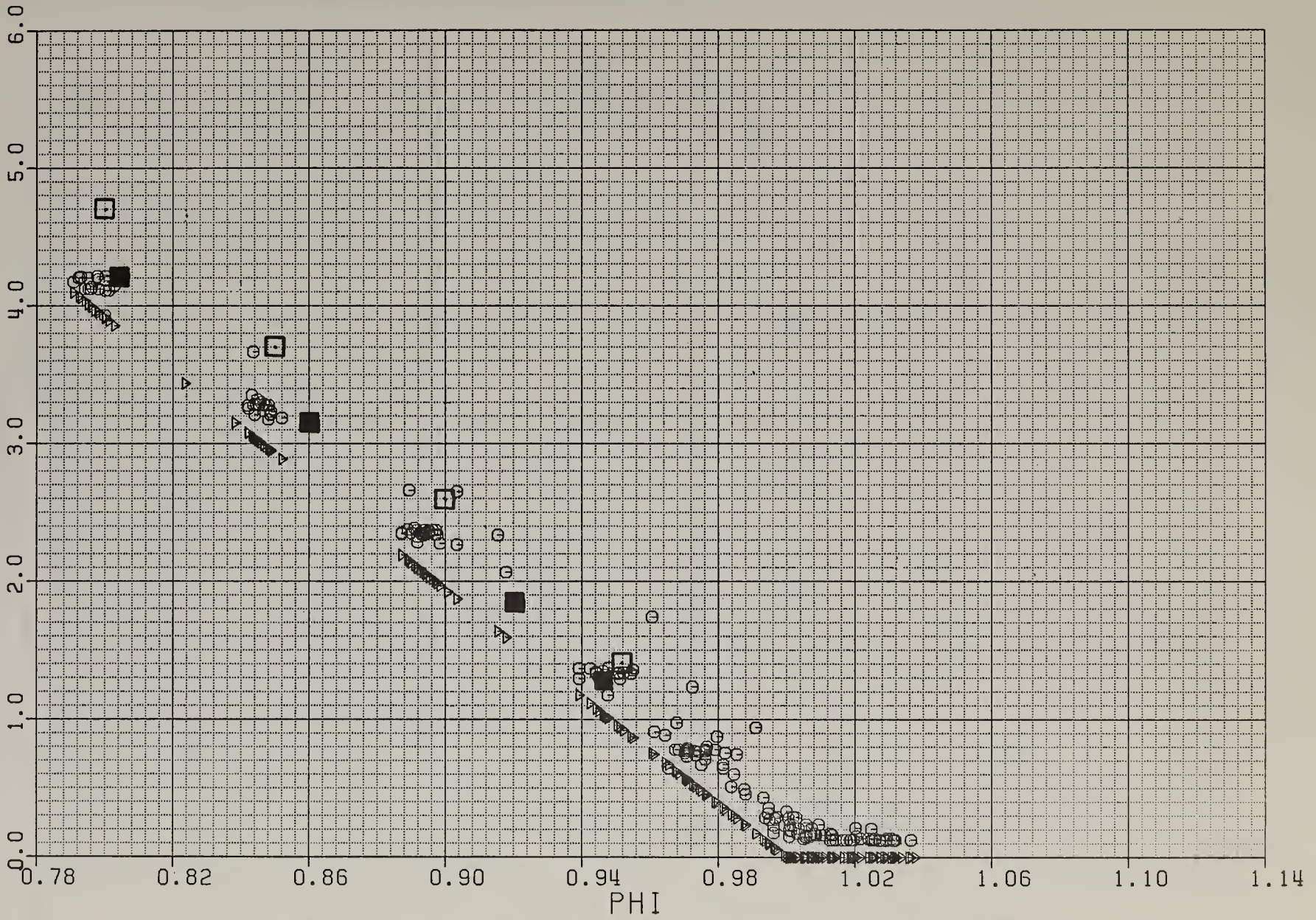

Fig. 8 - Variation of O_2 concentration with equivalence ratio; Fuel = No. 2 Fuel Oil; Sampling Below recuperator; (o - Gas Sampling; Δ - Equilibrium Calculation Based on Stack Temperature; □ - In-Situ Monitor - Sample 1; ■ - In-Situ Monitor - Sample 2).

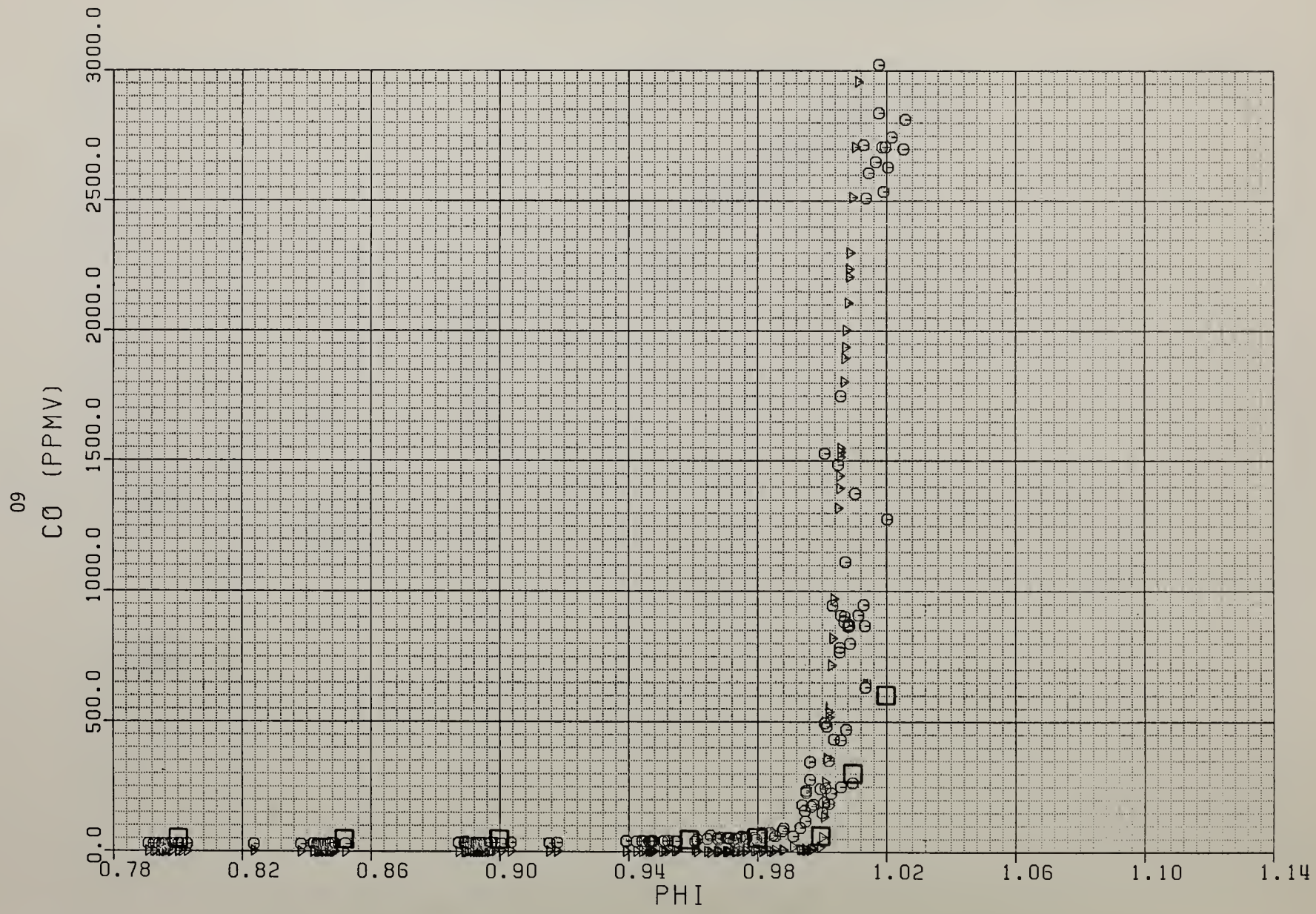

Fig. 9 - Variation of CO concentration with equivalence ratio; Fuel = No. 2 Fuel Oil; Sampling below recuperator; (o - Gas Sampling; Δ - Equilibrium Calculation Based on Stack Temperature; □ - In-Situ Monitor).

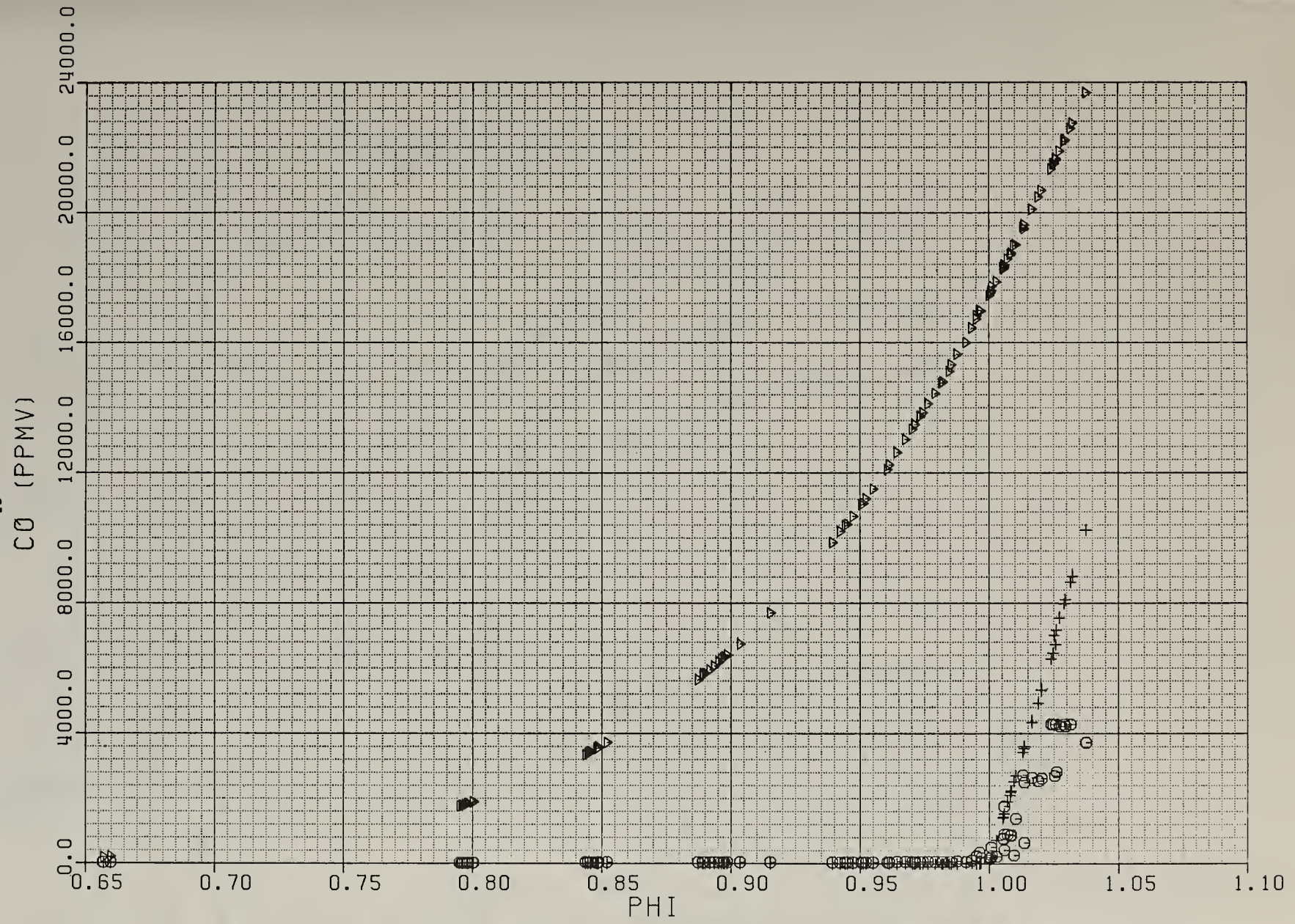

Fig. 10 - Variation of CO concentration with equivalence ratio; Fuel = No. 2 Fuel Oil; Sampling below recuperator; Included are CO equilibrium levels based on flame temperature; (o - Gas Sampling; + - Equilibrium Calculation Based on Stack Temperature; Δ - Equilibrium Calculation Based on Flame Temperature).

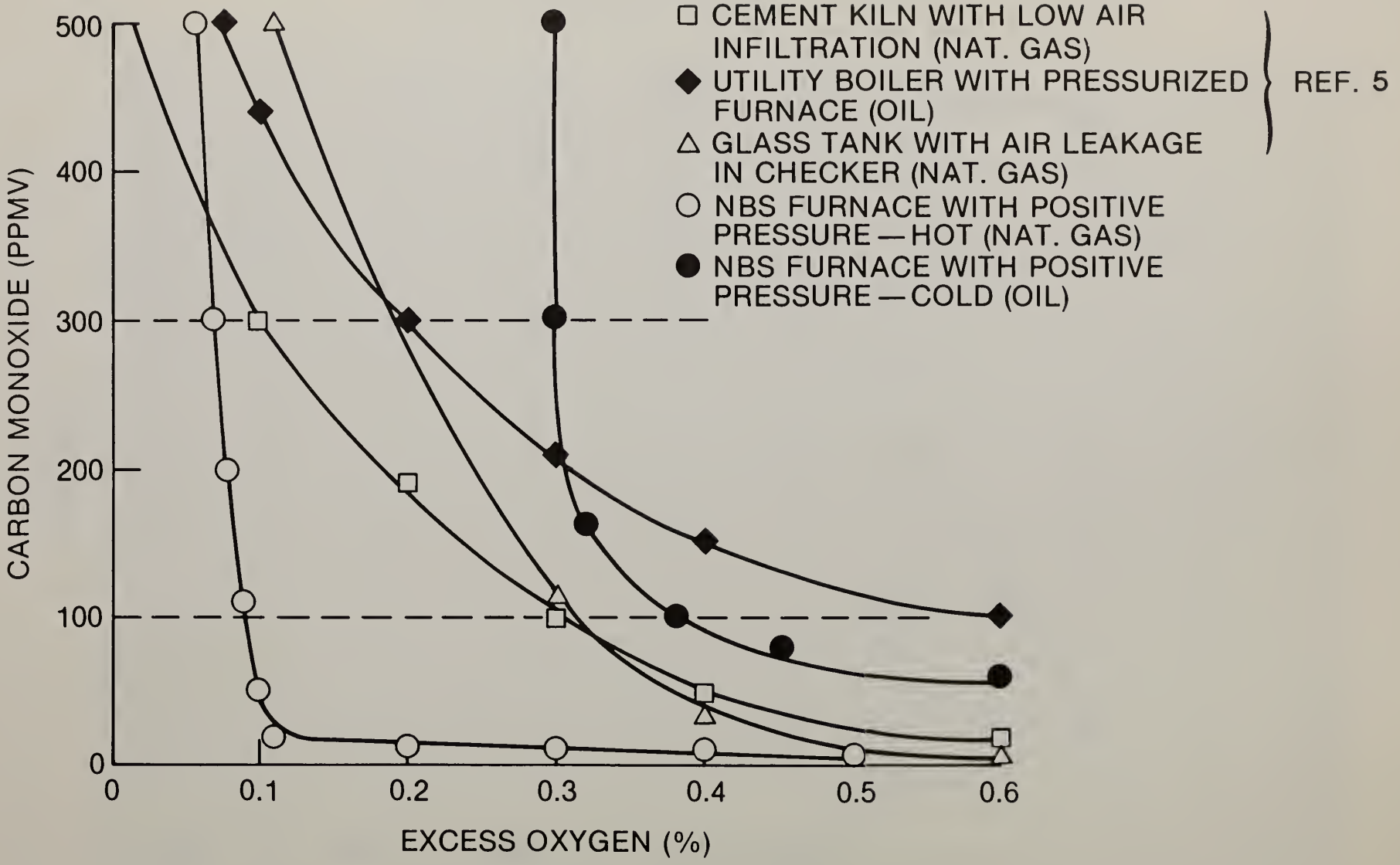

Fig. 11 - Variation of CO with excess O_2 for several boilers and furnaces.

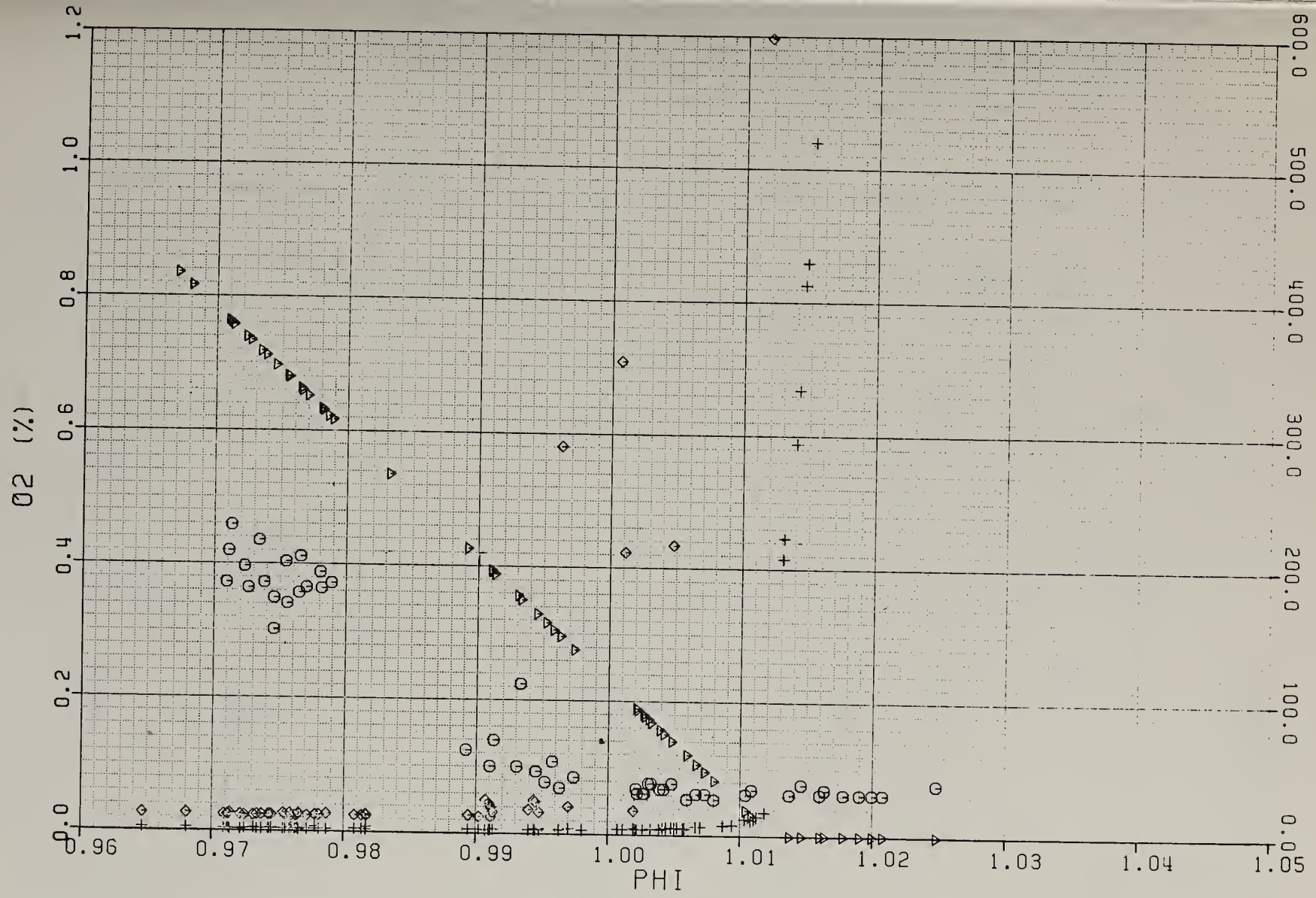

Fig. 12 - Variation of CO and O_2 concentration with equivalence ratio; Expanded Scale; Fuel = Natural Gas; Sampling below recuperator; (o - Gas Sampling for O_2 Analyzer; Δ - Equilibrium Calculation Based on Stack Temperature for O_2 Analyzer; ◇ - Gas Sampling for CO Analyzer; + - Equilibrium Calculation Based on Stack Temperature for CO Analyzer).

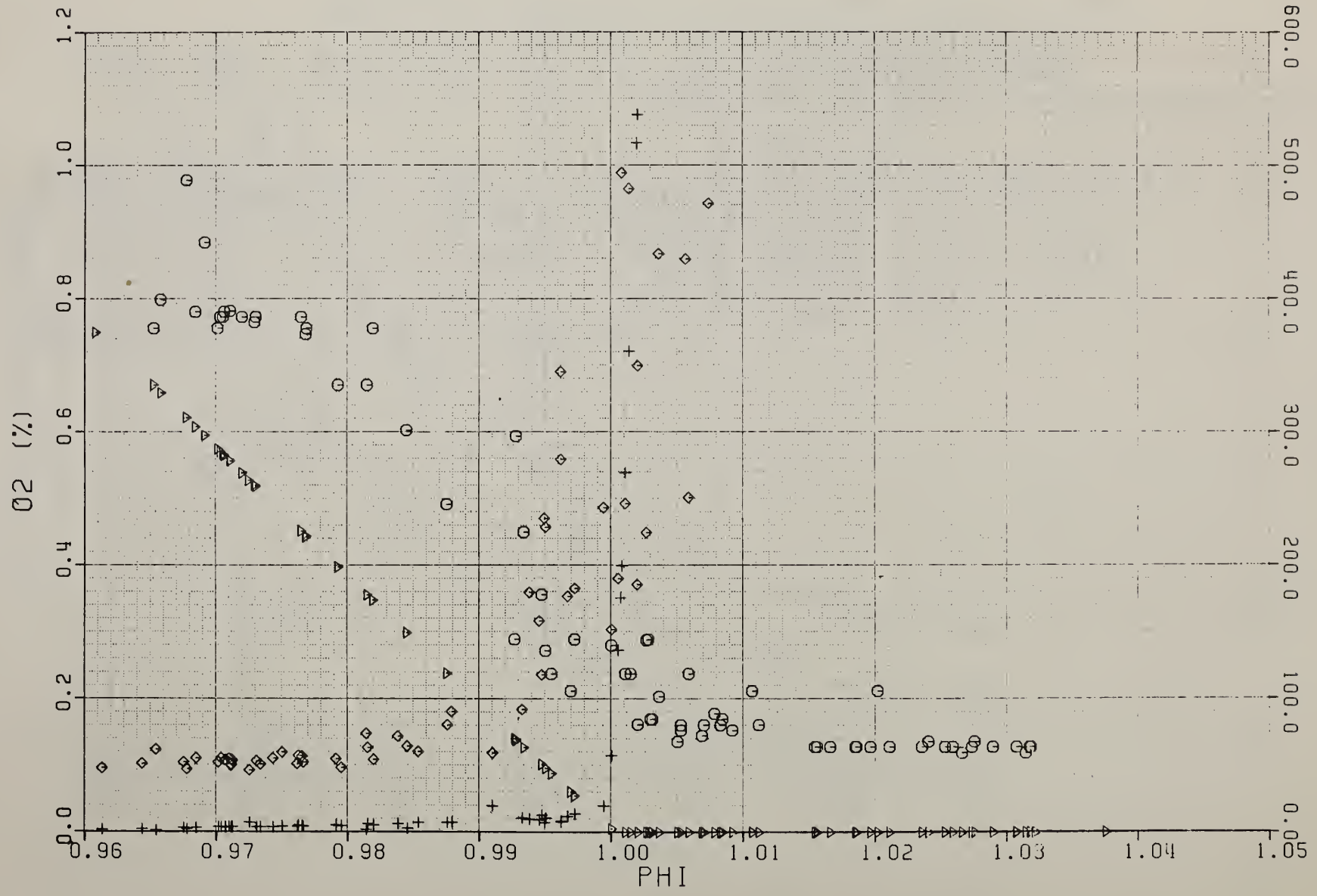

Fig. 13 - Variation of CO and O_2 concentration with equivalence ratio; Expanded scale; Fuel = No. 2 Fuel Oil; Sampling below recuperator; (o - Gas Sampling for O_2 Analyzer; Δ - Equilibrium Calculation Based on Stack Temperature for O_2 Analyzer; ◇ - Gas Sampling for CO Analyzer; + - Equilibrium Calculation Based on Stack Temperature for CO Analyzer).

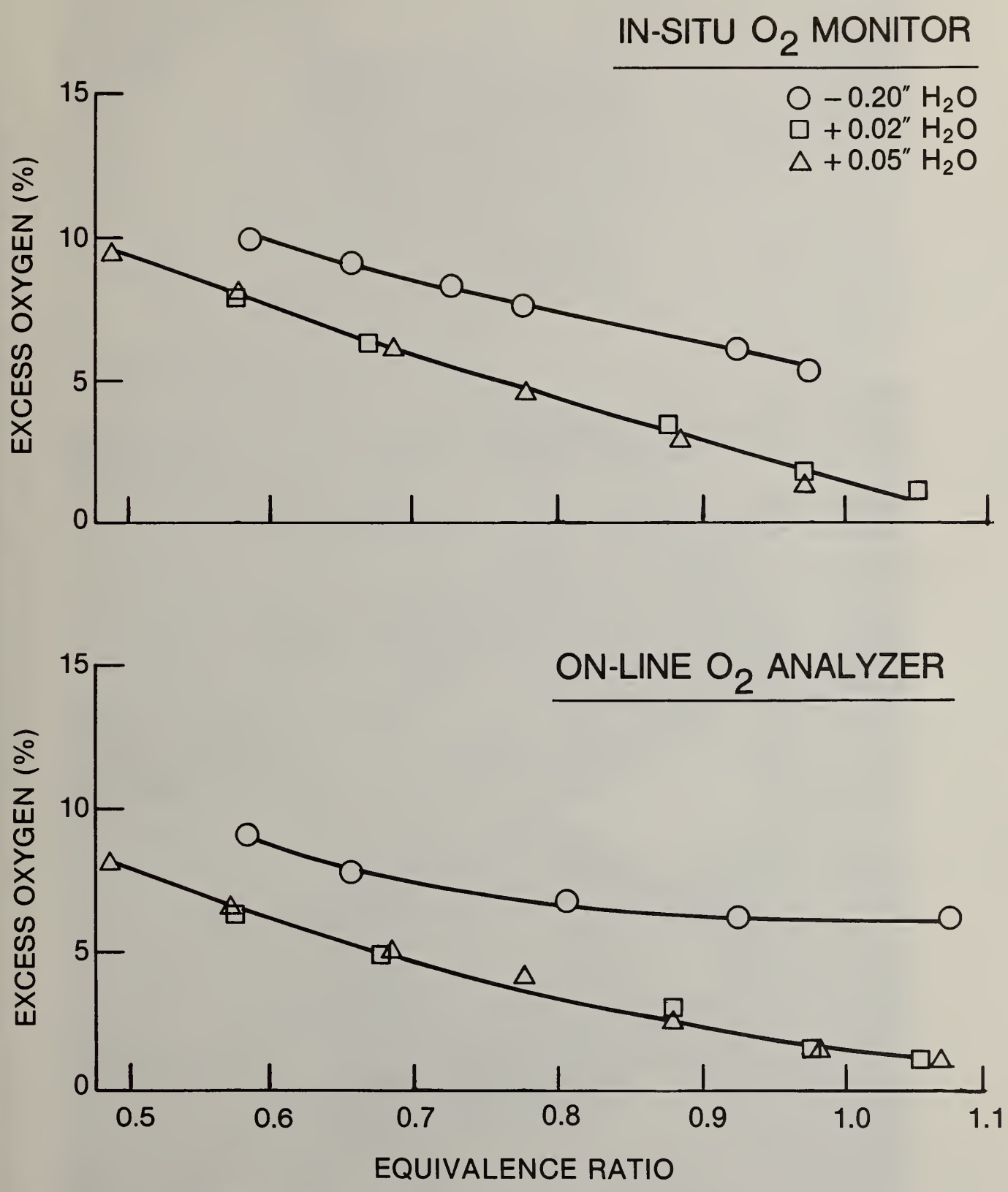

Fig. 14 - Variation of Excess O_2 with equivalence ratio at different furnace pressures; Fuel = No. 2 Fuel Oil.

Fig. 15 - View of the CO monitoring system as installed in the stack above the recuperator.

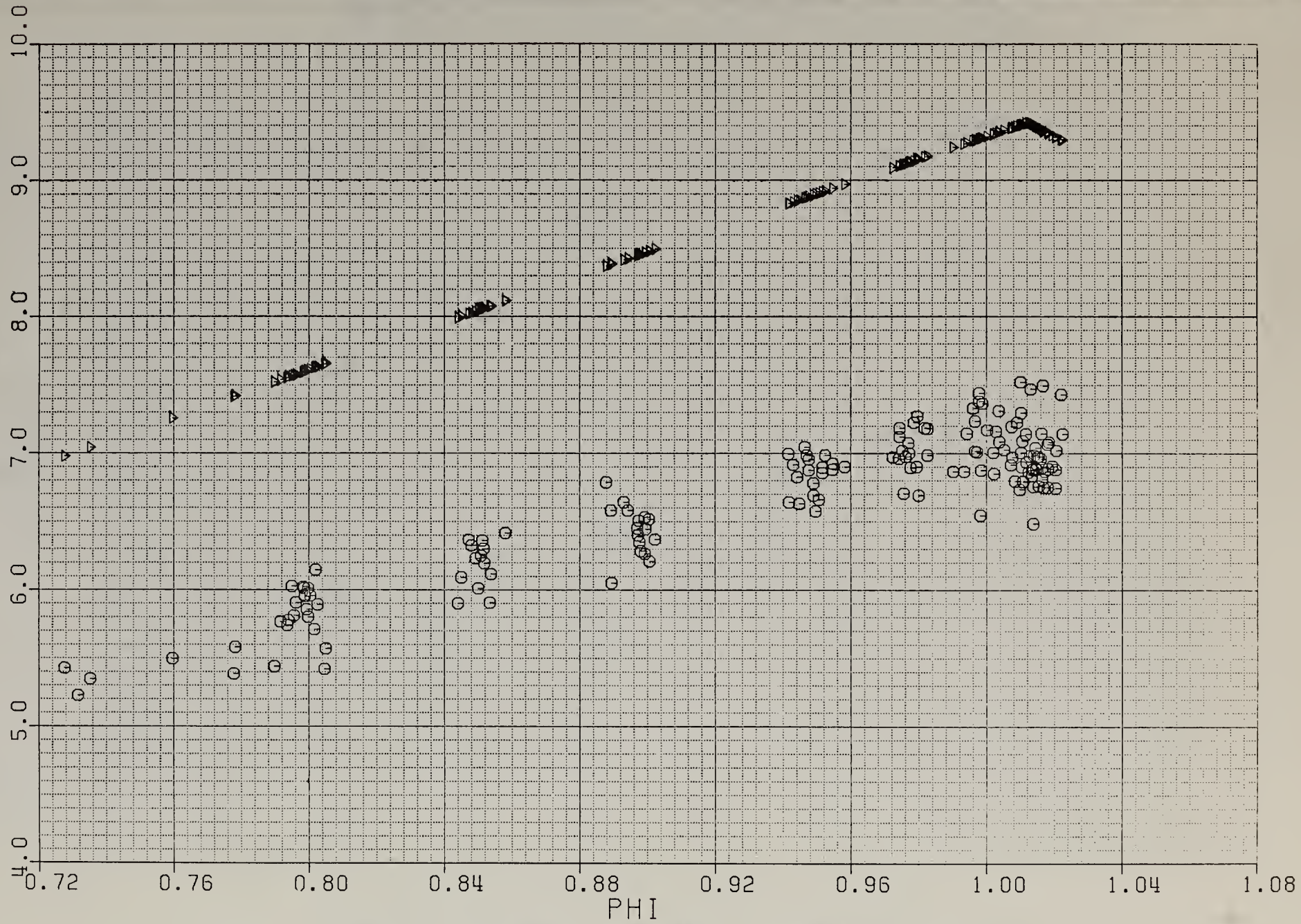

Fig. 16 - Variation of CO_2 concentration with equivalence ratio; Fuel = Natural Gas; Sampling above recuperator; Dilution observed due to CO monitor cooling air; (o - Gas Sampling; Δ - Equilibrium Calculation Based on Stack Temperature).

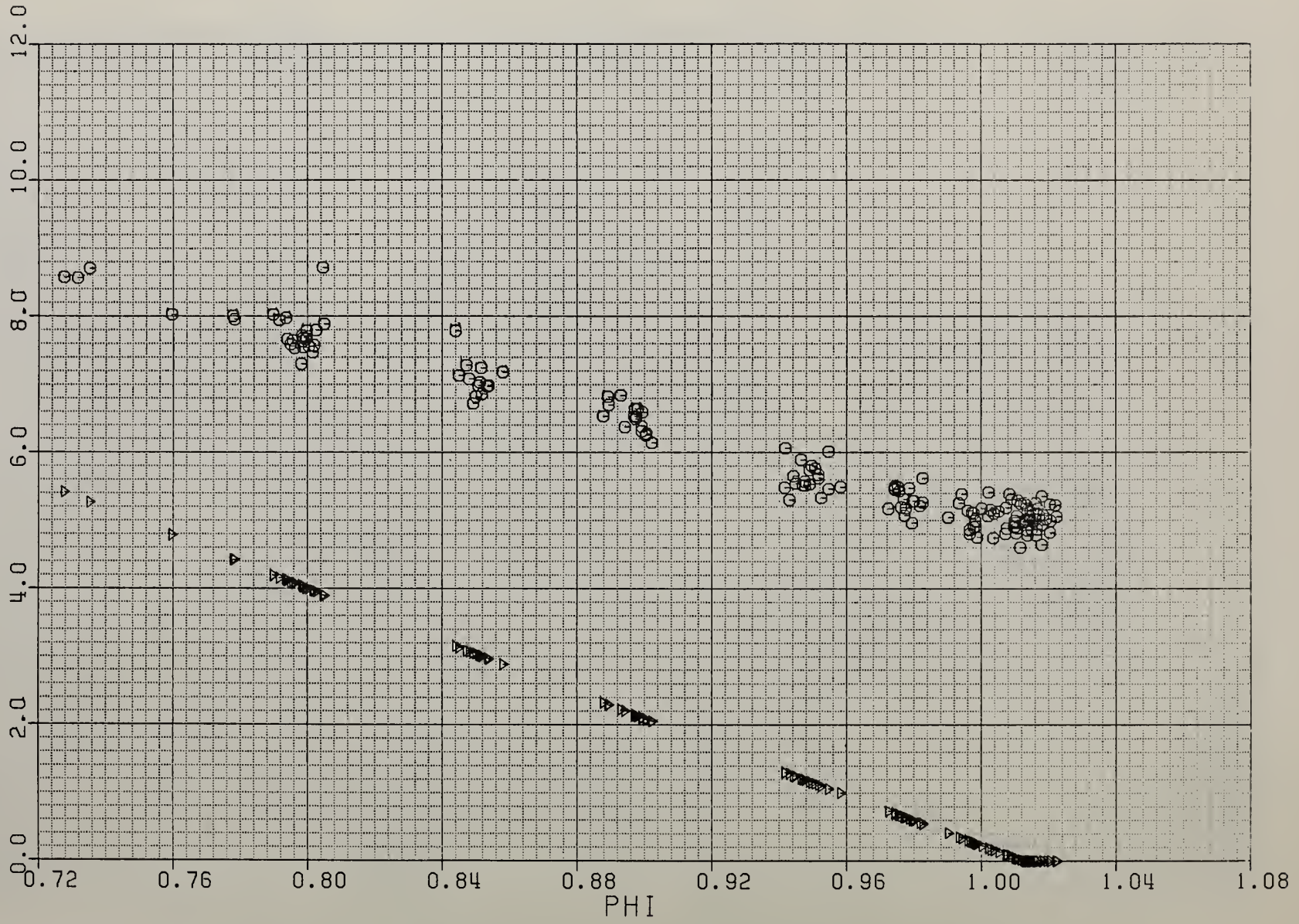

Fig. 17 - Variation of O_2 concentration with equivalence ratio; Fuel = Natural Gas; Sampling above recuperator; Dilution observed due to CO monitor cooling air; (o - Gas Sampling; Δ - Equilibrium Calculation Based on Stack Temperature).

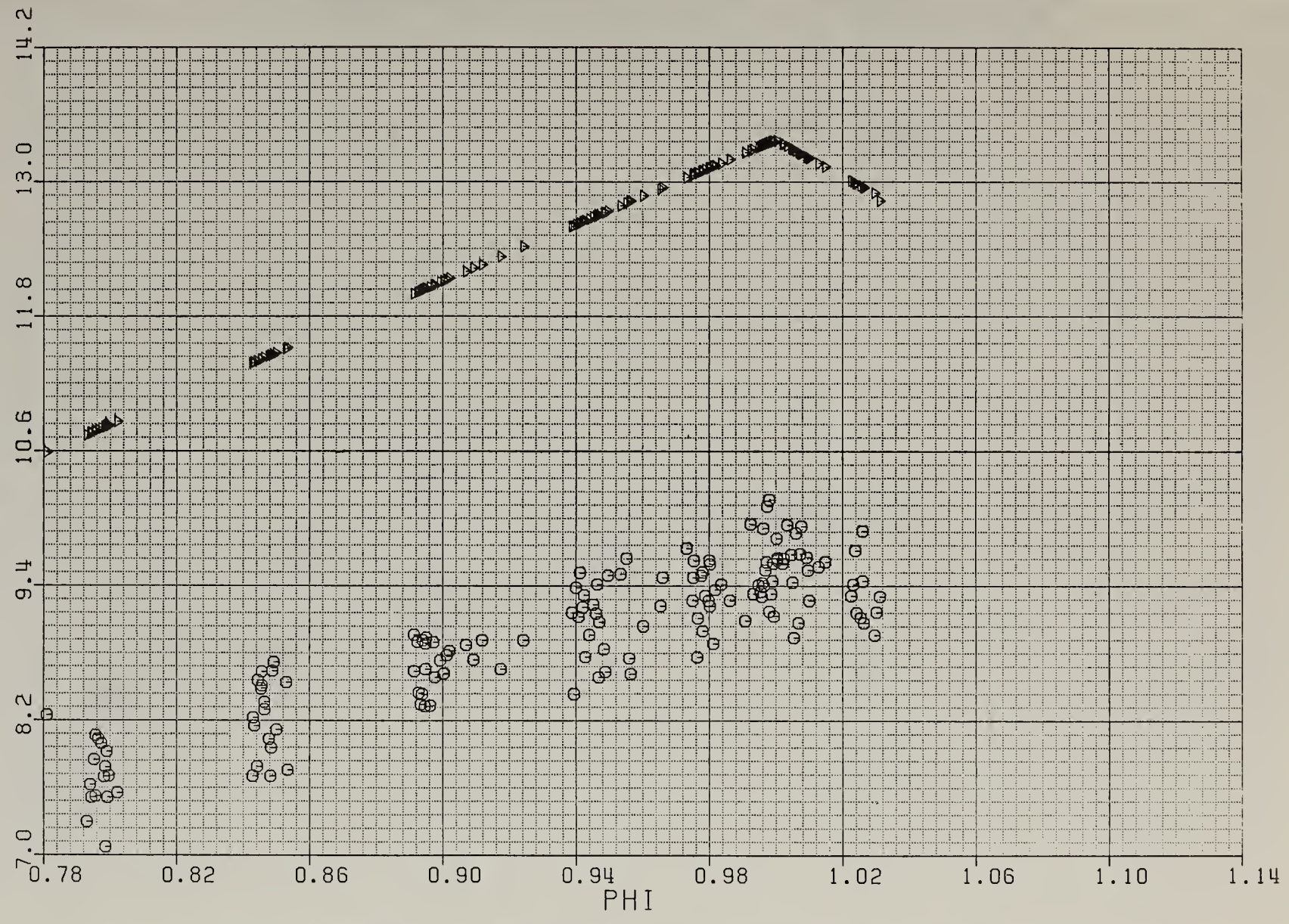

Fig. 18 - Variation of CO_2 concentration with equivalence ratio; Fuel = No. 2 Fuel Oil; Sampling above recuperator; Dilution observed due to CO monitor cooling air; (o - Gas Sampling; Δ - Equilibrium Calculation Based on Stack Temperature).

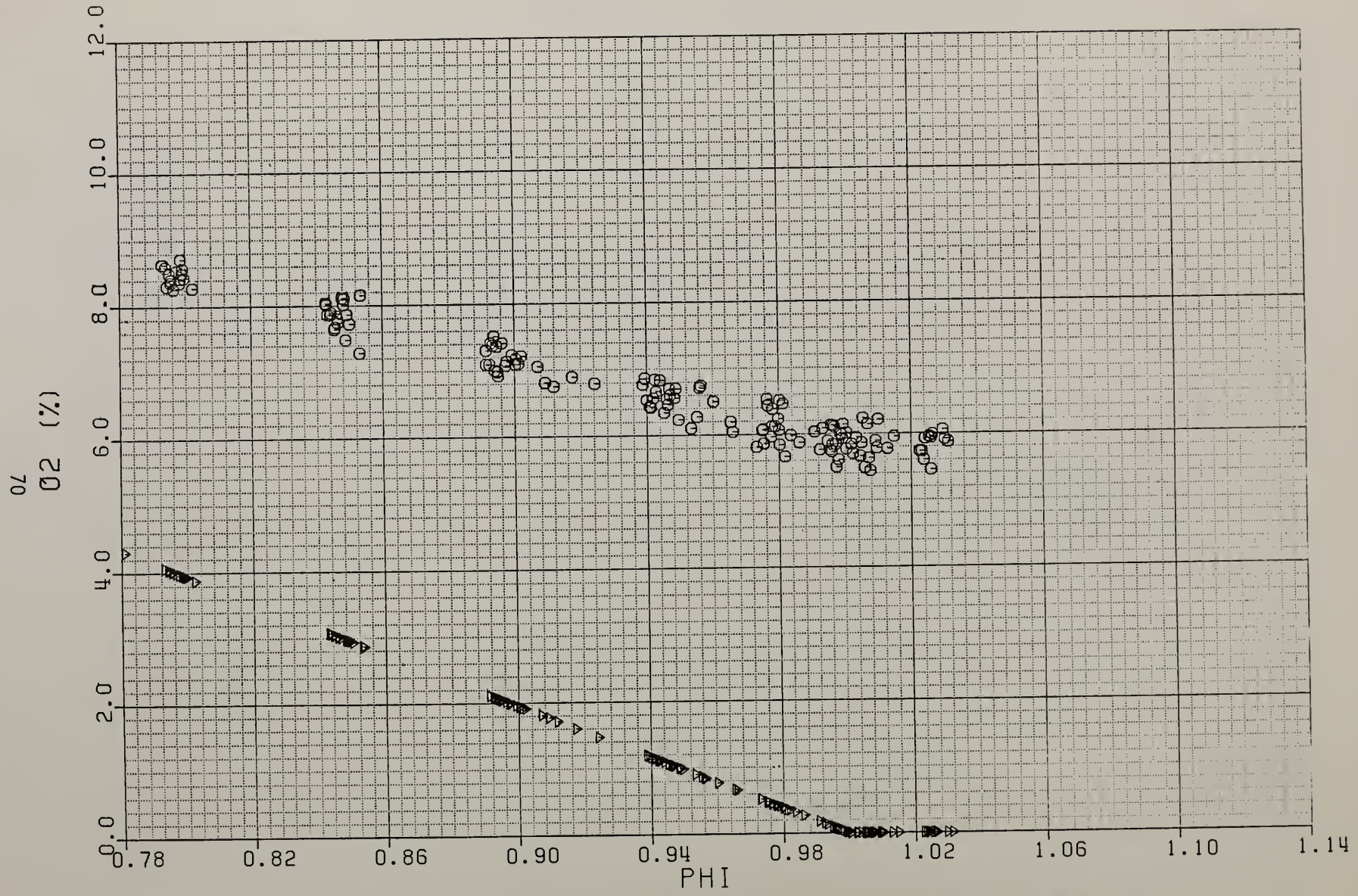

Fig. 19 - Variation of O_2 concentration with equivalence ratio; Fuel = No. 2 Fuel Oil; Sampling above recuperator; Dilution observed due to CO monitor cooling air; (o - Gas Sampling; Δ - Equilibrium Calculation Based on Stack Temperature).

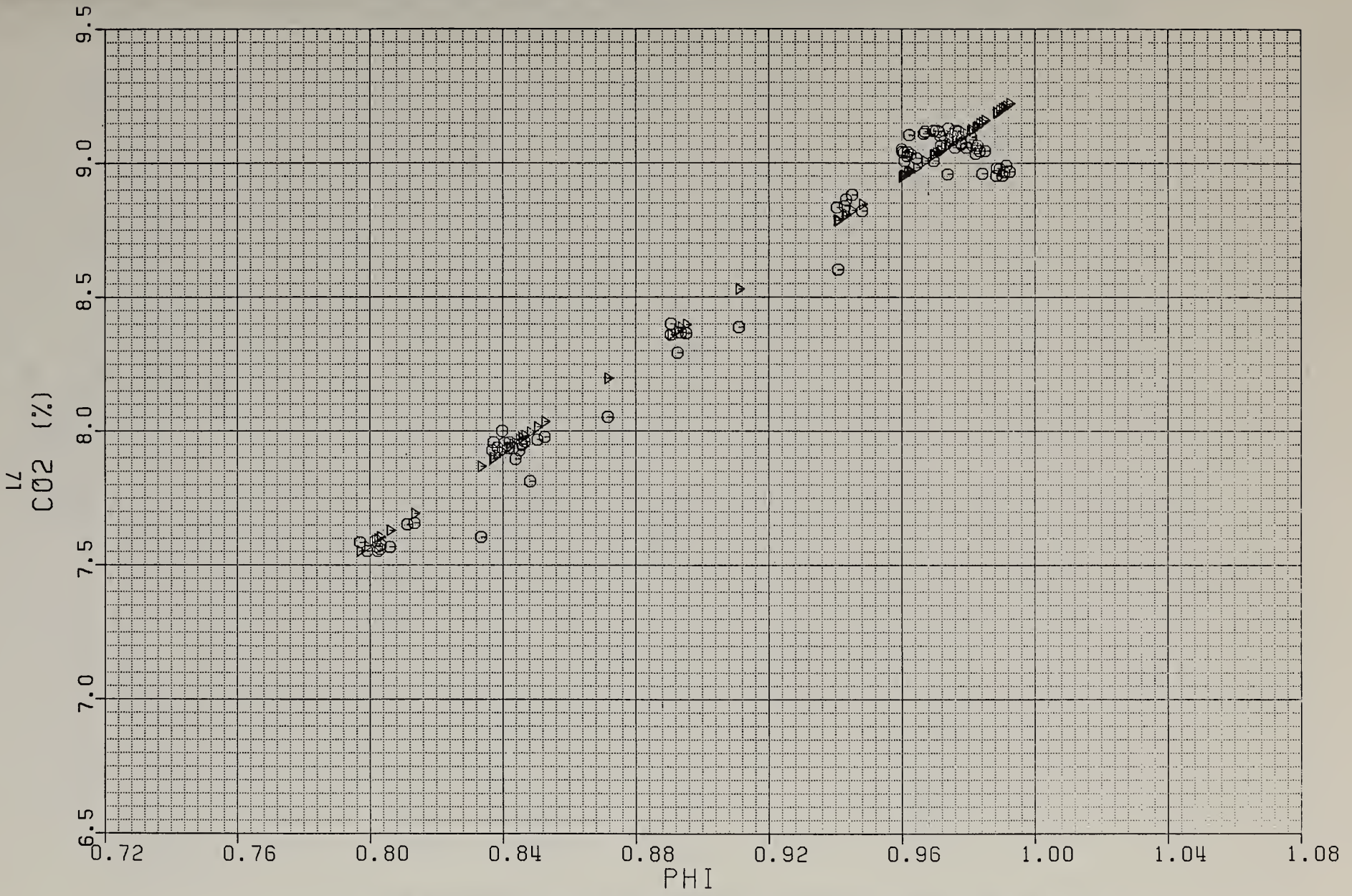

Fig. 20 - Variation of CO_2 concentration with equivalence ratio; Fuel = Natural Gas; Sampling above recuperator; With pilot flame on; Minimum cooling air dilution; (o - Gas Sampling; Δ - Equilibrium Calculation Based on Stack Temperature).

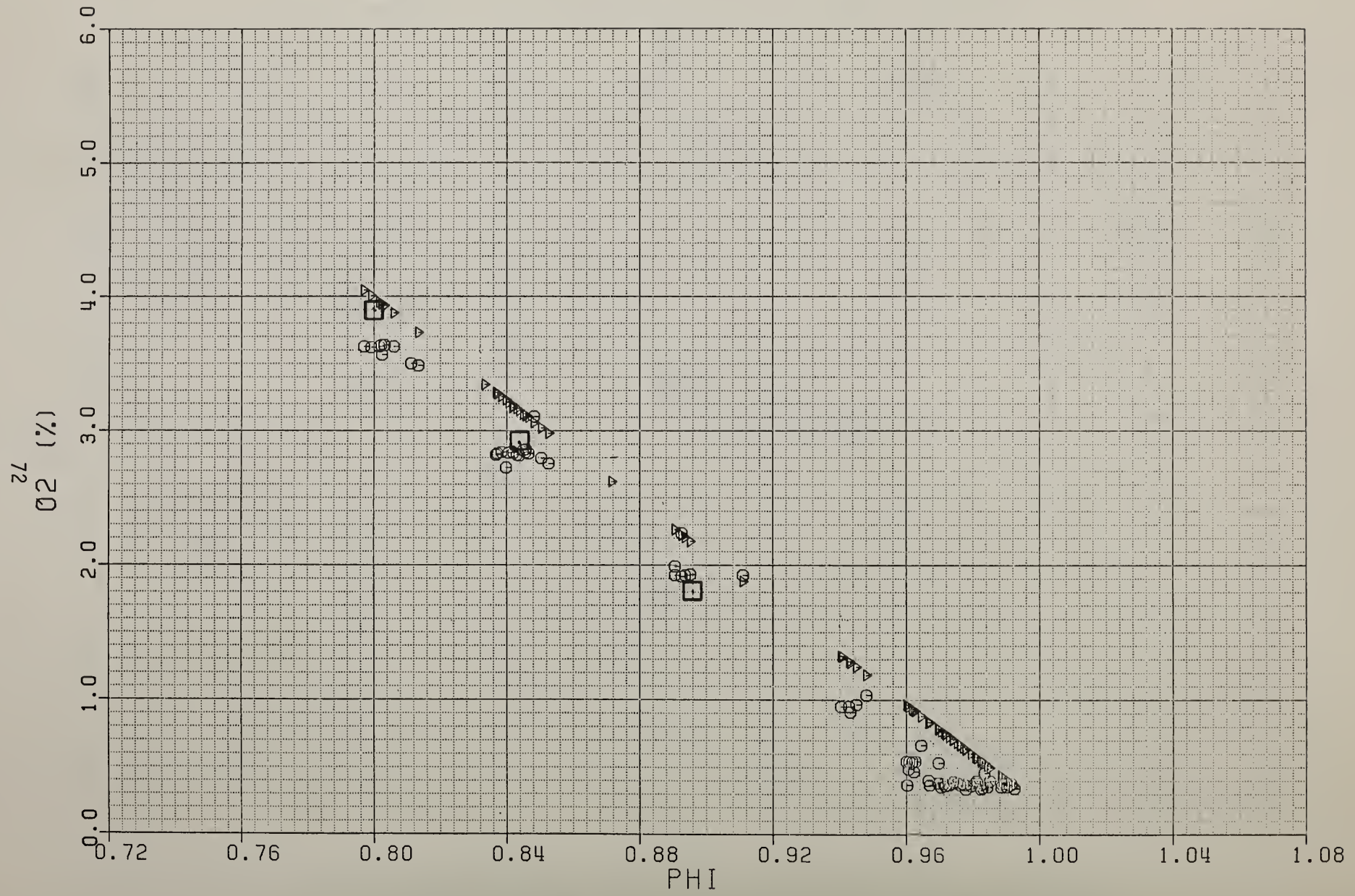

Fig. 21 - Variation of O_2 concentration with equivalence ratio; Fuel = Natural Gas; Sampling above recuperator; With pilot flame on; Minimum cooling air dilution; (o - Gas Sampling; Δ - Equilibrium Calculation Based on Stack Temperature; □ - In-Situ Monitor).

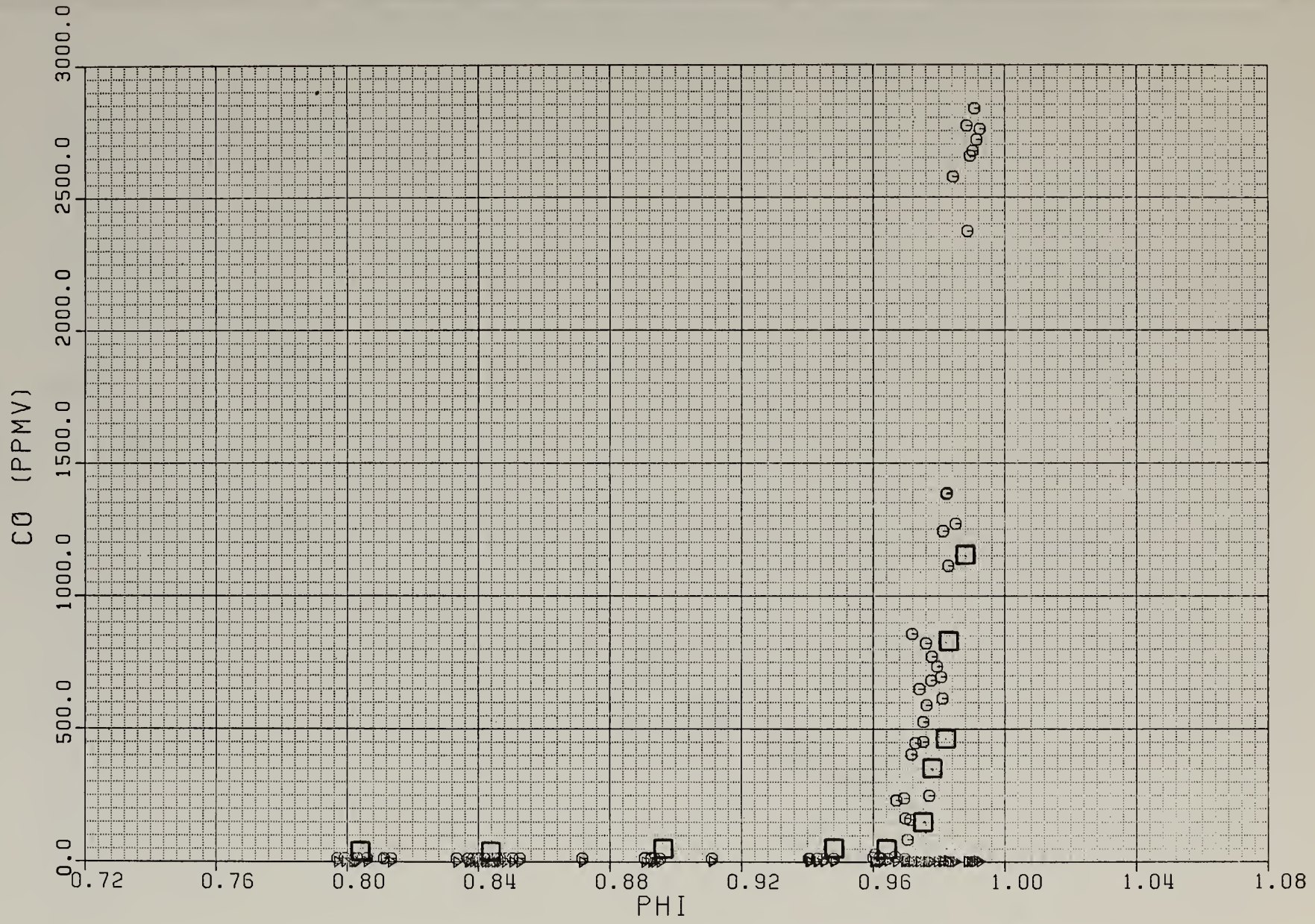

Fig. 22 - Variation of CO concentration with equivalence ratio; Fuel = Natural Gas; Sampling above recuperator; With pilot flame on; Minimum cooling air dilution; (o - Gas Sampling; Δ - Equilibrium Calculation Based on Stack Temperature; □ - In-Situ Monitor).

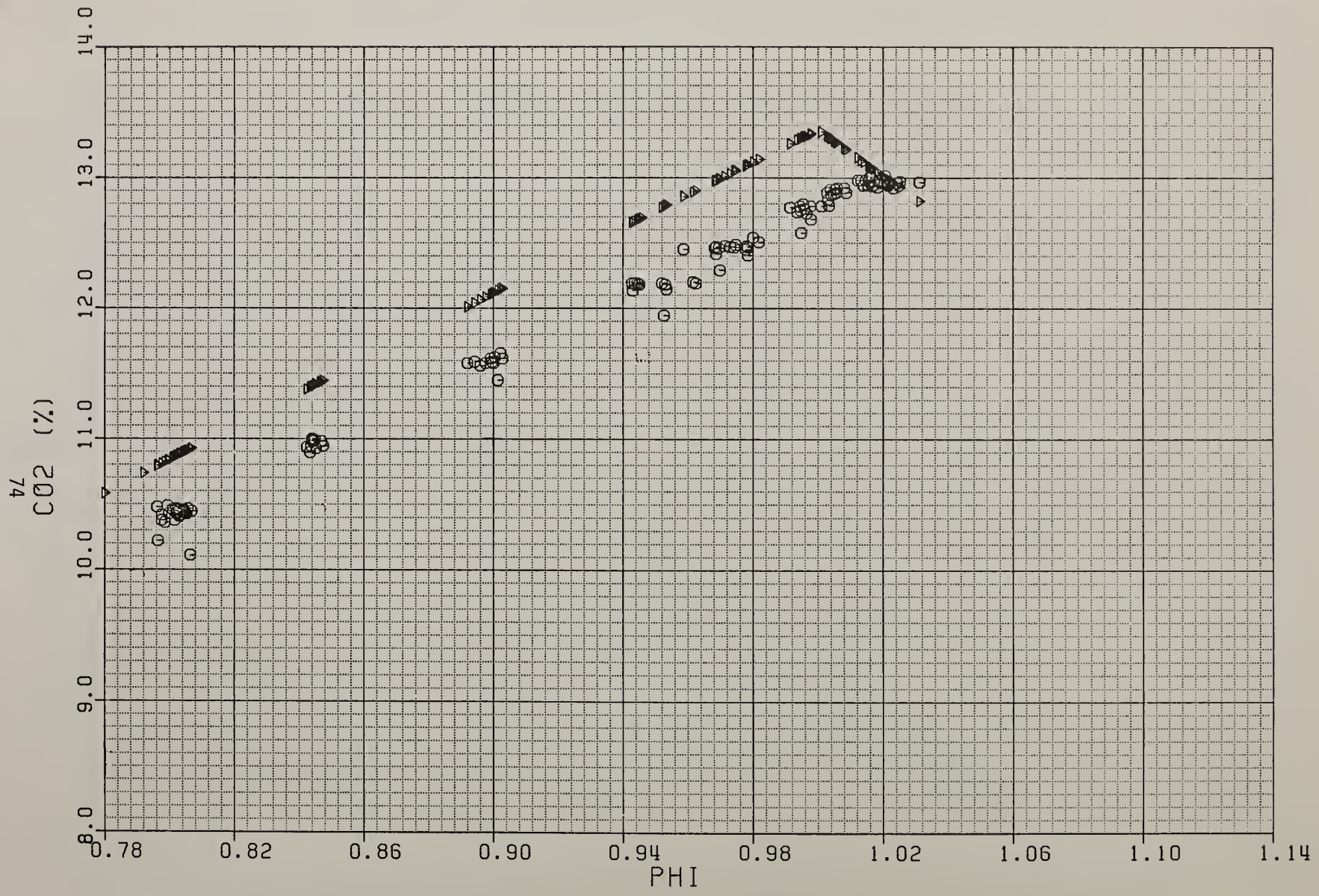

Fig. 23 - Variation of CO_2 concentration with equivalence ratio; Fuel = No. 2 Fuel Oil; Sampling above recuperator; T_F = 888°C; Minimum cooling air dilution; (o - Gas Sampling; Δ - Equilibrium Calculation Based on Stack Temperature).

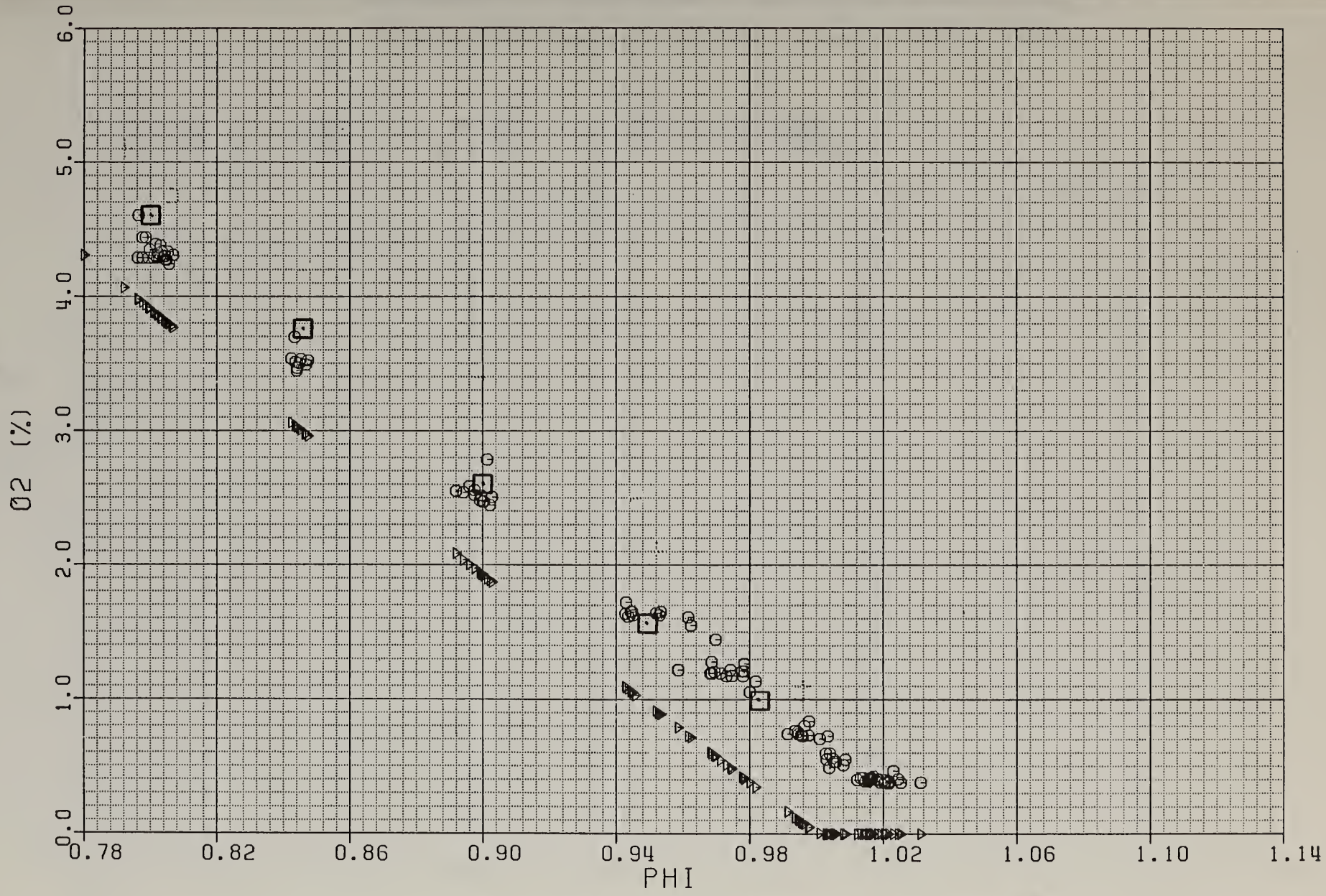

Fig. 24 - Variation of O_2 concentration with equivalence ratio; Fuel = No. 2 Fuel Oil; Sampling above recuperator; T_F = 888°C; Minimum cooling air dilution; (o - Gas Sampling; Δ - Equilibrium Calculation Based on Stack Temperature; □ - In-Situ Monitor).

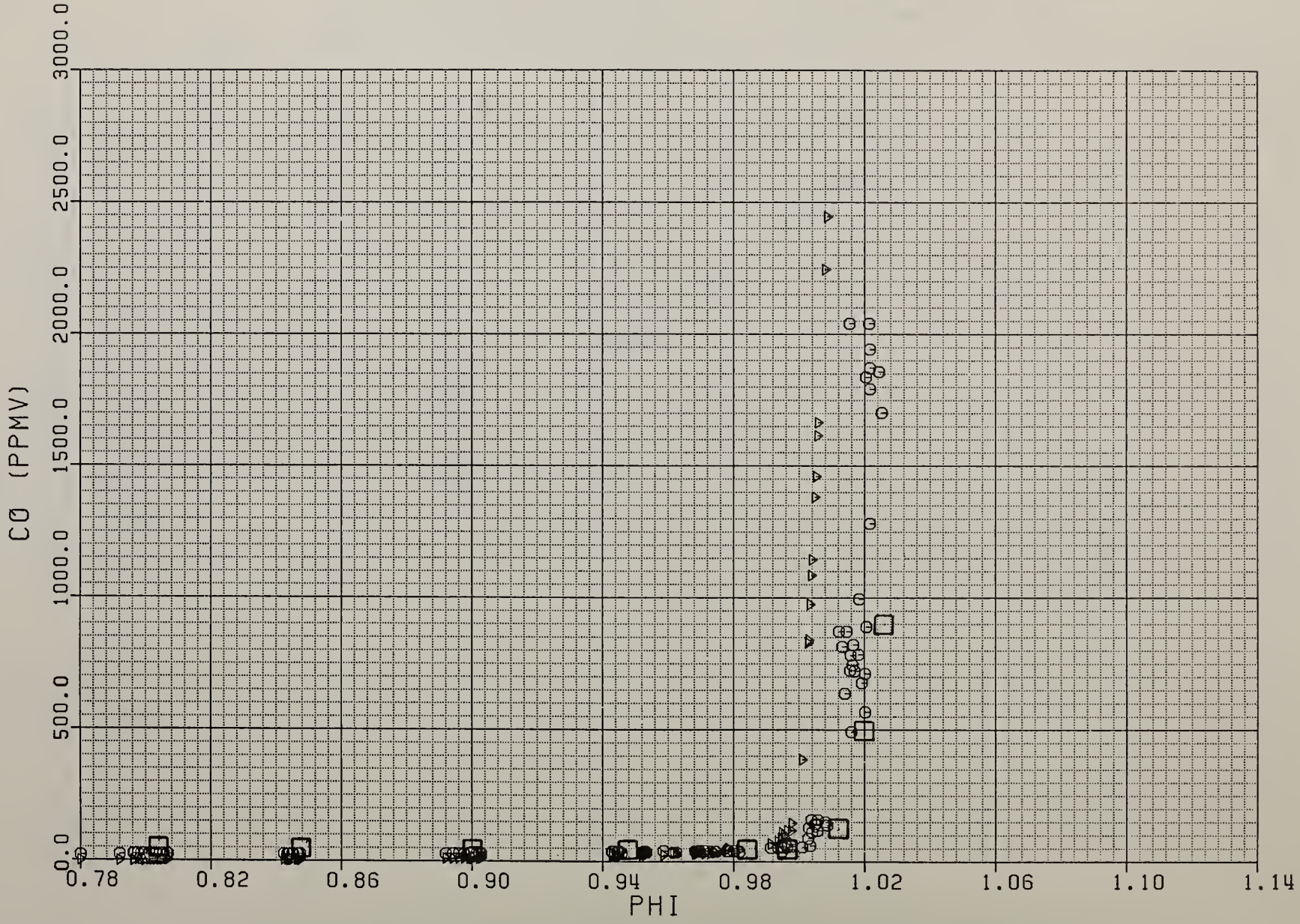

Fig. 25 - Variation of CO concentration with equivalence ratio; Fuel = No. 2 Fuel Oil; Sampling above recuperator; T_F = 888°C; Minimum cooling air dilution; (o - Gas Sampling; Δ - Equilibrium Calculation Based on Stack Temperature; □ - In-Situ Monitor).

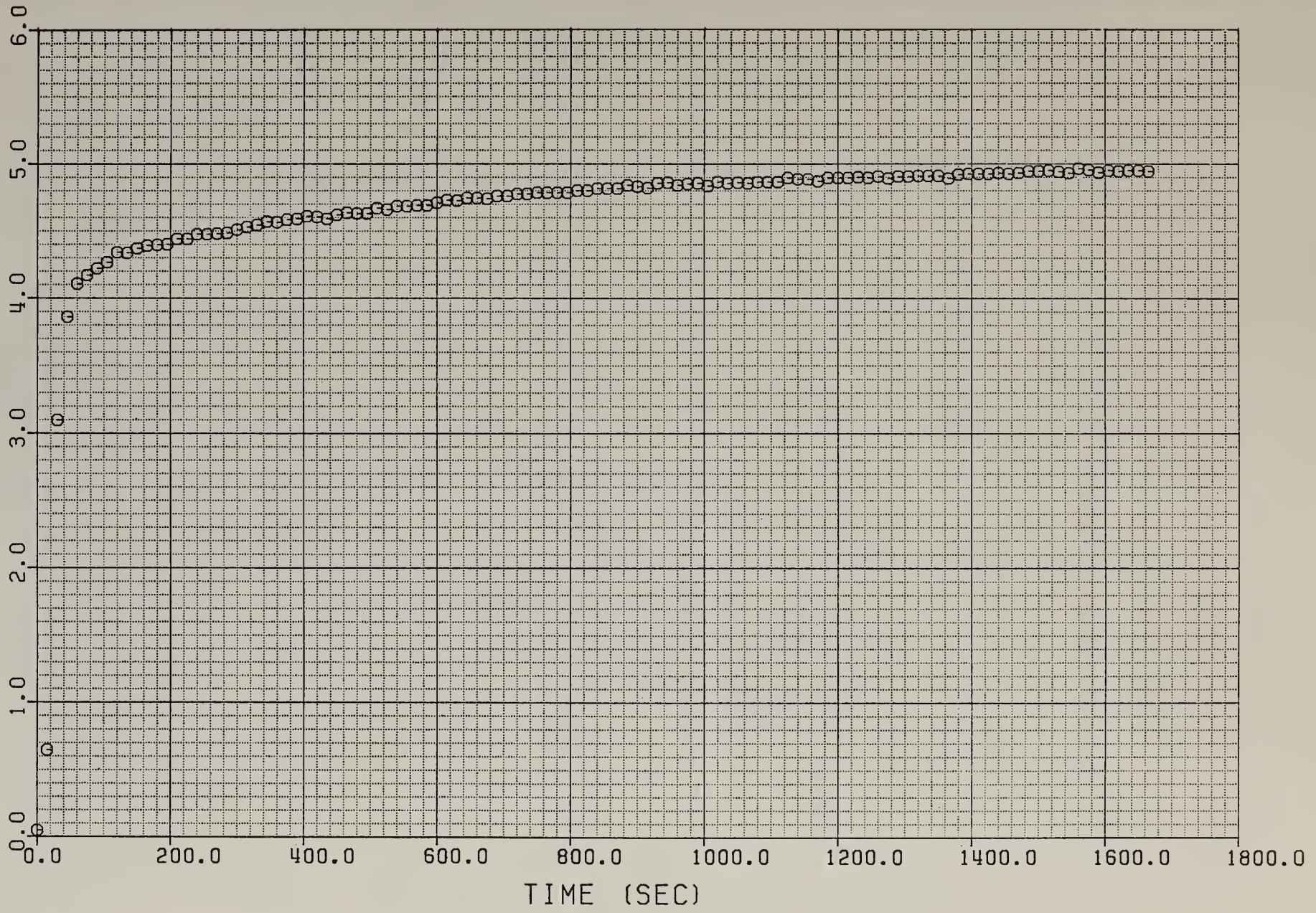

Fig. 26 - Start-up transient test: CO_2 variation with time; ϕ = 0.5; Fuel = Natural Gas; Sampling above recuperator; (o - Gas Sampling).

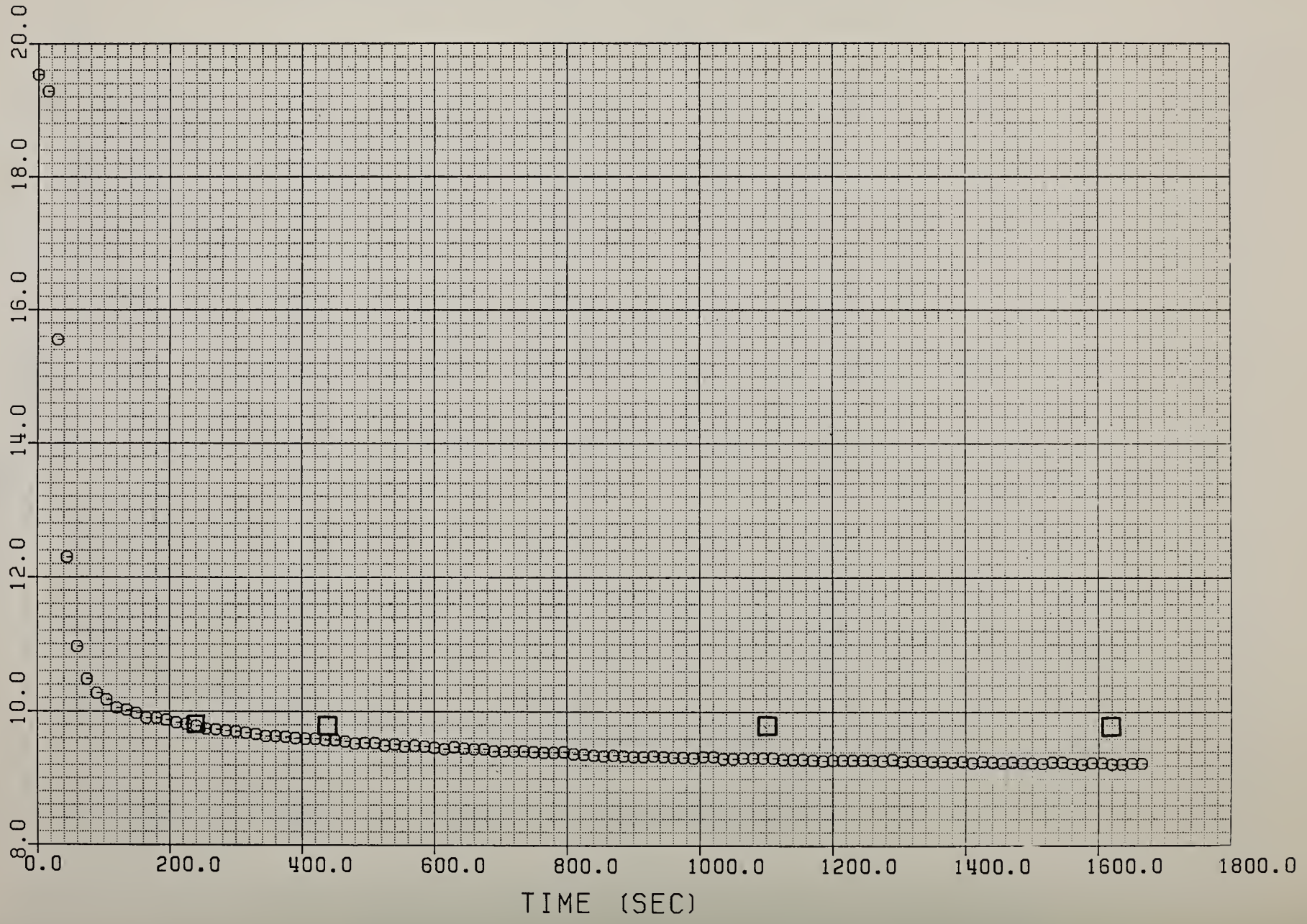

Fig. 27 - Start-up transient test: O_2 variation with time; ϕ = 0.5; Fuel = Natural Gas; Sampling above recuperator; In-situ O_2 monitor below recuperator; (o - Gas Sampling; □ - In-Situ Monitor).

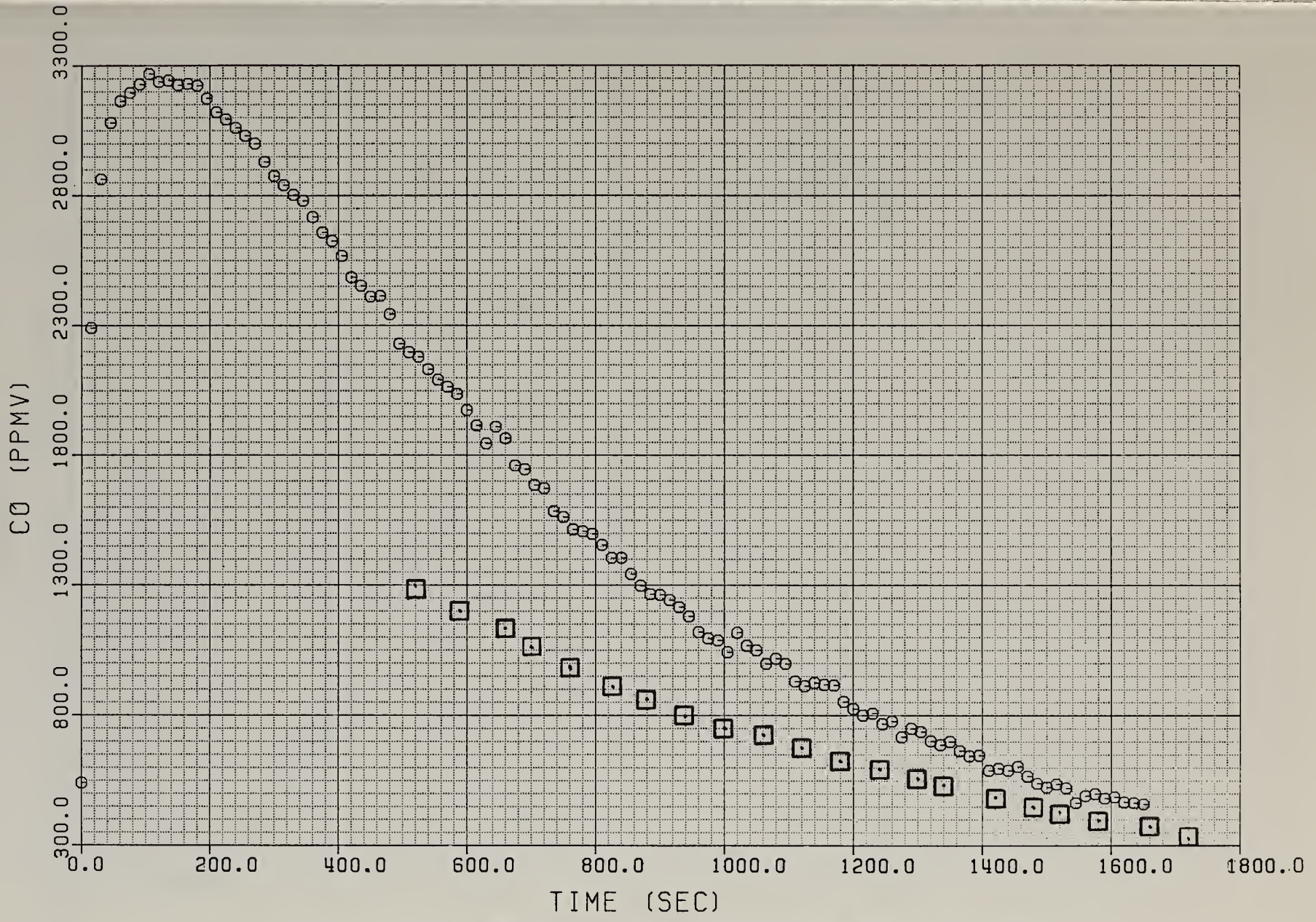

Fig. 28 - Start-up transient test: CO variation with time; ϕ = 0.5; Fuel = Natural Gas; Sampling above recuperator; (o - Gas Sampling; □ - In-Situ Monitor).

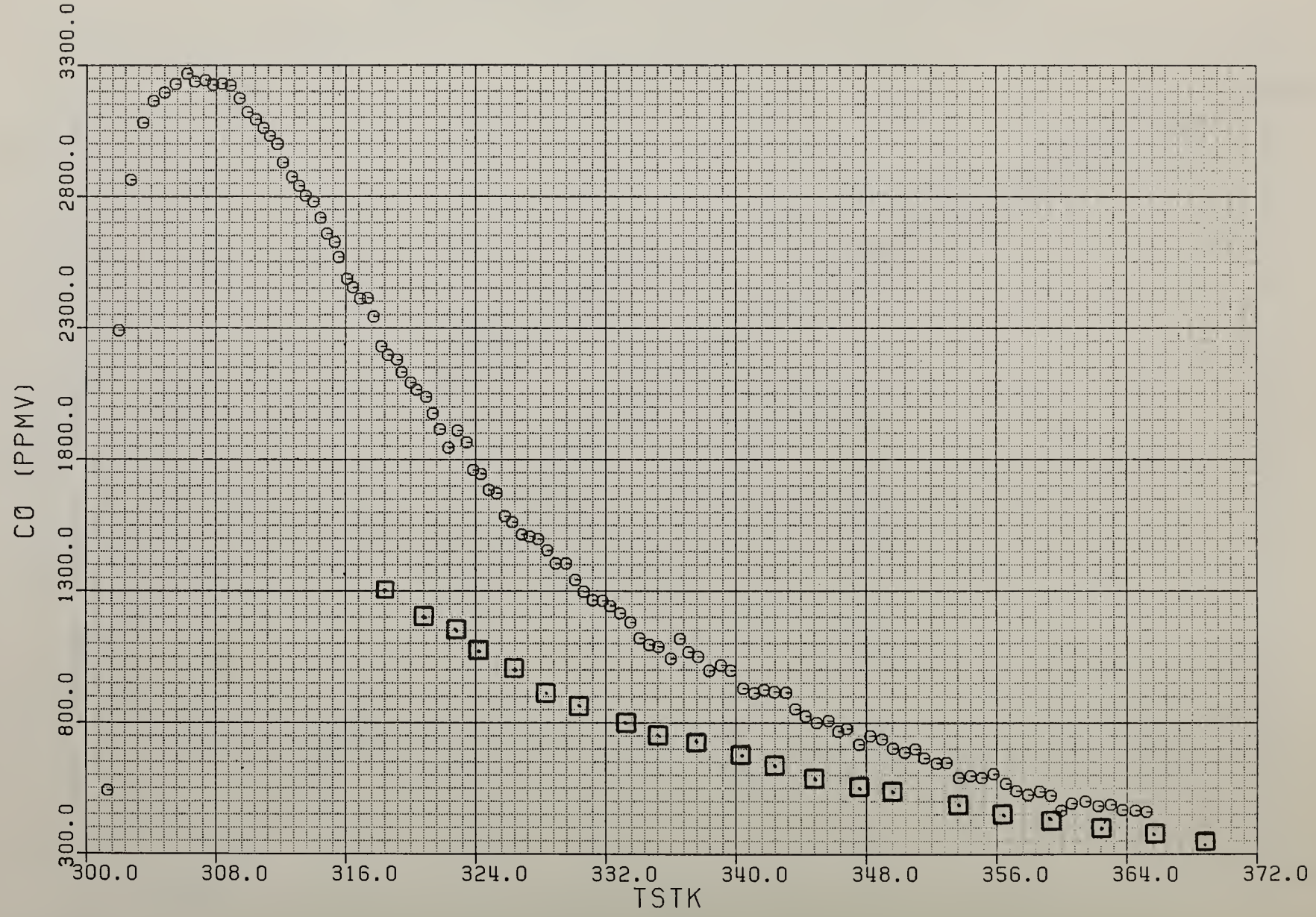

Fig. 29 - Start-up transient test: CO variation with stack gas temperature; ϕ = 0.5; Fuel = Natural Gas; Sampling above recuperator; (o - Gas Sampling; □ - In-Situ Monitor).

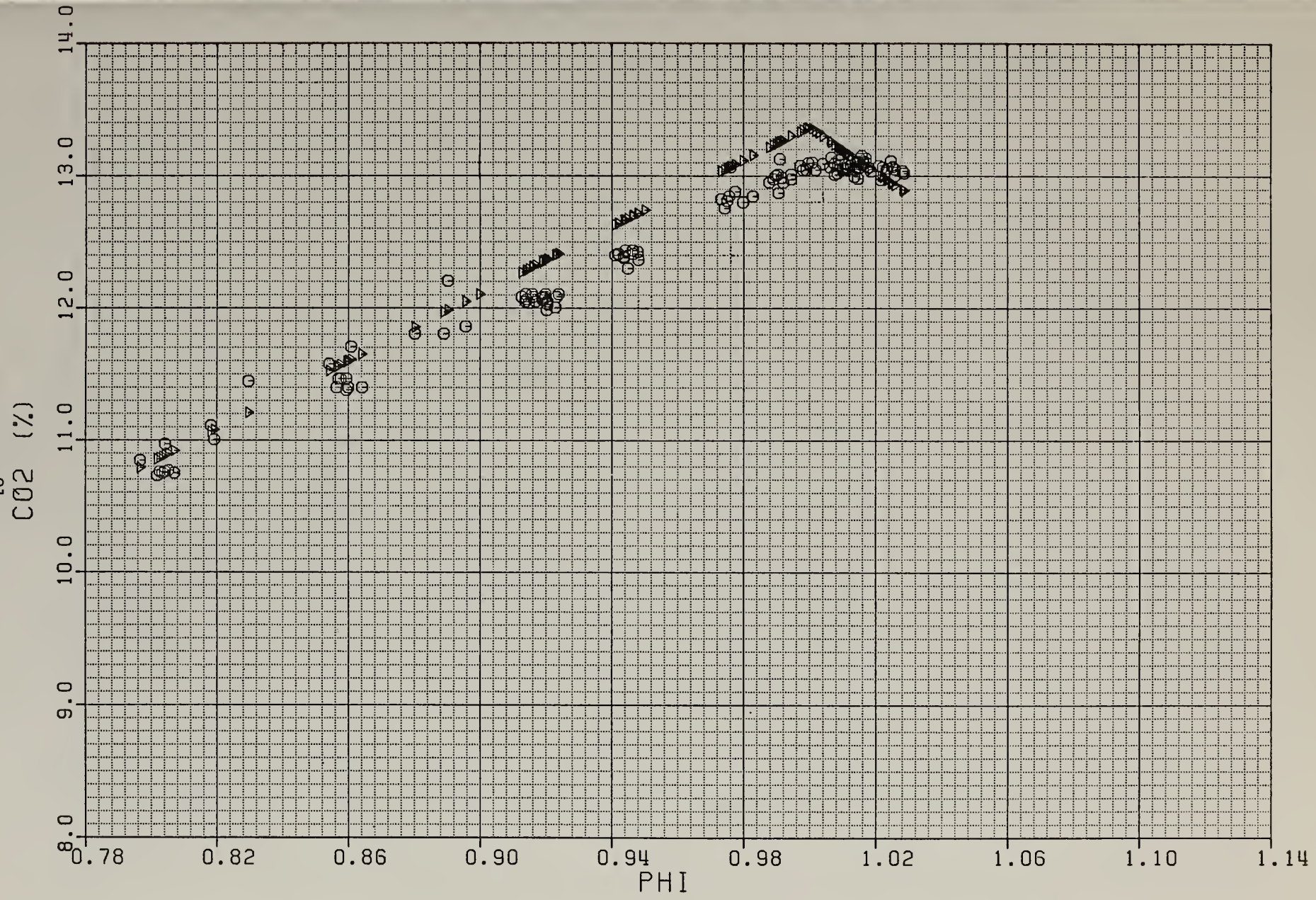

Fig. 30 - Variation of CO_2 concentration with equivalence ratio; Fuel = No. 2 Fuel Oil; Sampling above recuperator; T_F = 920°C; (o - Gas Sampling; Δ - Equilibrium Calculation Based on Stack Temperature).

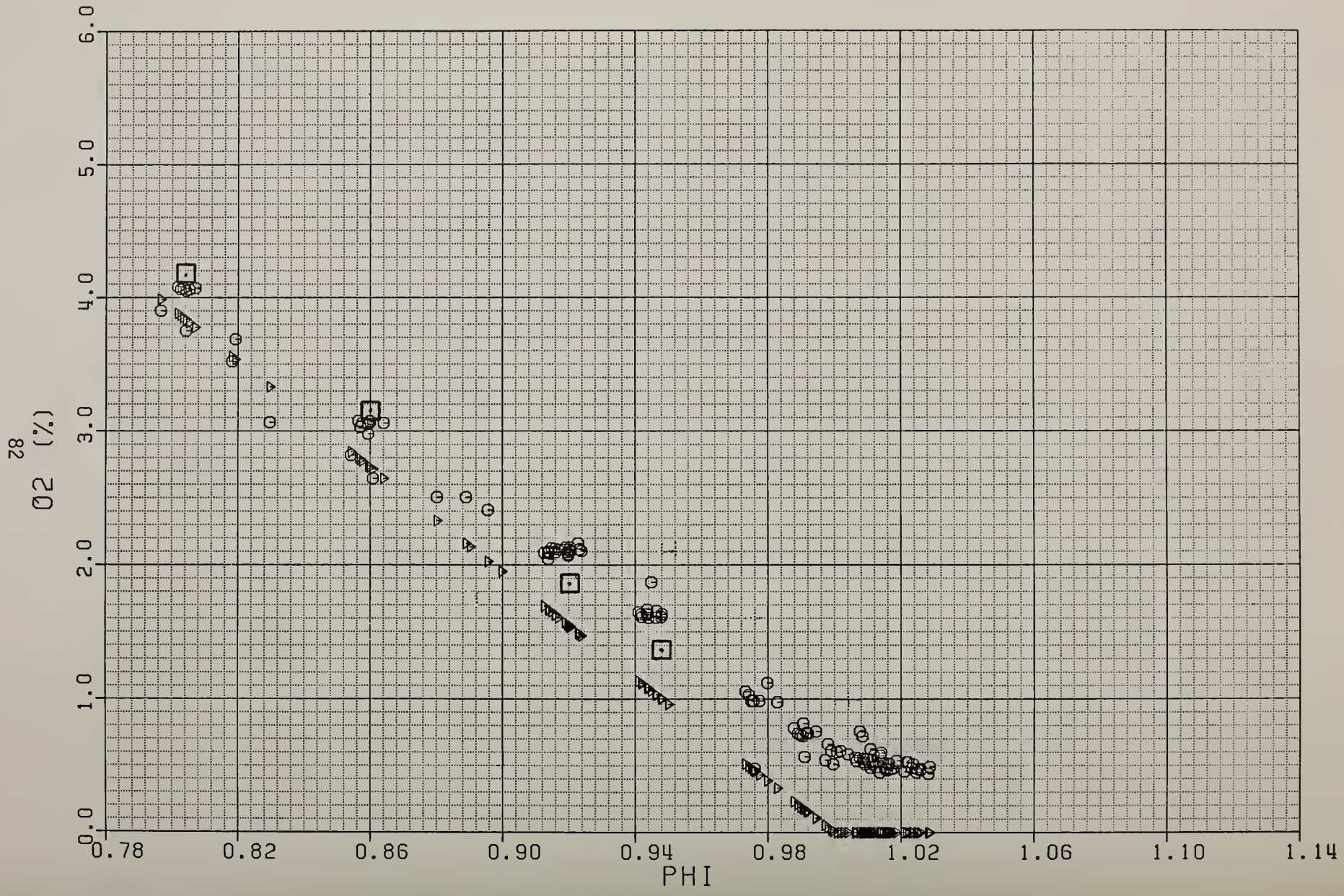

Fig. 31 - Variation of O_2 concentration with equivalence ratio; Fuel = No. 2 Fuel Oil; Sampling above recuperator; T_F = 920°C; (o - Gas Sampling; Δ - Equilibrium Calculation Based on Stack Temperature; □ - In-Situ Monitor).

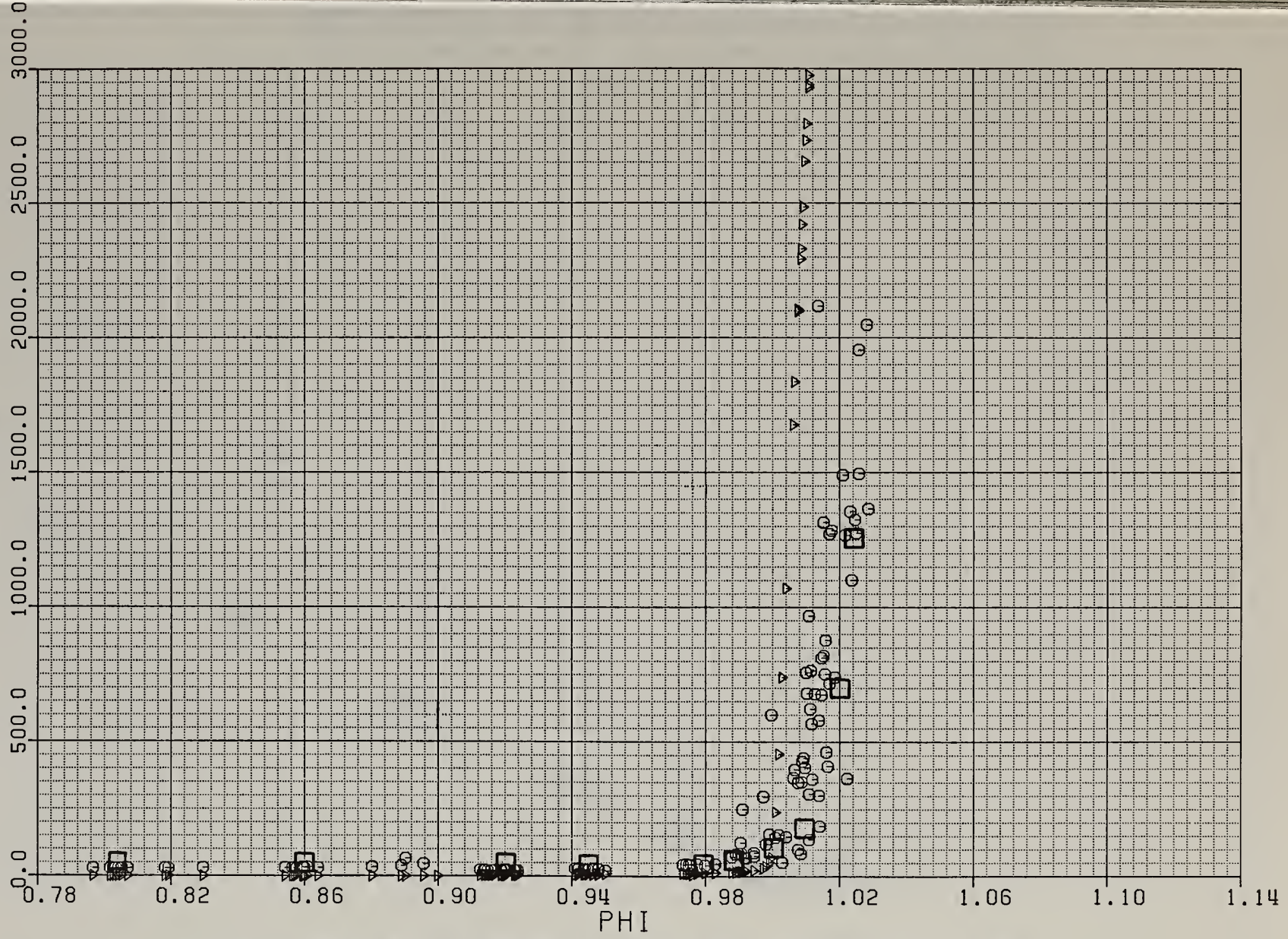

Fig. 32 - Variation of CO concentration with equivalence ratio; Fuel = No. 2 Fuel Oil; Sampling above recuperator; T_F = 920°C; (o - Gas Sampling; Δ - Equilibrium Calculation Based on Stack Temperature; □ - In-Situ Monitor).

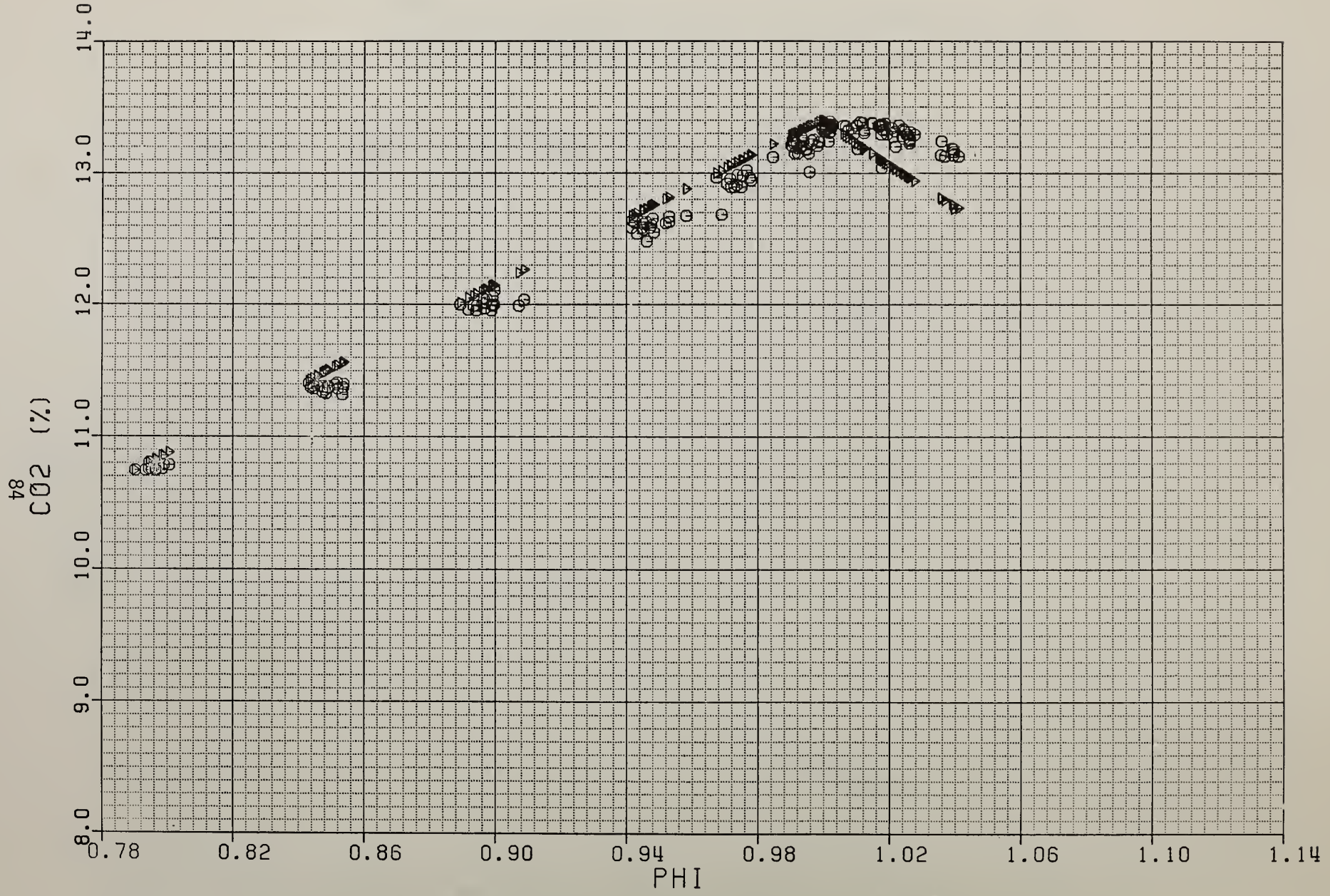

Fig. 33 - Long-term transient tests: Cool Furnace; T_F = 870°C; T_A = 177°C; Fuel = No. 2 Fuel Oil; Variation of CO_2 concentration with equivalence ratio; Sampling below recuperator; (o - Gas Sampling; Δ - Equilibrium Calculation Based on Stack Temperature).

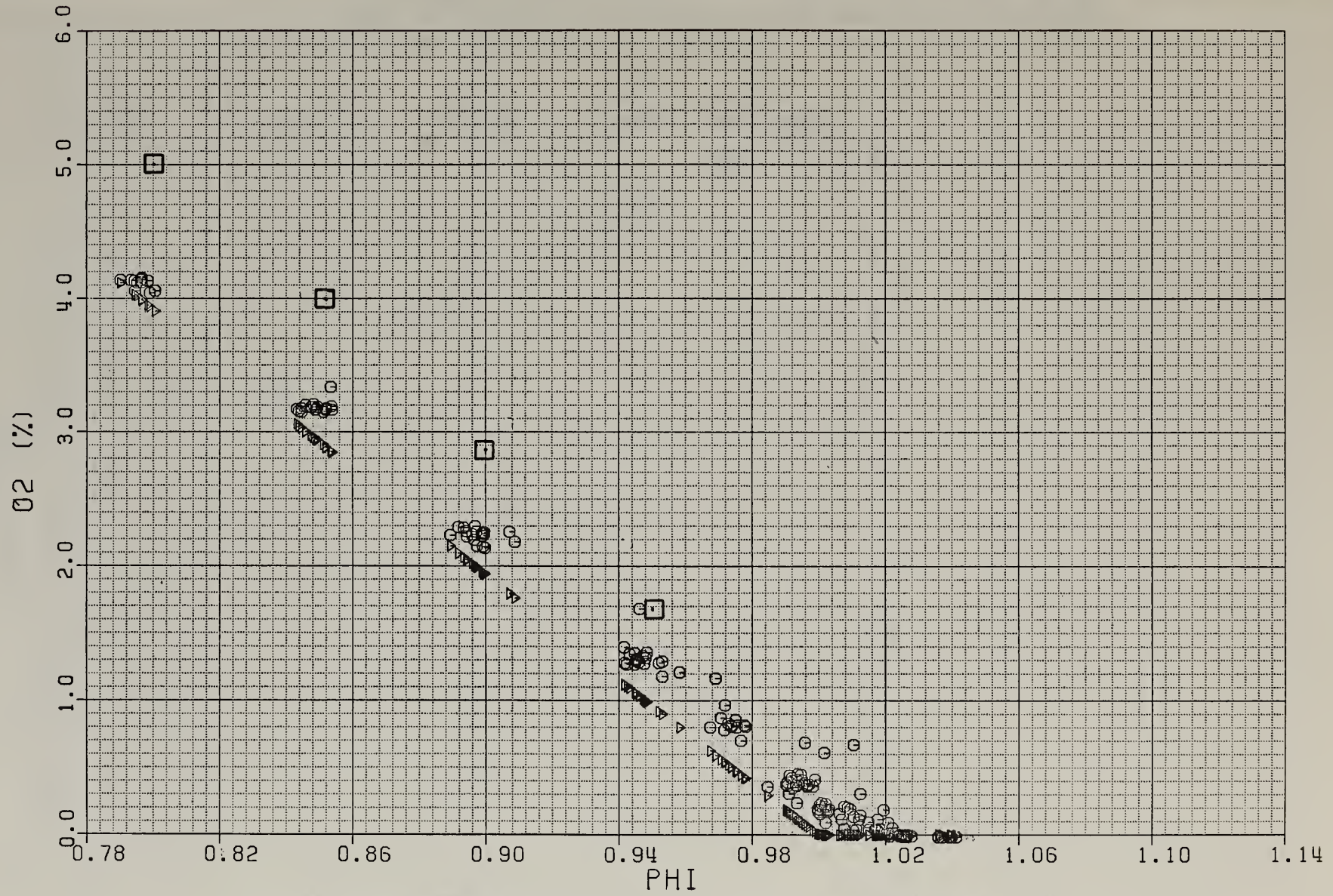

Fig. 34 - Long term transient tests: Cool Furnace; T_F = 870°C; T_A = 177°C; Fuel = No. 2 Fuel Oil; Variation of O_2 concentration with equivalence ratio; Sampling below recuperator; (o - Gas Sampling; Δ - Equilibrium Calculation Based on Stack Temperature; □ - In-Situ Monitor).

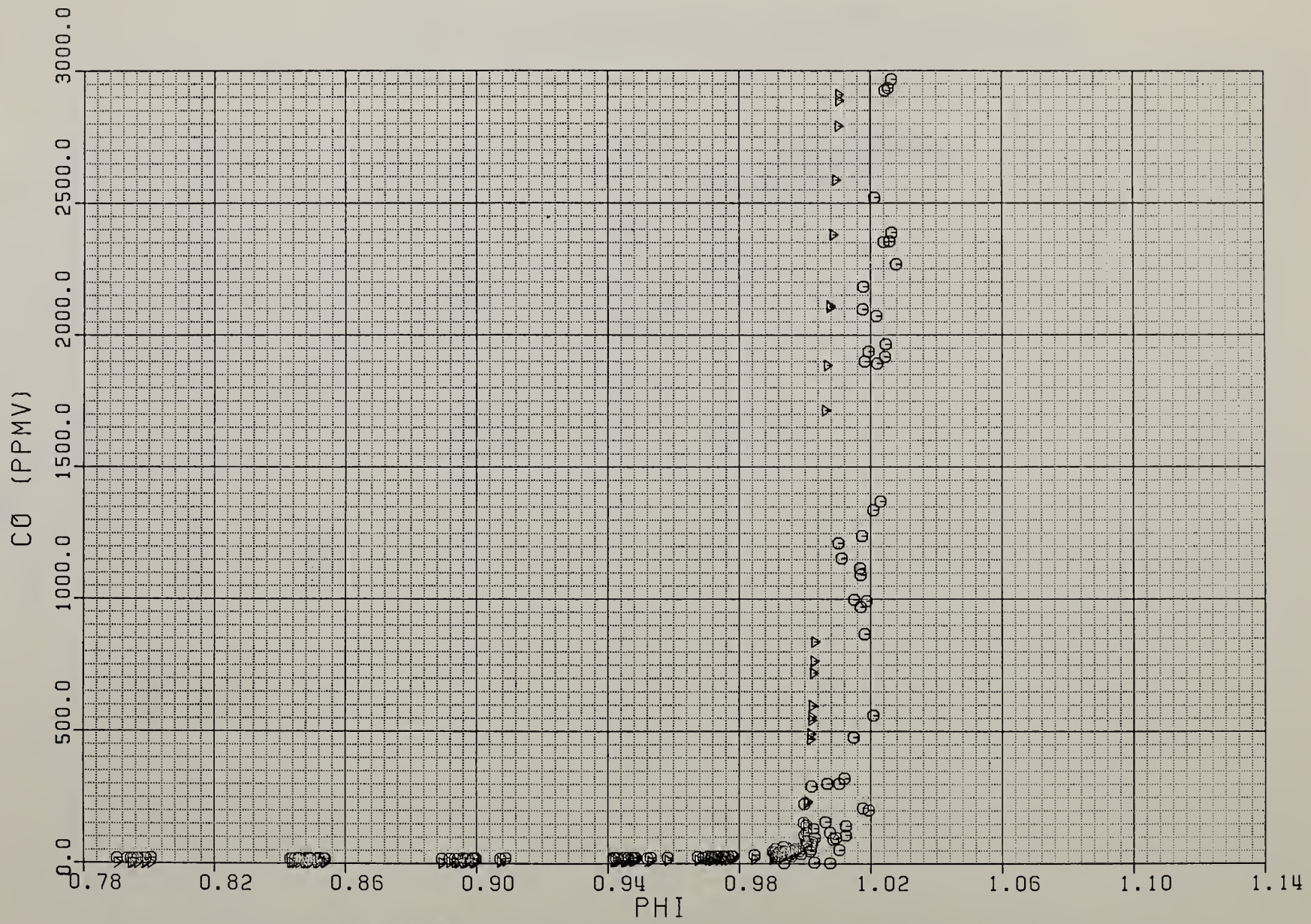

Fig. 35 - Long term transient tests: Cool Furnace; T_F = 870°C; T_A = 177°C; Fuel = No. 2 Fuel Oil; Variation of CO concentration with equivalence ratio; Sampling below recuperator; (o - Gas Sampling; Δ - Equilibrium Calculation Based on Stack Temperature).

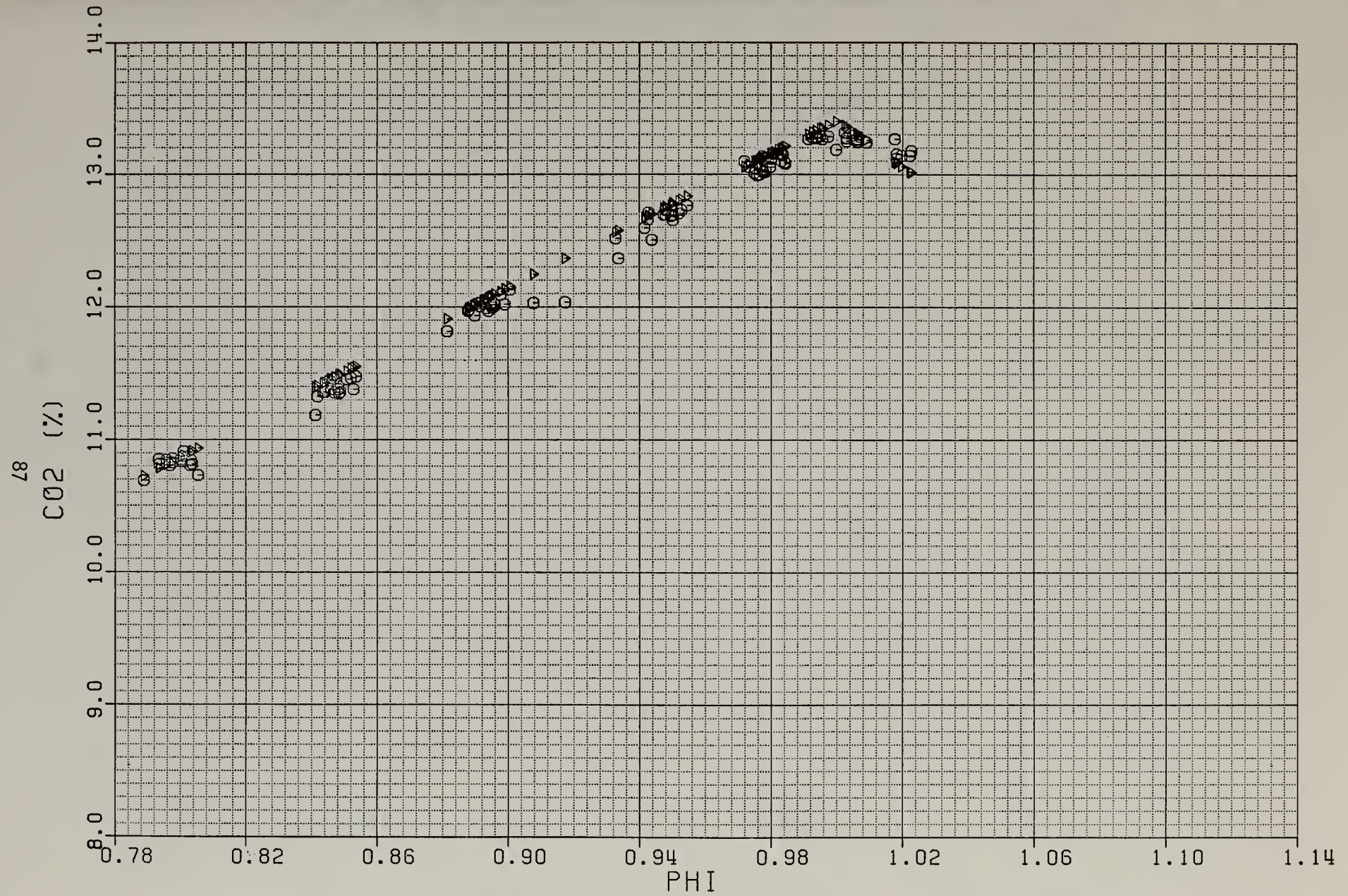

Fig. 36 - Long term transient tests: Warm Furnace; T_F = 910°C; T_A = 249°C; Fuel = No. 2 Fuel Oil; Variation of CO_2 concentration with equivalence ratio; Sampling below recuperator; (o - Gas Sampling; Δ - Equilibrium Calculation Based on Stack Temperature).

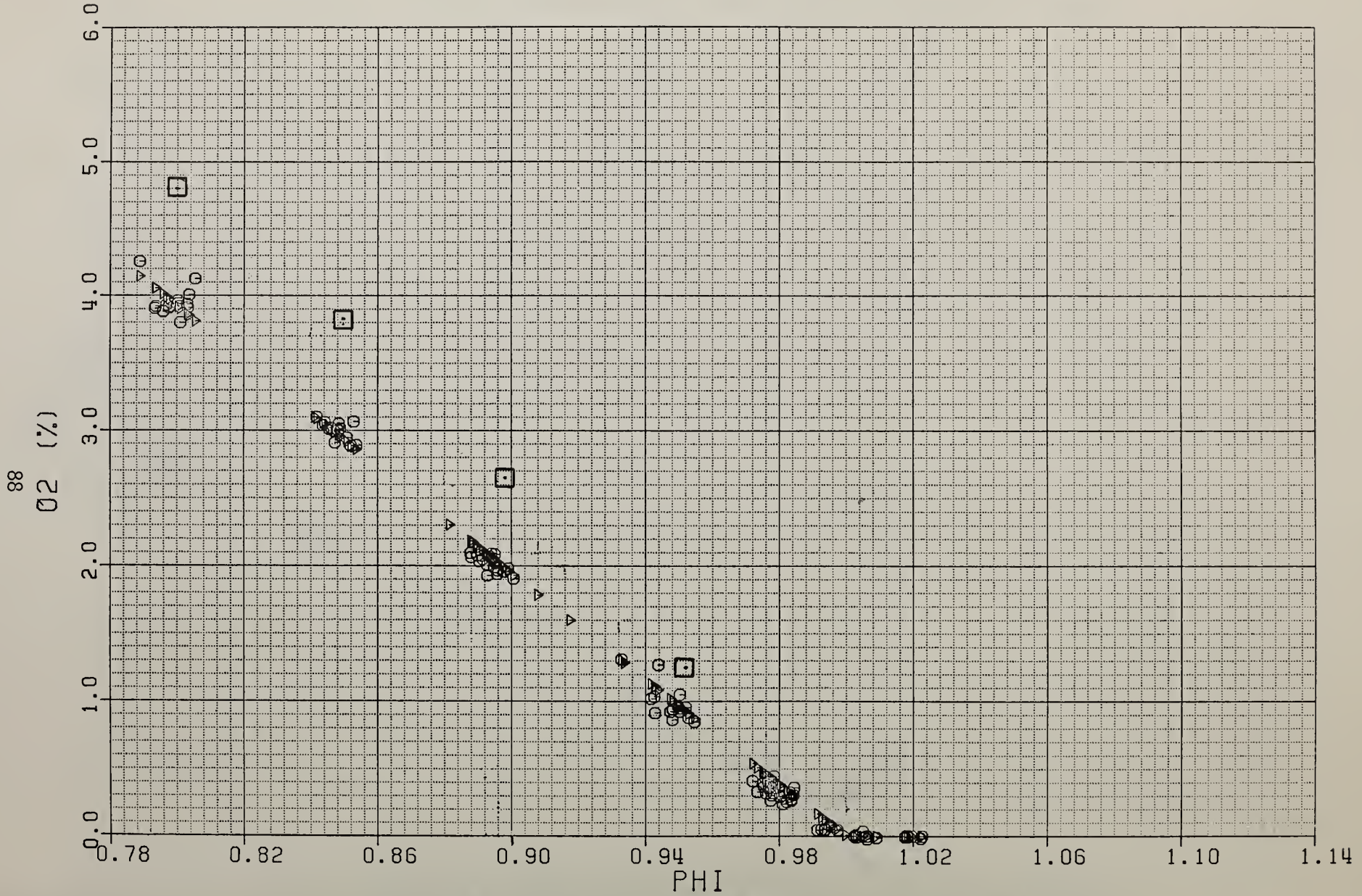

Fig. 37 - Long term transient tests: Warm Furnace; T_F = 910°C; T_A = 249°C; Fuel = No. 2 Fuel Oil; Variation of O_2 concentration with equivalence ratio; Sampling below recuperator; (o - Gas Sampling; Δ - Equilibrium Calculation Based on Stack Temperature; □ - In-Situ Monitor).

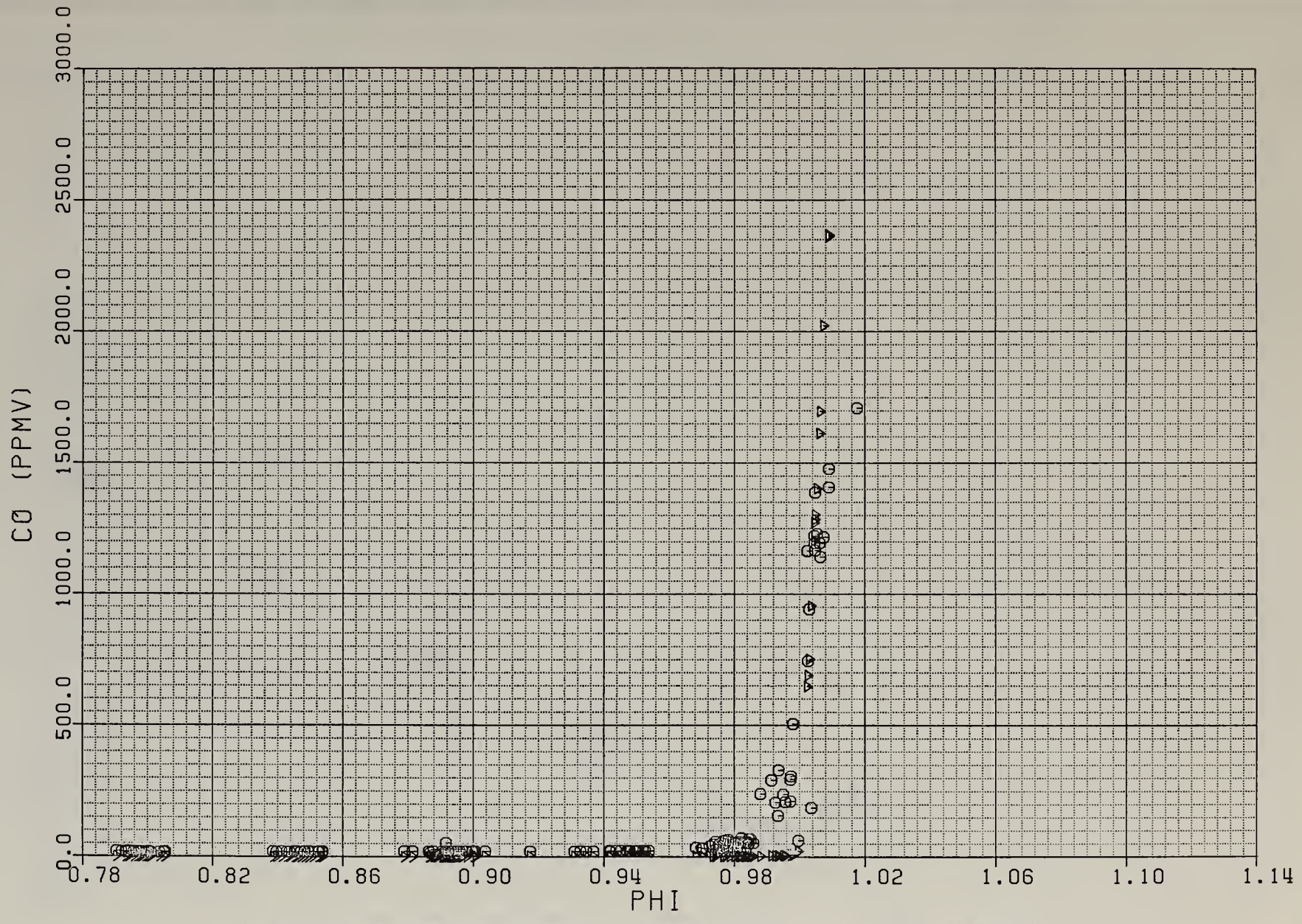

Fig. 38 - Long term transient tests: Warm Furnace; T_F = 910°C; T_A = 249°C; Fuel = No. 2 Fuel Oil; Variation of CO concentration with equivalence ratio; Sampling below recuperator; (o - Gas Sampling; Δ - Equilibrium Calculation Based on Stack Temperature).

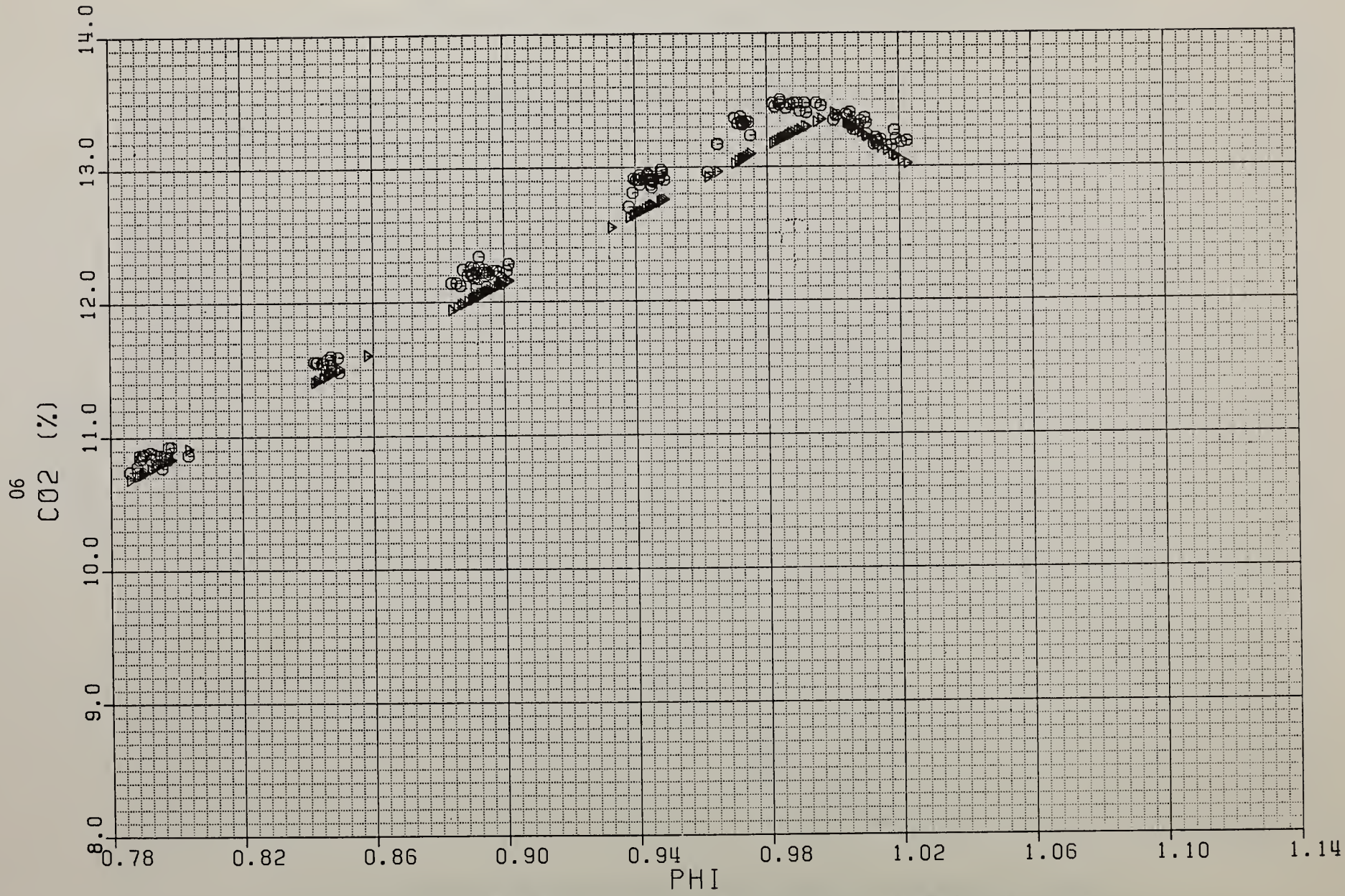

Fig. 39 - Long term transient tests: Hot Furnace; T_F = 945°C; T_A = 270°C; Fuel = No. 2 Fuel Oil; Variation of CO_2 concentration with equivalence ratio; Sampling below recuperator; (o - Gas Sampling; Δ - Equilibrium Calculation Based on Stack Temperature).

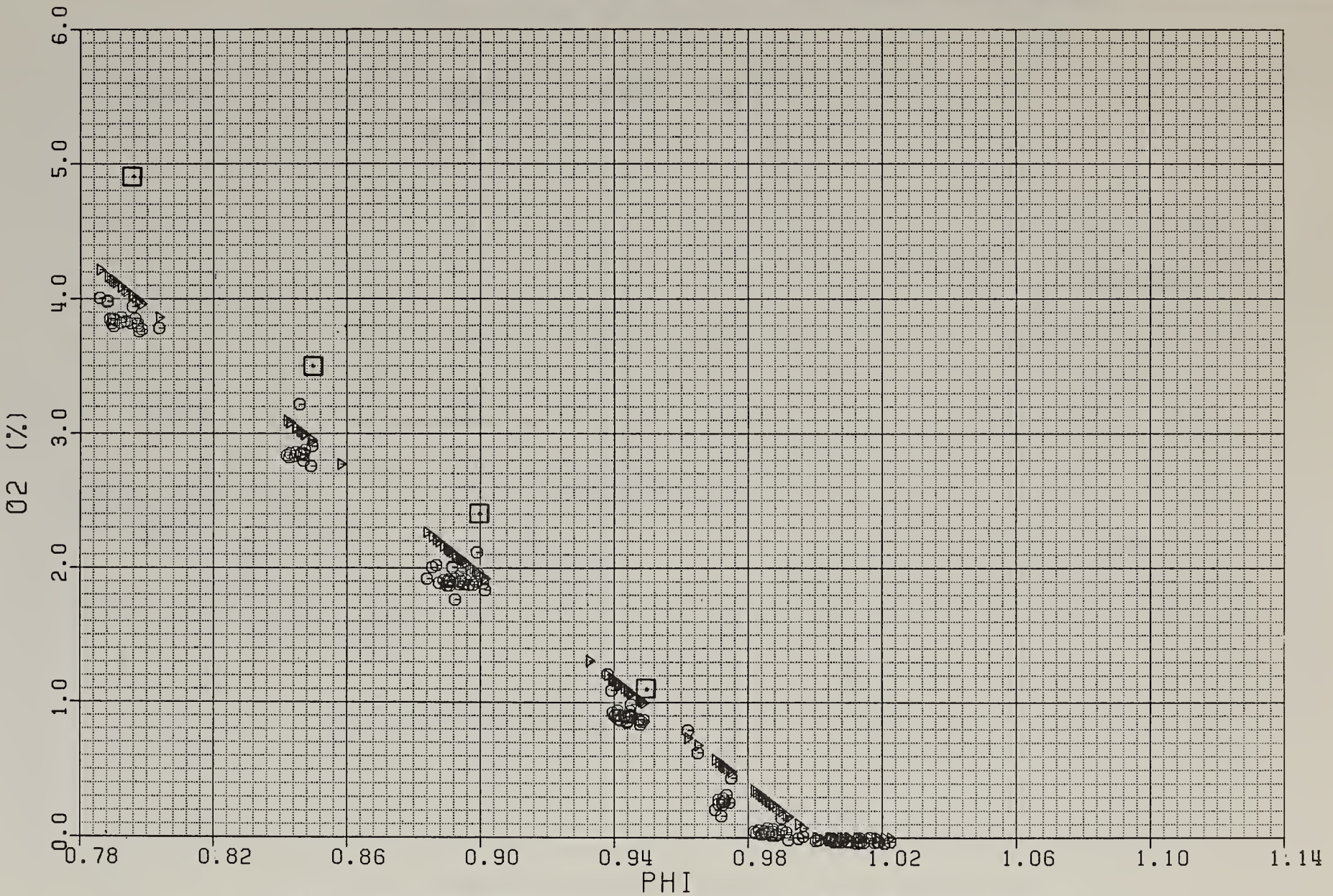

Fig. 40 - Long term transient tests: Hot Furnace; T_F = 945°C; T_A = 270°C; Fuel = No. 2 Fuel Oil; Variation of O_2 concentration with equivalence ratio; Sampling below recuperator; (o - Gas Sampling; Δ - Equilibrium Calculation Based on Stack Temperature; □ - In-Situ Monitor).

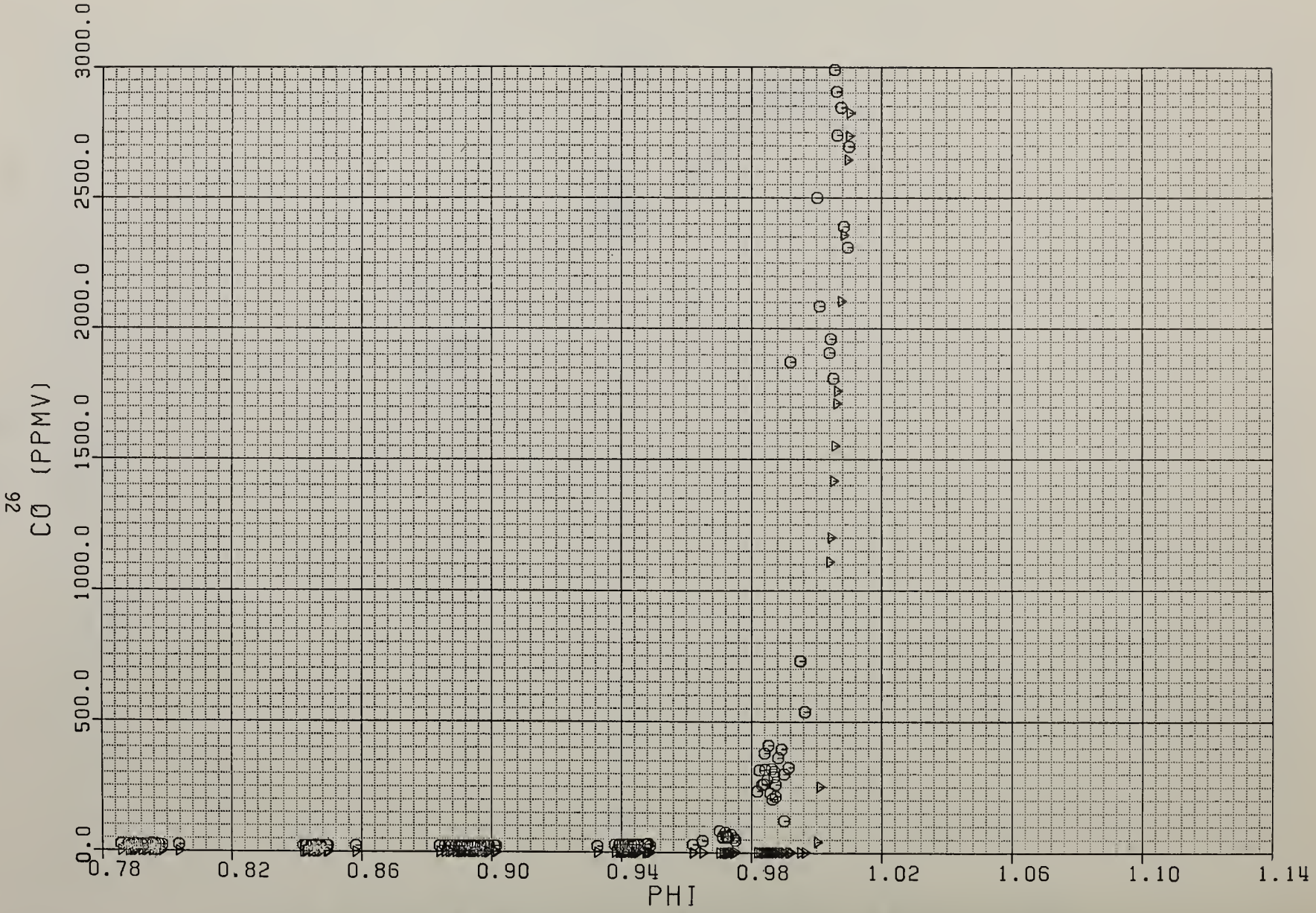

Fig. 41 - Long term transient tests: Hot Furnace; T_F = 945°C; T_A = 270°C; Fuel = No. 2 Fuel Oil; Variation of CO concentration with equivalence ratio; Sampling below recuperator; (o - Gas Sampling; Δ - Equilibrium Calculation Based on Stack Temperature).

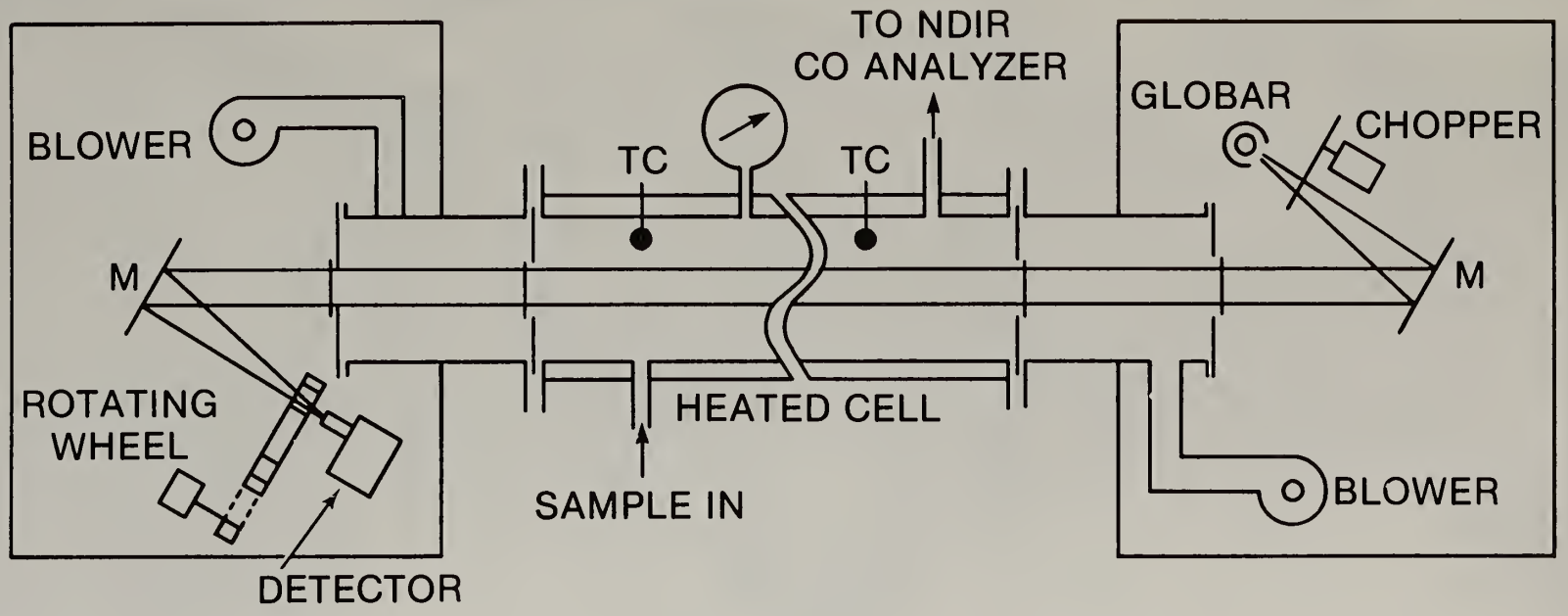

Fig. 42 - Schematic of heated absorption test cell assembly.

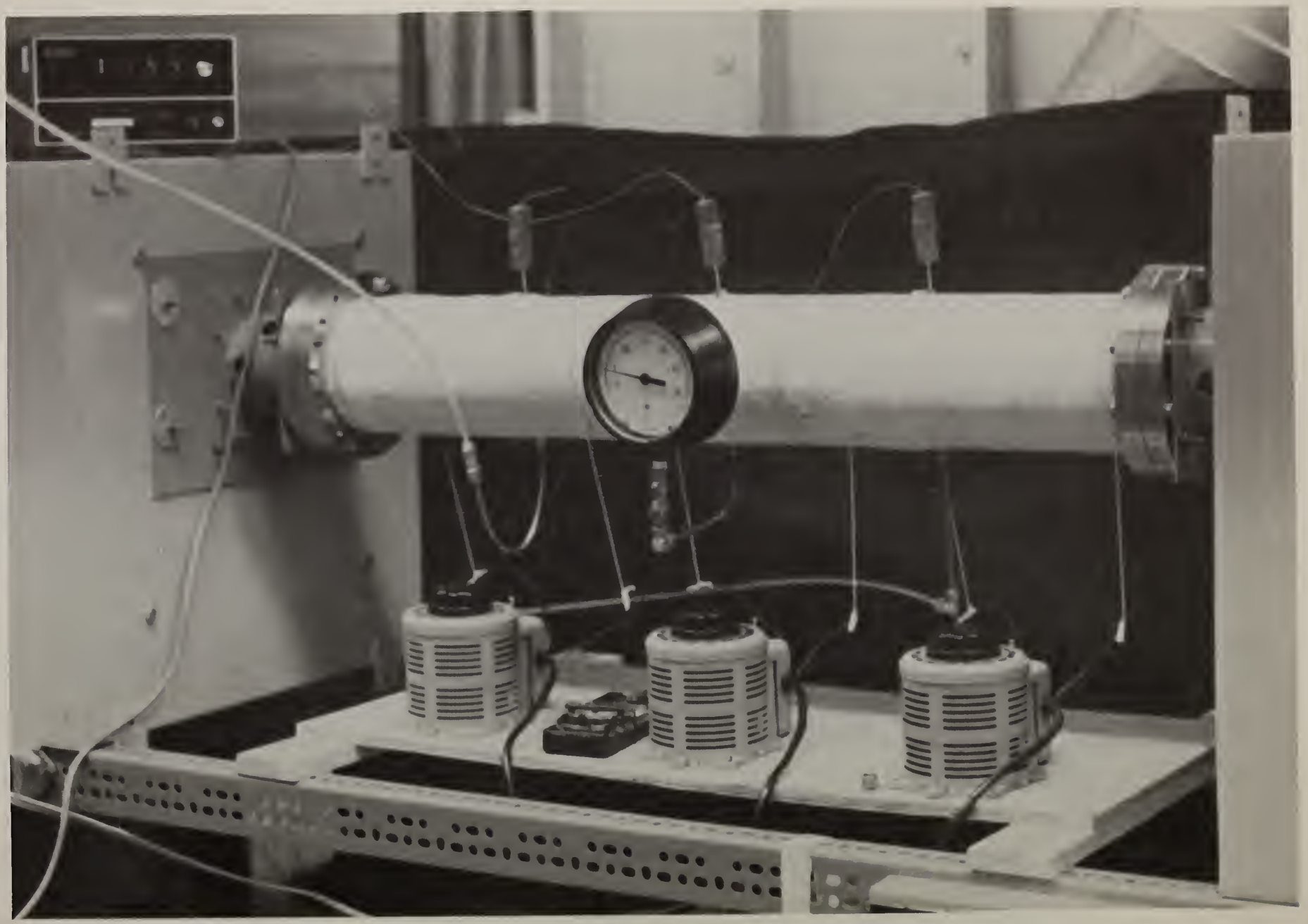

Fig. 43 - View of heated absorption test cell assembly.

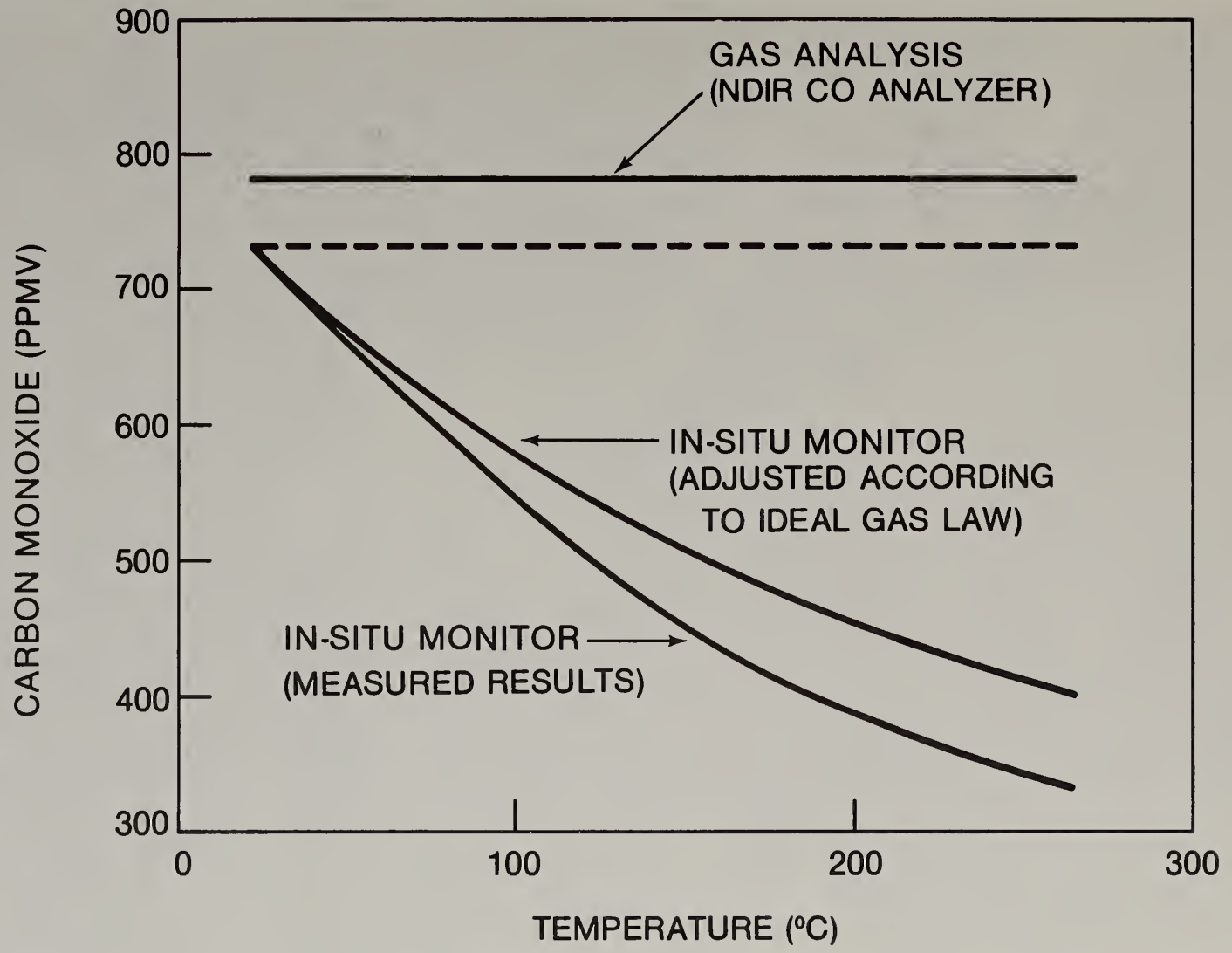

Fig. 44 - Dependence of CO measurements on test cell temperature.

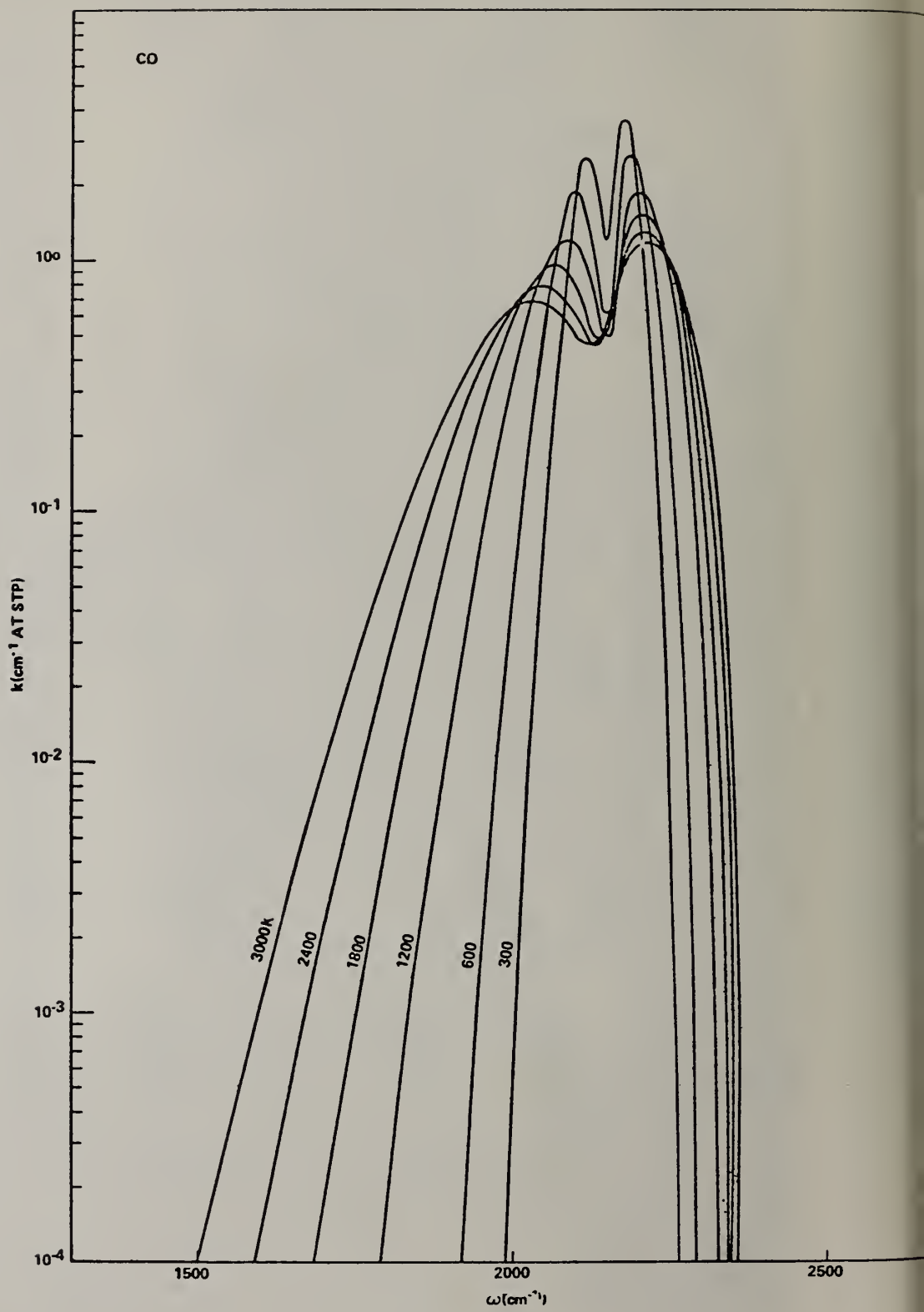

Fig. 45 - Absorption coefficient of CO as a function of temperature.

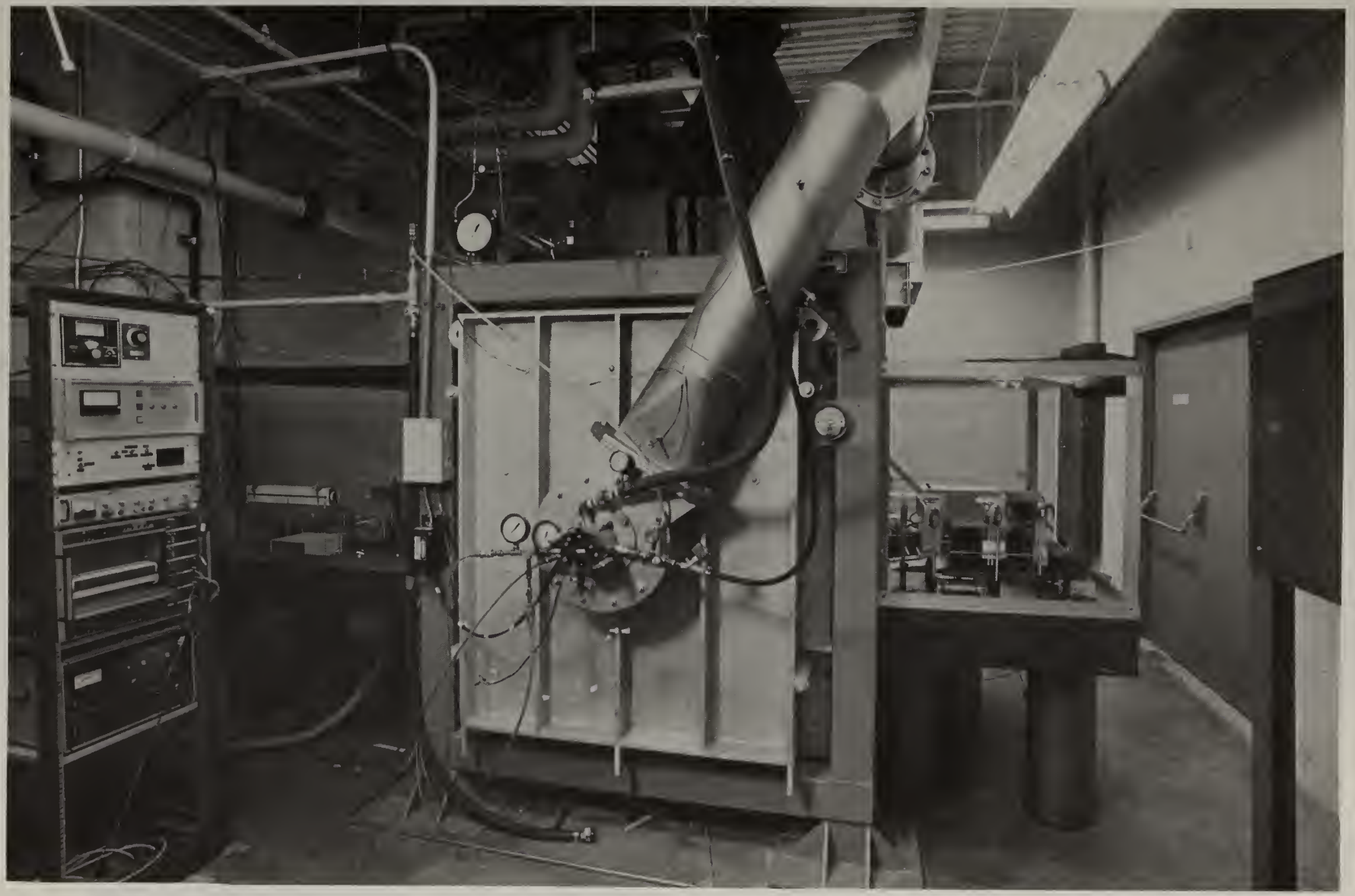

Fig. 46 - NBS Experimental Furnace Facility.

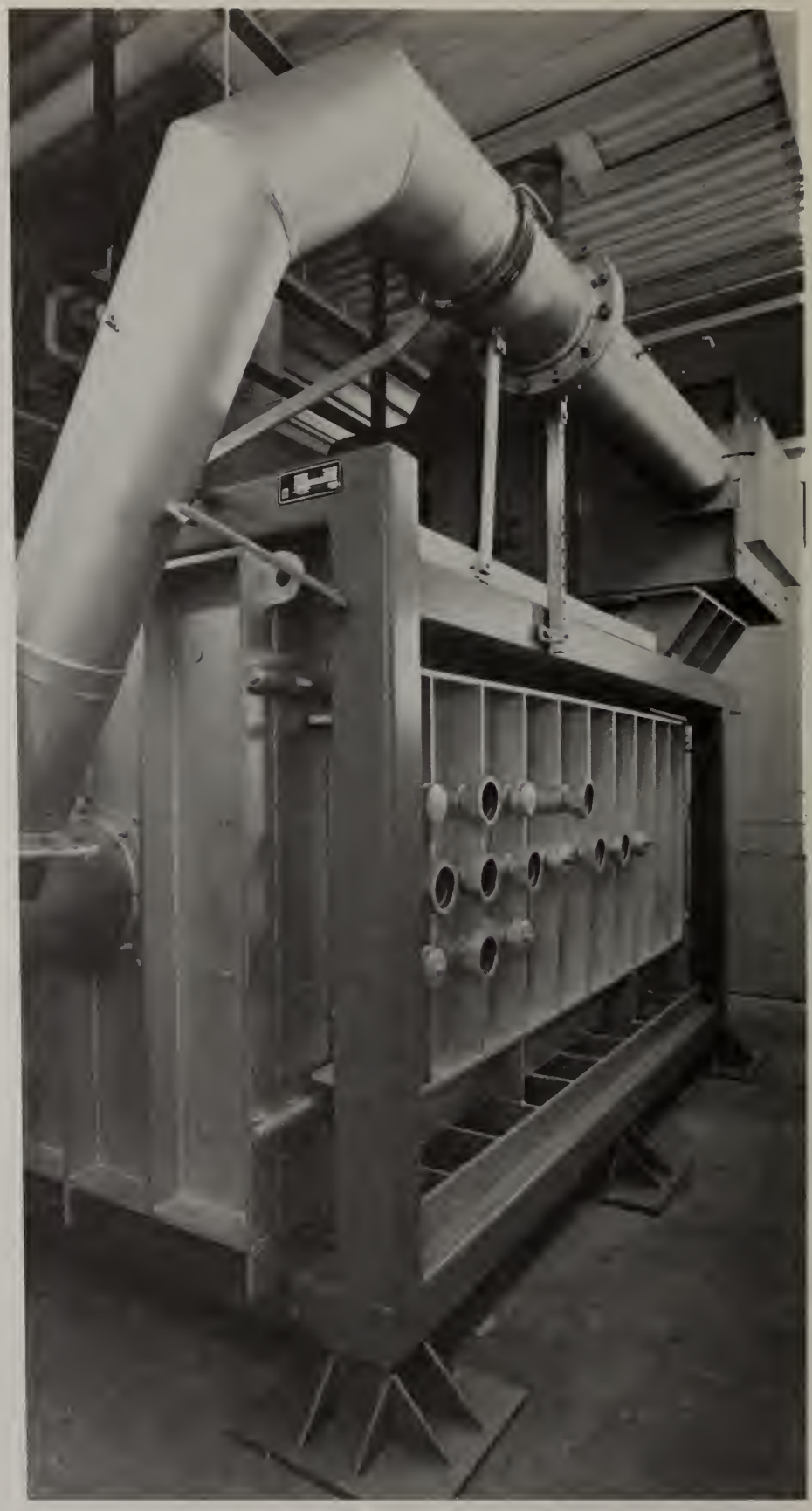

Fig. 47 - NBS Experimental Furnace: Sideview of furnace.

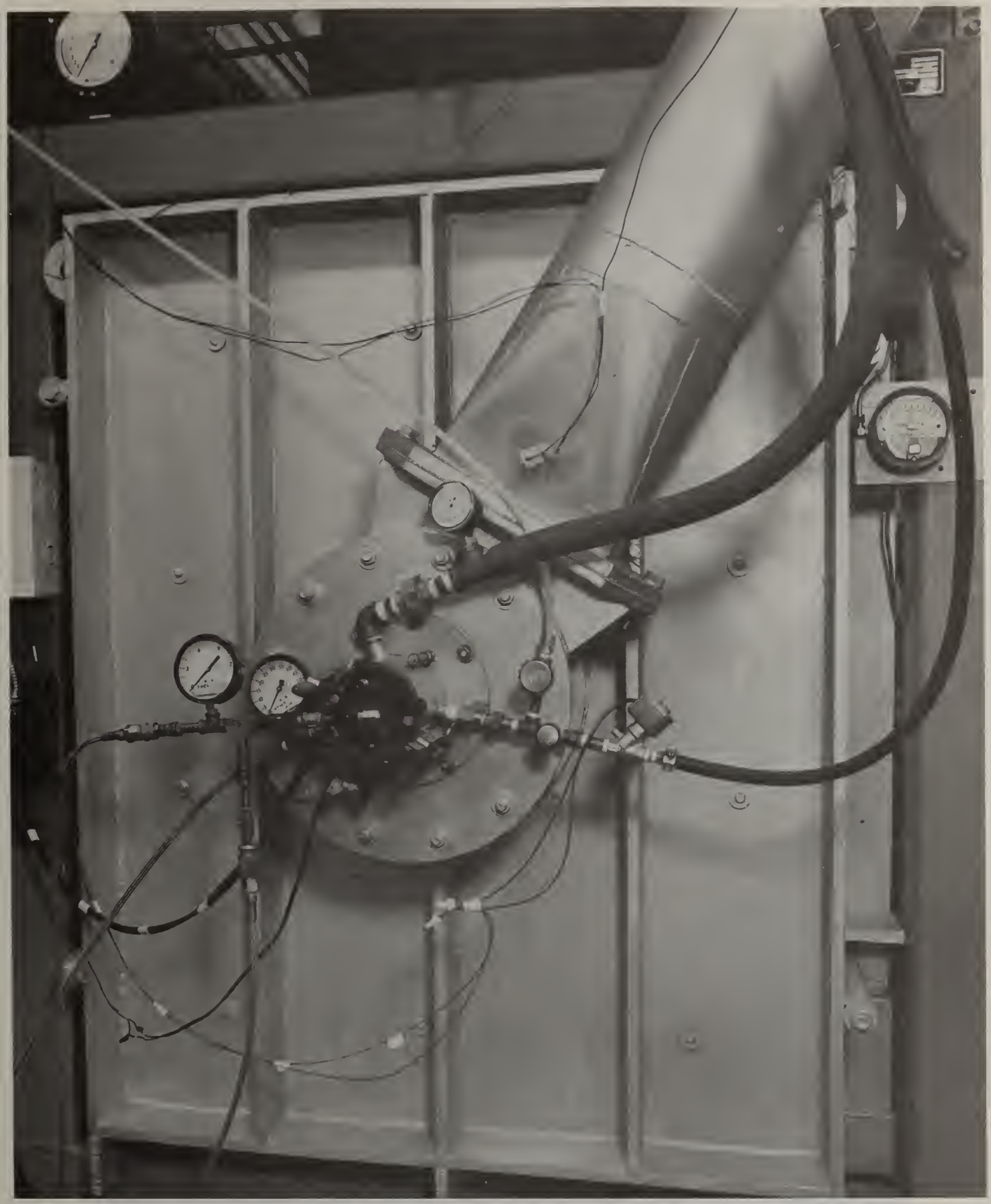

Fig. 48 - NBS Experimental Furnace and Burner.

Fig. 49 - NBS Experimental Furnace: The Recuperator.

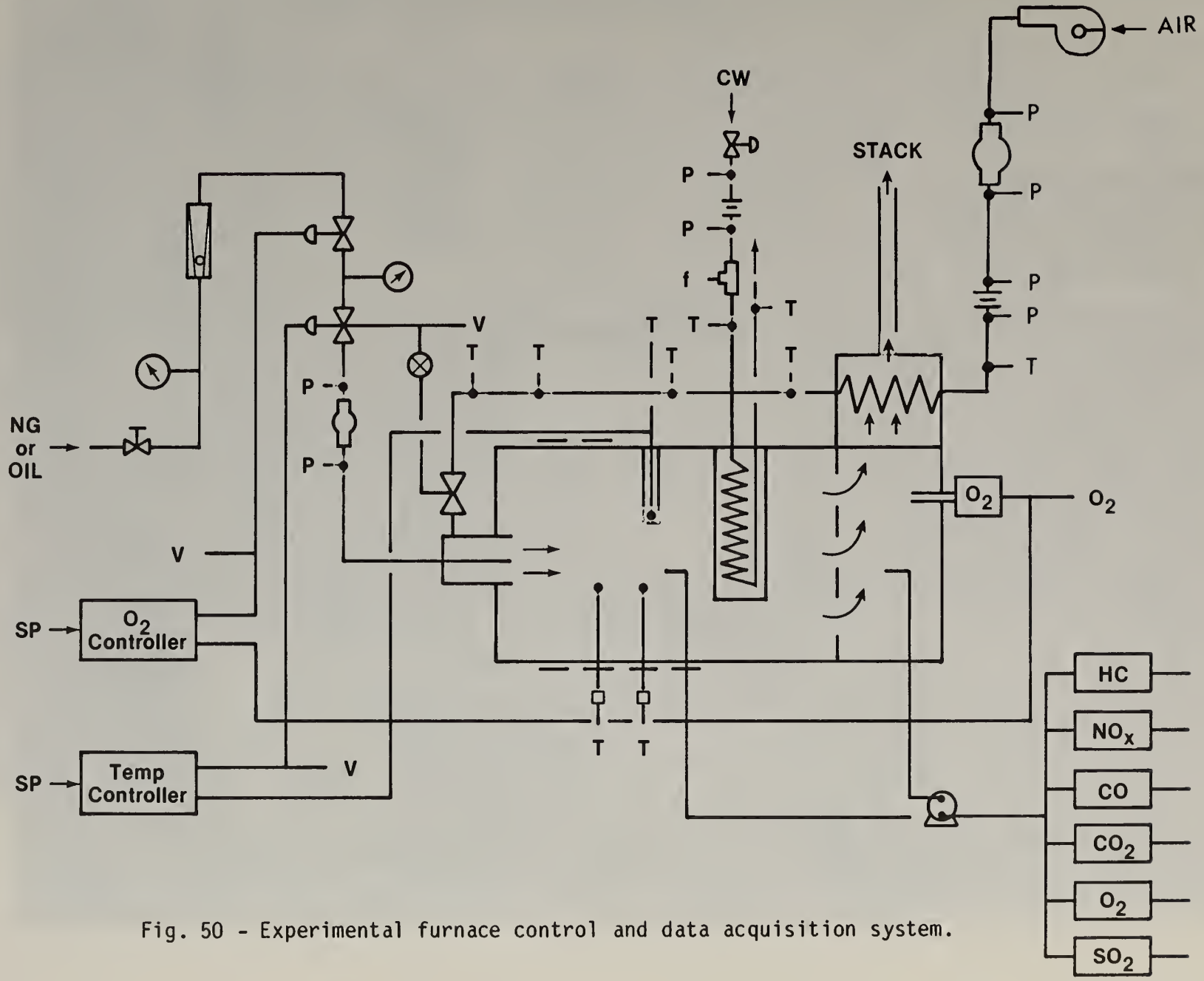

Fig. 50 - Experimental furnace control and data acquisition system.

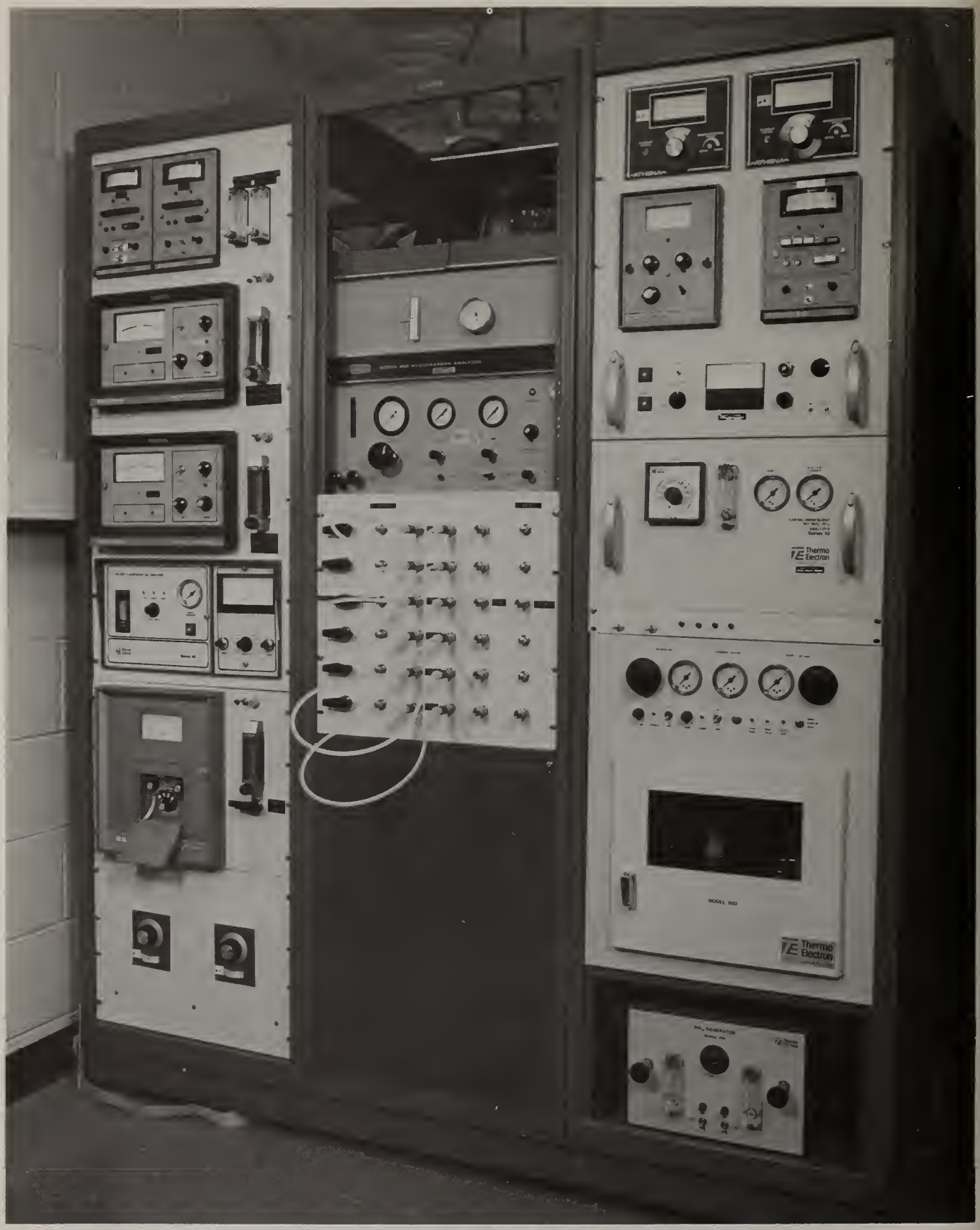

Fig. 51 - View of gas sampling and analysis system.

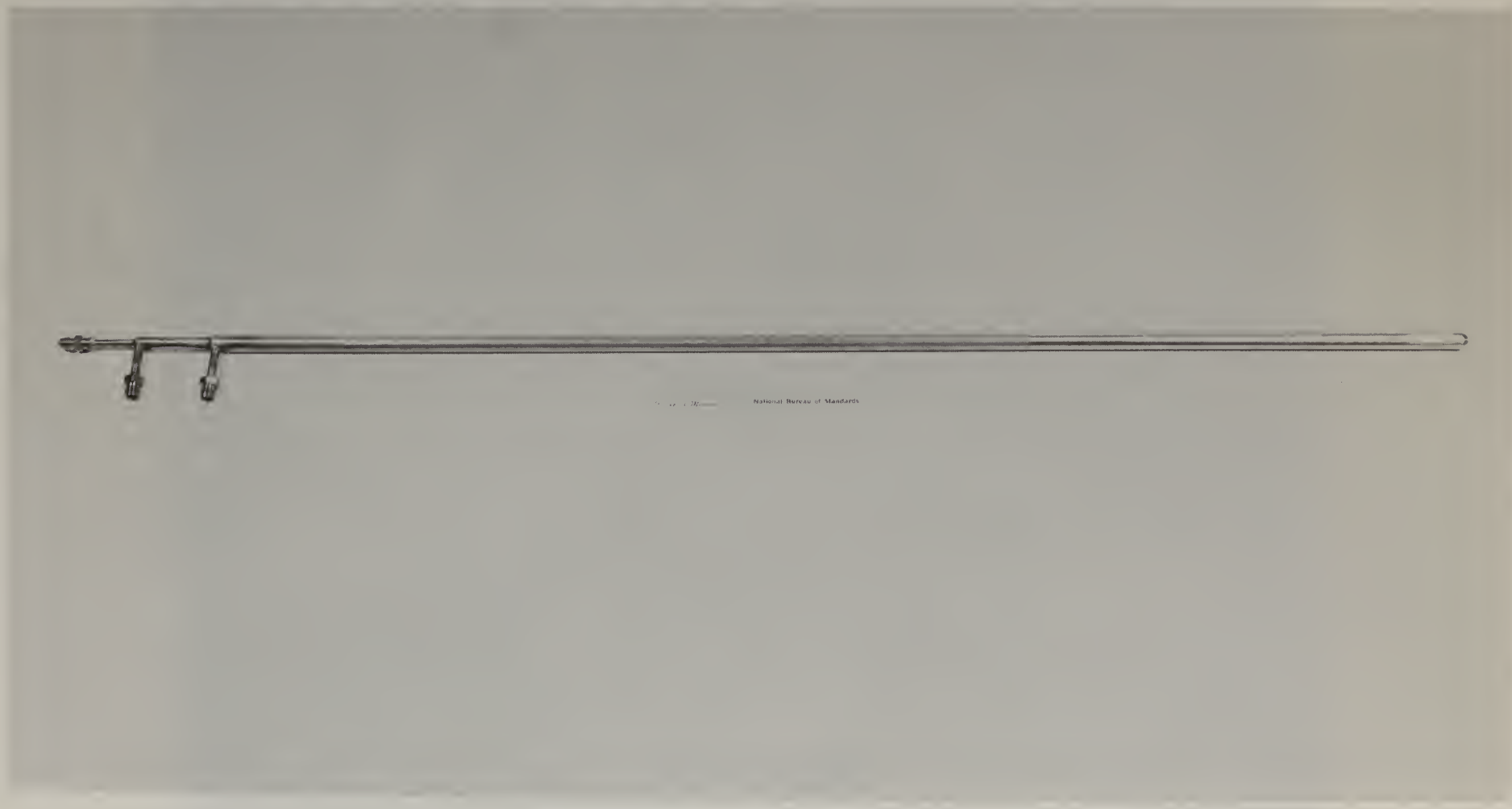

Fig. 52 - Water cooled gas sampling probe.

Fig. 53 - Location of water cooled gas sampling probe.

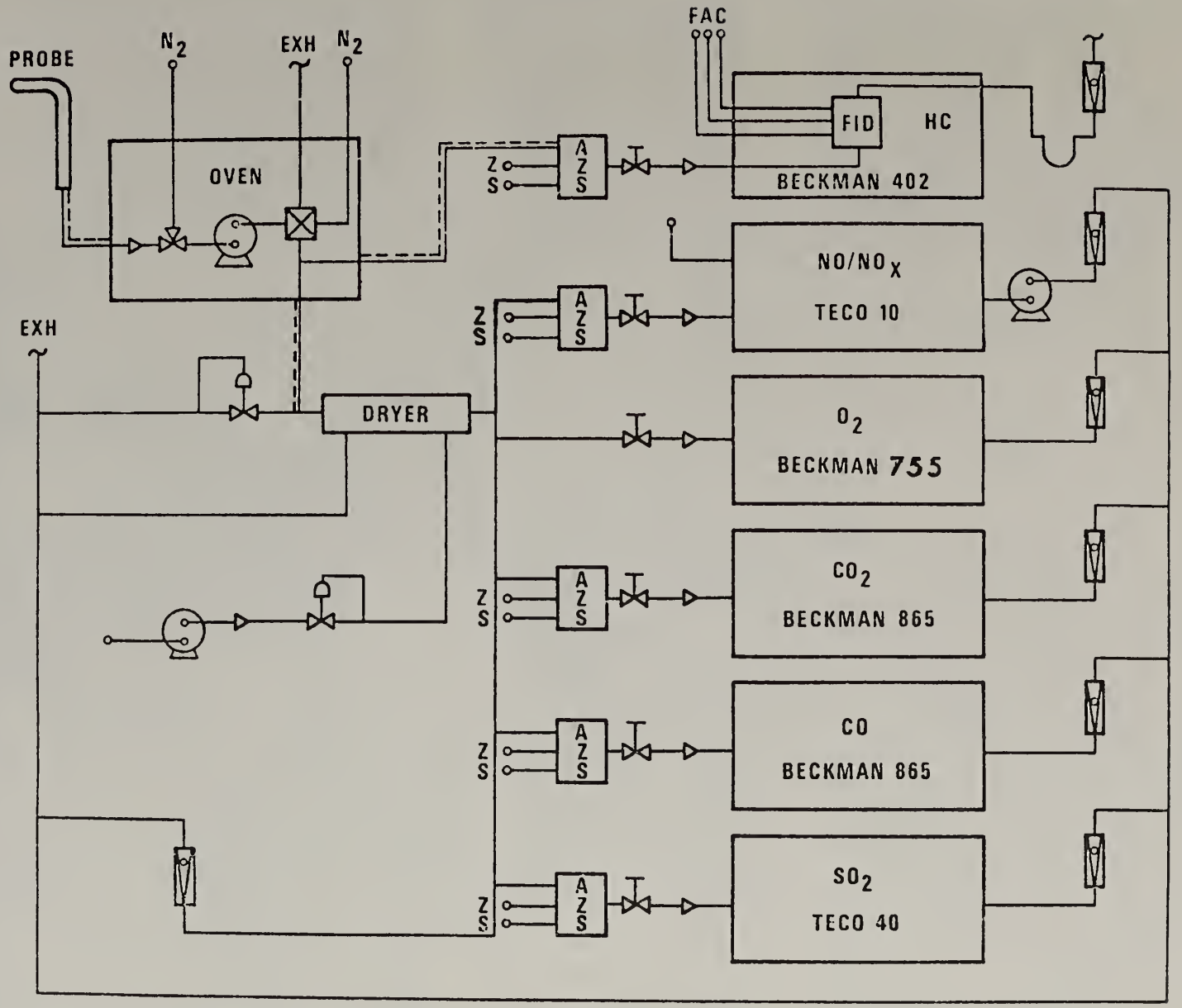

Fig. 54 - Schematic of gas analysis and sampling system.

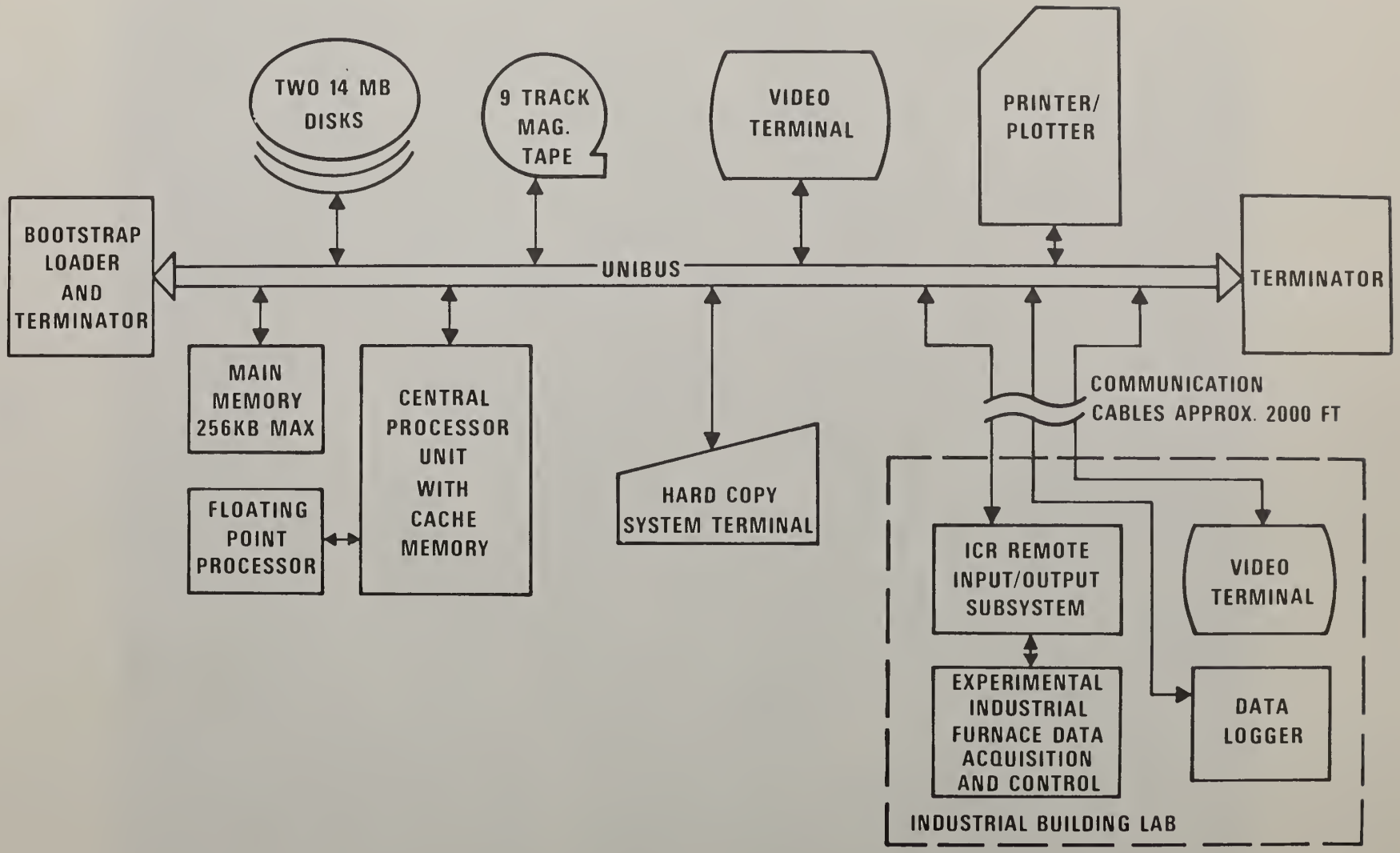

Fig. 55 - DEC PDP 11/60 minicomputer based data acquisition and control system.

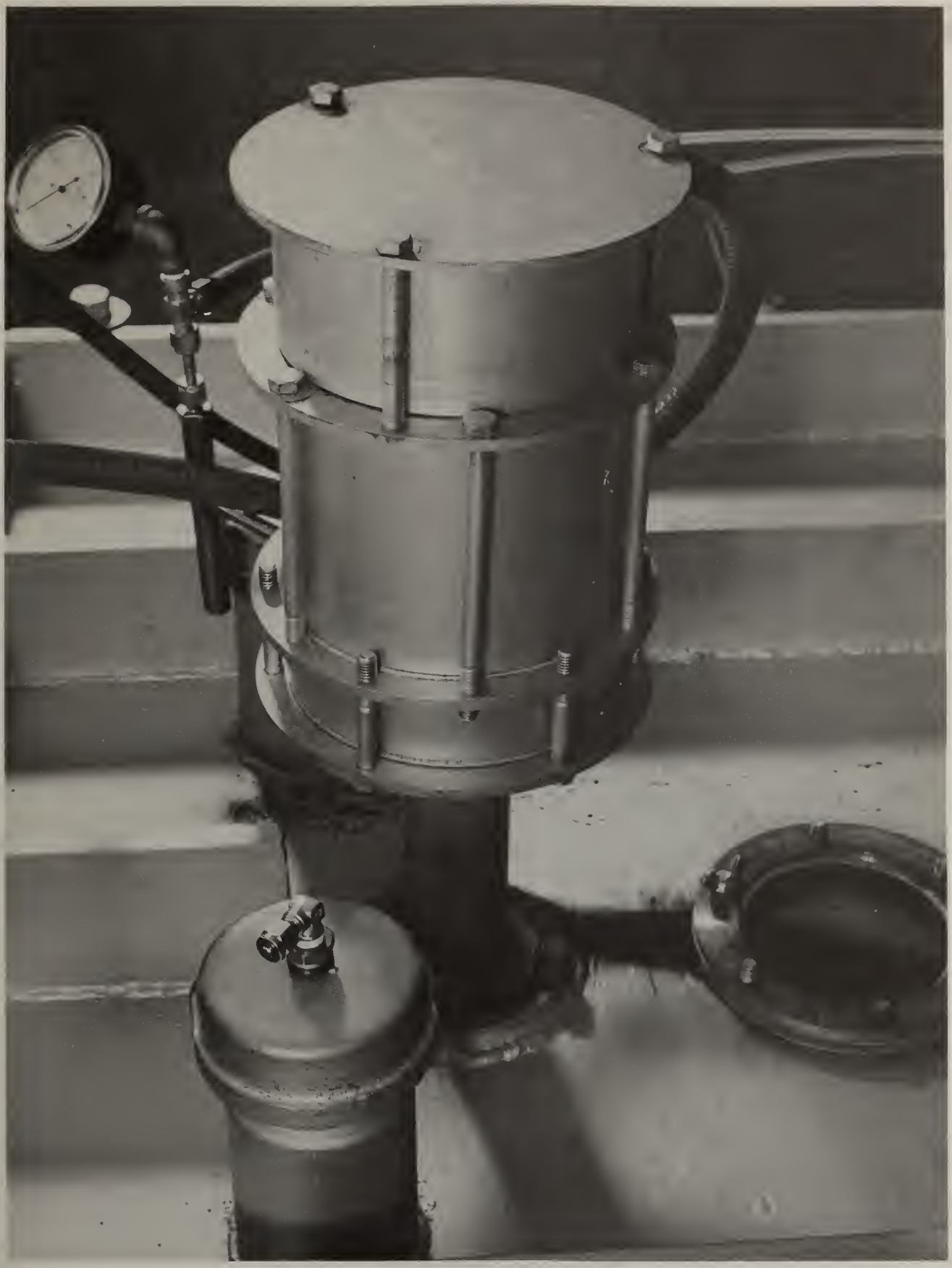

Fig. 56 - Location of in-situ O_2 monitor.

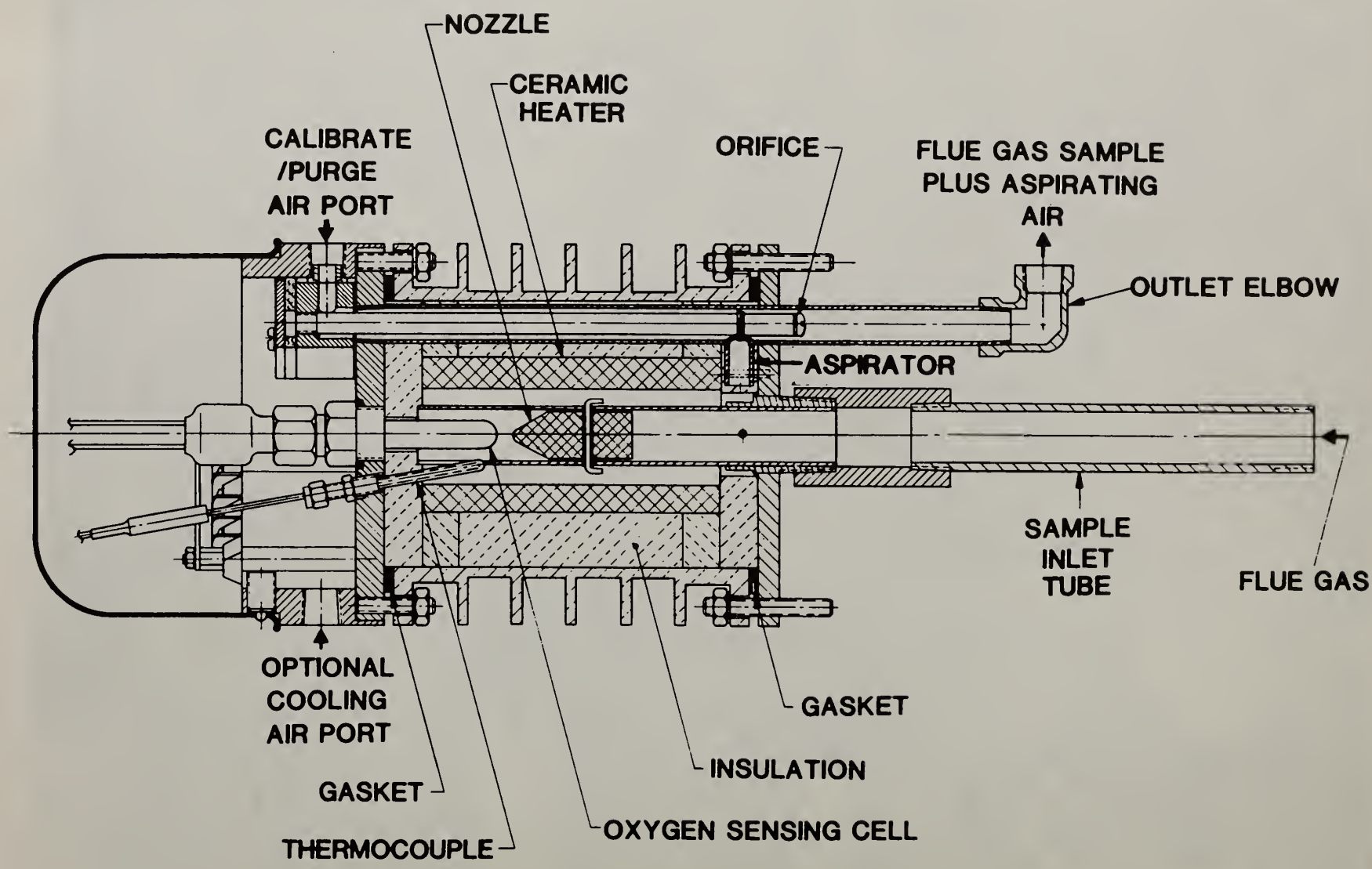

Fig. 57 - Schematic of O_2 probe.

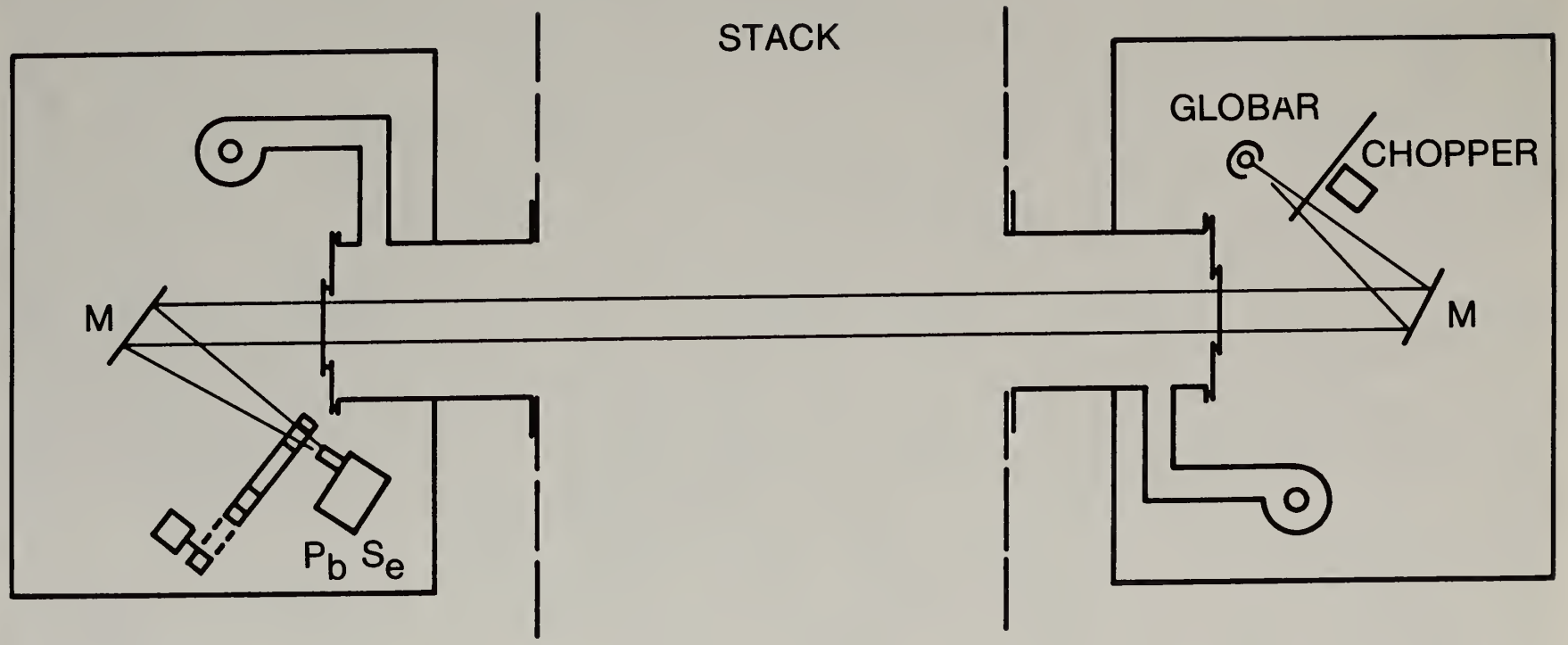

Fig. 58 - Schematic of the in-situ CO monitoring system.

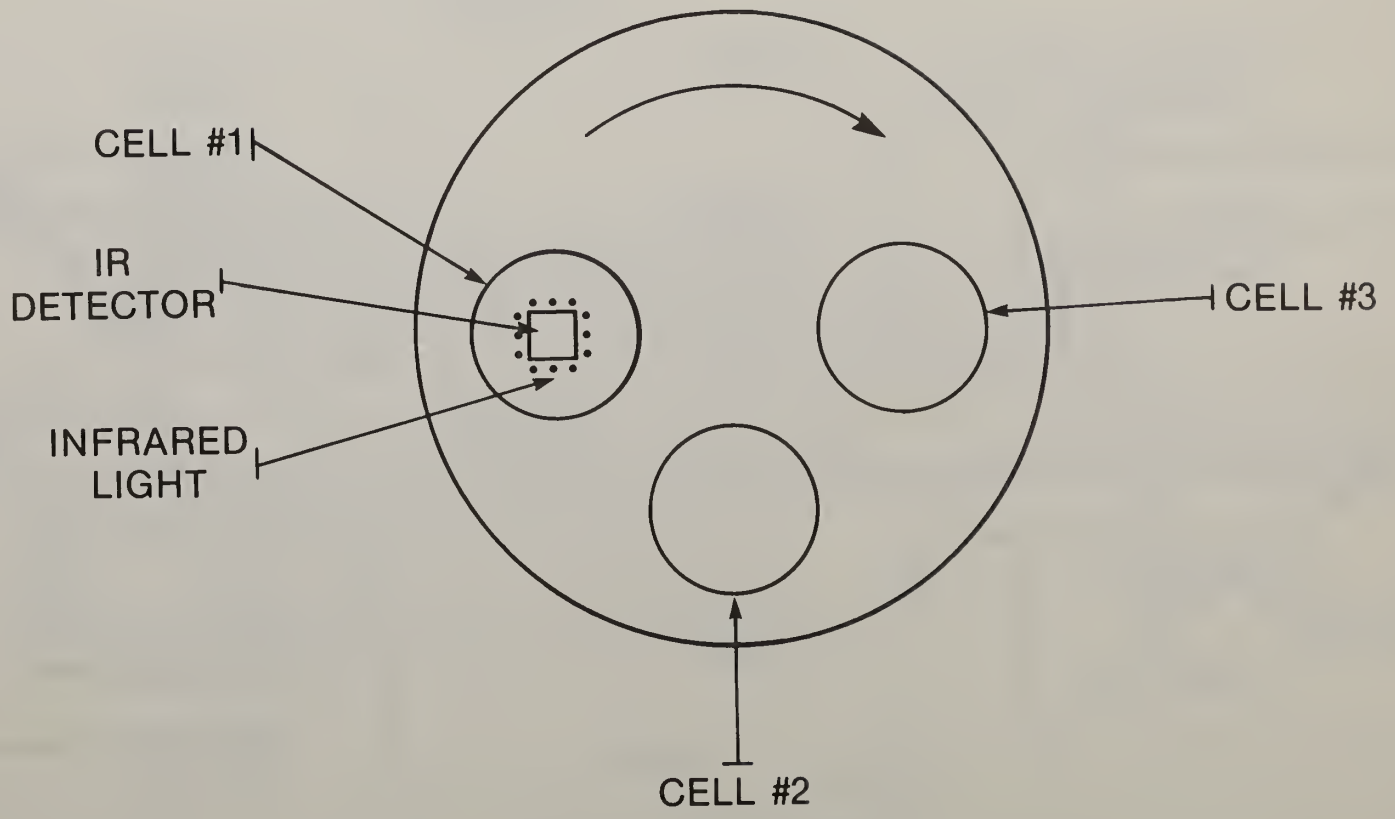

Fig. 59 - Schematic of the rotating wheel and three sealed gas cells inside the CO monitor.

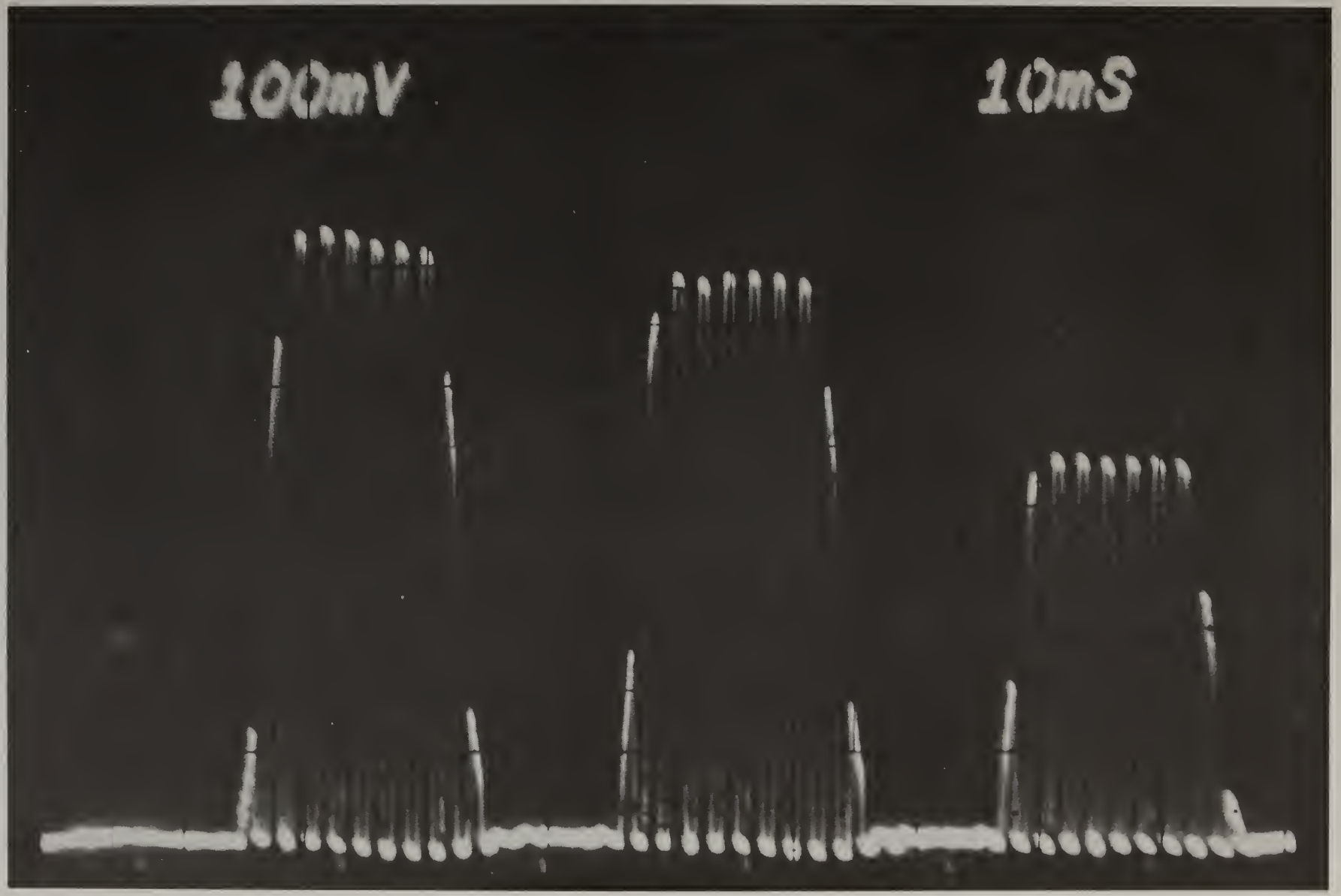

Fig. 60 - Typical output from the CO detector.